The Dual Function of the *Chlamydia pneumoniae* Cpn0572 Protein in Modulating the Host Actin Cytoskeleton

Inaugural-Dissertation
zur Erlangung des Doktorgrades
der Mathematisch-Naturwissenschaftlichen Fakultät
der Heinrich-Heine Universität Düsseldorf
(Fachbereich Biologie)

vorgelegt von
Rafat Zrieq
aus Irbid

Düsseldorf 2009

Aus dem Institut für
Funktionelle Genomforschung der Mikroorganismen
der Heinrich-Heine Universität Düsseldorf

Gedruckt mit der Genehmigung der
Mathematisch-Naturwissenschaftlichen Fakultät der
Heinrich-Heine Universität Düsseldorf

Referent: Prof. Dr. Johannes H. Hegemann
Koreferent: Prof. Dr. Olaf Bossinger

Tag der mündlichen Prüfung: 19. 06. 2009

CONTENTS

ABBREVIATIONS

%	Percentage
°C	Degree Celsius
µl	Microlitre
µM	Micromolar
µm	Micrometer
ABPs	The acting-binding proteins
ADP	Adenosine diphosphate
Aip1	The actin interacting protein 1
Arp	Actin related protein
ATP	Adenosine-5'-triphosphate
bp	Base pair
BSA	Bovine serum albumin
C.	*Chlamydia*
CH	Calponin homology
CPAF	The chlamydial protease-like activity factor
ddH2O	Distilled deionized water
DNA	Deoxyribonucleic acid
dNTP	Desoxyribonucleoside-5’-triphosphate
DUF	Domain of Unknown Function
EB	The chlamydial Elementary Body
F-actin	Filamentous actin/ actin filaments
g	Gram
G-actin	Globular monomeric actin
GAG	Glycosaminoglycans
GAPs	GTPase activating proteins
GDP	Guanosine diphosphate
GEFs	Guanine nucleotide exchange factors
GFP	The green fluorescent protein
GST	Glutathione S-transferase
GTP	Guanosine triphosphate
h	Hour
HEPES	4-(2-hydroxyethyl)-1-piperazineethanesulfonic acid
IF	Immunofluorescence
IFs	Intermediate filaments
Incs	The chlamydial inclusion membrane proteins
IPTG	Isopropyl-â-D-1-thiogalactopyranoside

l	Liter
Lat-A	Latrunculin-A
LB	Luria-Bertani medium
M	Molar
MAPK	Mitogen activated protein kinase
MEM	Minimum essential medium
mg	Milligram
MIF	Microimmunofluorescence
min	Minute
ml	Milliliter
mM	Millimolar
MOI	Multiplicity of infection
MOMP	The chlamydial major outer membrane protein
NF-$_k\beta$	The nuclear factor kappa-light-chain-enhancer of activated B cells
NPFs	Nucleation promoting factors
nt	Nucleotide
N-WASP	Neural WASP
OD	Optical density
OmcB	The chlamydial outer membrane complex protein B
ORF	Open reading frame
PBS	Phosphate buffered saline
PCR	Polymerase Chain Reaction
PEG	Polyethyleneglycol
pH	Potential of hydrogen
PI3K	Phosphoinositol 3-kinase
PIP3	Phosphatidylinositol- 3,4,5 triphosphate
Pmp21	The *Chlamydia* Polymorphic membrane protein 21
PtdIns(4,5)P2, PI(4,5)P2 or PIP2	Phosphatidylinositol (4,5)-bisphosphate
RB	The chlamydial Reticulate Body
RNA	Ribonucleic acid
rpm	Revolution per minutes
SD	Synthetic medium
SDS-PAGE	SDS-Polyacrylamide-Gel electrophoresis
sec	Second
SPG	Chlamydia transportation medium (sucrose-phosphate-glutamate dilution)

Tarp	The *C. trachomatis* translocated actin recruiting protein
TIIISS	Type three secretion system
U	Units
V	Volt
WASP	Wiskott–Aldrich syndrome protein
WAVE	WASP verprolin homologous protein
Wb	Western blot
WH	WASP homology
WIP	WASP-interacting protein
X	Time/fold
YPD	Yeast extract peptone dextrose

SUMMARY

Chlamydiae are gram-negative obligate intracellular bacterial pathogens of humans and animals. *C. pneumoniae* is a common respiratory pathogen that has been associated with a variety of chronic diseases including asthma and atherosclerosis.

Chlamydiae display a biphasic developmental cycle with an infectious, but metabolically inactive elementary body (EB) and a non-infectious metabolically active reticulate body (RB). Uptake of EBs is a crucial step for infection. Like other pathogenic bacteria, it is believed that *Chlamydiae* species deliver their effector proteins to trigger their own entry and survival within the host cell. Among the few chlamydial effector proteins identified, the *C. trachomatis* Tarp is the only identified protein translocated into the host cell where it colocalizes with actin pedestals underneath the attached EB (Clifton, Fields et al. 2004). In a follow up study, it has been shown that Tarp nucleates actin polymerization *in vitro* (Jewett, Fischer et al. 2006). Several studies analyzing Tarp investigated the biochemical properties of the protein *in vitro*, however the molecular mechanism of how Tarp interacts and modulates the host actin *in vivo* has not been shown.

In this study, we analyzed the *C. pneumoniae* homologous protein Cpn0572. Both proteins share high homology in the central region but are markedly different in the N-terminal and the C-terminal regions. To investigate the role of Cpn0572 in modulating host cell processes, we used the yeast *Saccharomyces cerevisiae* as an eukaryotic model system. Therefore, we expressed Cpn0572 in yeast and performed a phenotypic analysis. Cpn0572-expressing yeast cells exhibited irreversible reduced growth and increased sensitivity against the actin destabilizing drug Latrunculin-A (Lat-A). Further studies revealed that *cpn0572* interacts genetically with actin mutant alleles. Cpn0572 transformed the yeast wild type actin into clumps and the GFP-Cpn0572 fusion protein exclusively colocalized with these actin clumps and stabilized them against Lat-A. The actin phenotype induced by Cpn0572 and the colocalization between GFP-Cpn0572 and actin clumps were also observed in the transfected human HEK-239 cells.

A deletion analysis identified a central domain of Cpn0572 (DUF) which is conserved in all homologues proteins of Cpn0572 from different *Chlamydia* species. We could show that this conserved domain is crucial for colocalization with and stabilization of filamentous actin (F-actin) structures. DUF alone could bind *in vitro* pre-assembled mammalian F-actin and pulled down actin from HEp-2 cells lysates. Using *in vivo* and *in vitro* experiments, mutations introduced in the conserved amino acids within DUF resulted in loss of Cpn0572 capability in actin clumping, colocalization with actin structures and binding F-actin.

The combination of DUF with other domains of Cpn0572 protein yielded different actin and yeast growth phenotypes. The C-terminal region of the Cpn0572 protein increased

the actin stabilization activity of DUF (which on its own is not lethal for yeast growth) and caused yeast lethality. On the other hand, the N-terminal region containing DUF induced actin clumping and lethality in yeast cells.

Using the advantages of yeast, we showed that Cpn0572 stabilizes actin by competing with and/or displacing of the actin-depolymerizing factor cofilin from binding F-actin. These results have been extended and verified *in vitro* using mammalian actin and cofilin proteins. Competition with cofilin in binding F-actin has also been shown for DUF and the C-terminus of Cpn0572.

Like Tarp, Cpn0572 induced actin nucleation *in vitro* independent from other cellular proteins and DUF required a region of 110 amino acid residues upstream of DUF to achieve this activity. Mutations within this fragment identified a crucial stretch of proline amino acids surrounding a central glutamic acid that is crucial for Cpn0572 actin clumping activity in yeast and human cells expressing Cpn0572, however this proline stretch is not required for Cpn0572-induced actin nucleation activity *in vitro*.

Using antibodies raised against the recombinant Cpn0572 protein, the expression of Cpn0572 was confirmed by western blot analysis in both infectious EBs and human cells infected with *C. pneumoniae*. Microscopical analysis showed that Cpn0572 is translocated 10 minutes after infection underneath the attached EBs into the human cells.

Collectively, our study suggests a model showing the possible dual function of Cpn0572 in stabilizing and nucleating actin *in vivo* during infection. Further experiments which are currently being carried out in yeast and human cells will advance our understanding of the role of Cpn0572 in *C. pneumoniae* infection.

1. INTRODUCTION

*Chlamydia*e are obligate intracellular gram-negative bacteria. They infect a wide spectrum of hosts and cause a variety of diseases. To date, only three *Chlamydia* species are known to infect humans that are *Chlamydia trachomatis*, *Chlamydia psittaci* and *Chlamydia pneumoniae*. *Chlamydia* cannot grow freely in the environment, therefore they have to gain access to a host cell where they can grow and replicate. To do so, *Chlamydiae* species share a unique developmental cycle during which they perform multiple interactions with the host cell to establish its niche for growth and replication.

1.1. Taxonomy of *Chlamydia*

The taxonomic classification of *Chlamydia* has been initially based on phenotypic, morphological and genetic criteria. *Chlamydia* is a genus of bacteria in the family *Chlamydiaceae*, order *Chlamydiales*, class and phylum *Chlamydiae*. In the past, the known species in this genus were *Chlamydia trachomatis*, *Chlamydia pneumoniae*, *Chlamydia psittaci* and *Chlamydia pecorum*. 10 years ago, a revised classification was suggested which is based on an analysis of the ribosomal operon of *Chlamydia* and *Chlamydia*-like organisms. The new classification increased the number of species in the *Chlamydiaceae* family to nine and grouped these species into two genera: *Chlamydia* (3 species: *C. trachomatis*, *C. suis* and *C. muridarum*) and *Chlamydophila* (6 species: *Ch. abortus*, *Ch. psittaci*, *Ch. felis*, *Ch. caviae*, *Ch. pecorum* and *Ch. pneumoniae*) . This new classification considered also three novel families within the order *Chlamydiales* including *Parachlamydiaceae*, *Simkaniaceae* and *Waddliaceae* (Everett, Bush et al. 1999) However, the taxonomic separation of the genus based on ribosomal sequences is neither consistent with the natural history of the organism nor widely used by the *Chlamydia* research community 10 years after its introduction. Recently, a new phylogenetic analysis confirms and strengthens the close and linked evolutionary relationship among *Chlamydia* (Stephens, Myers et al. 2009). Thus, it is proposed to reunite the *Chlamydiaceae* into a single genus, *Chlamydia* (Figure 1-1).

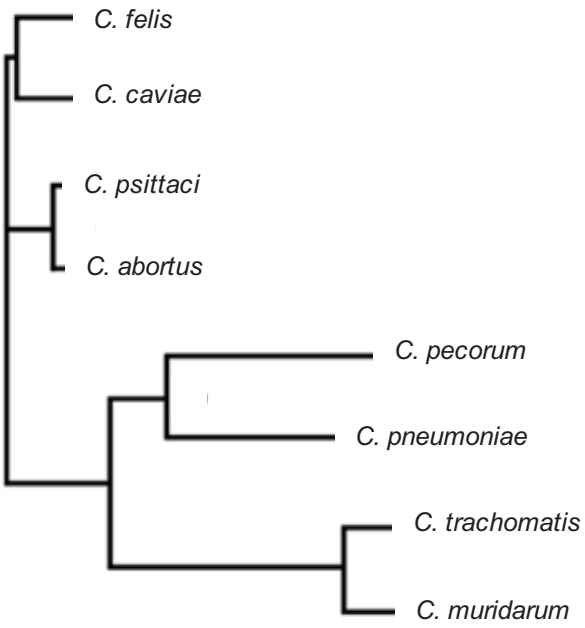

Figure 1-1: Diagram of the new classification of the genus *Chlamydia* (taken from Stephens et al., 2009)

1.2. *Chlamydiae* are important human pathogens

1.2.1. *C. trachomatis*

C. trachomatis strains (about 18 distinct serotypes) are the leading cause for a wide spectrum of acute and chronic diseases. For example, the *C. trachomatis* serovars A to C cause conjunctivitis and trachoma (a common cause of preventable blindness worldwide). *C. trachomatis* is responsible for about 15% of all cases of blindness and it has been estimated that about 600 million people live in areas where trachoma is endemic (Thylefors 1995; Thylefors 1998). The serovars D to K are the etiological agent of sexually transmitted genital and neonatal infections and an infection with these strains increases the risk of infertility (Land, Gijsen et al. 2002). The serovars L1,L2 and L3 are the leading cause of lymphogranuloma venereum. However, the infection with serovar L is generally considered to be rare. Recent reports found that the majority of serovar L infected people are HIV co-infected (Michael 2006). In USA, young adults aged 18-26 years have a prevalence of 4%. Women are more infected than men (Miller, Ford et al. 2004).

1.2.2. *C. psittaci*

The second *Chlamydia* species capable of a human infection is *C. psittaci* which causes psittacosis or ornithosis in human, after exposition to infected birds. Infection with *C. psittaci* is rare, only 50-100 cases are reported in USA every year, however anyone exposed to an infected bird is at the risk for infection and the infection results in a severe pneumonia. Despite antibiotic treatment, the mortality rate due to the infection is about 5%

(Roca 2007).

1.2.3. *C. pneumoniae*

The third species of *Chlamydia* that infects humans is *C. pneumoniae*. It has been estimated that half of the global adult population shows serological evidence of past infection with *C. pneumoniae* and it reaches 75% in the elderly population. *C. pneumoniae* causes human respiratory diseases. It is responsible for approximately 10% of community acquired pneumonia and for 5% of pharyngitis, bronchitis, asthma and sinusitis cases (Kuo, Grayston et al. 1995). Additionally, there is an increasing evidence for the association of *C. pneumoniae* infection with the risk of developing atherosclerosis, cardiovascular diseases (the leading cause of morbidity in the western world) and alzheimer's disease (Balin, Gerard et al. 1998; Sriram, Mitchell et al. 1998; Leinonen and Saikku 2000; Belland, Ouellette et al. 2004). However, a causal link has not been established yet. The mortality rate due to a *C. pneumoniae* infection is about 9%. A co-infection with other bacteria or the presence of other severe diseases increases the mortality risk (Oba and Salzman 2007).

1.3. *Chlamydial* developmental cycle

Chlamydia cannot grow and reproduce freely in nature, thus it needs a host cell as a niche to accomplish this task. *Chlamydia* have a developmental cycle (Figure 1-2) characterized by the small ~0.3 μm metabolically inactive and infectious form termed Elementary Body (EB) and the bigger ~1 μm metabolically active, but not infectious form termed Reticulate Body (RB) (Stephens 1999). To achieve this cycle EBs, like other pathogenic gram-negative bacteria, expose adhesins on their surface that bind certain receptors on the host cell surface. Indeed, initial attachment is mediated by electrostatic interactions to heparan sulfate moieties on the host cell, followed by irreversible binding to an unknown secondary receptor. Thus glycosaminoglycans (GAG) found on the surface of most nucleated cells are required for the initial phase of the *Chlamydia* EB attachment process (Zhang and Stephens 1992; Su, Raymond et al. 1996; Davis and Wyrick 1997; Wuppermann, Hegemann et al. 2001). For the murine (MoPn) biovar, it has been proposed that adhesion to mammalian cells can be mediated by the major outer membrane protein (MOMP) binding to host cell heparan sulphate-containing proteoglycans (Su, Raymond et al. 1996). Recently, the *Chlamydia* outer membrane complex protein B (OmcB) was characterized as an adhesin for *C. trachomatis* and *C. pneumoniae* that also binds the host surface GAG. It has been suggested that OmcB binding GAG stabilizes the bacterium on the host cell surface enabling more specific interactions between unidentified adhesins and host receptors (Moelleken and Hegemann 2008). Furthermore,

a recent study characterizing the *C. pneumoniae* Pmp21 surface protein showed that this protein is an adhesin (Schmidt and Hegemann, not published). However, our group has identified several additional potential adhesins and is currently analyzing them.

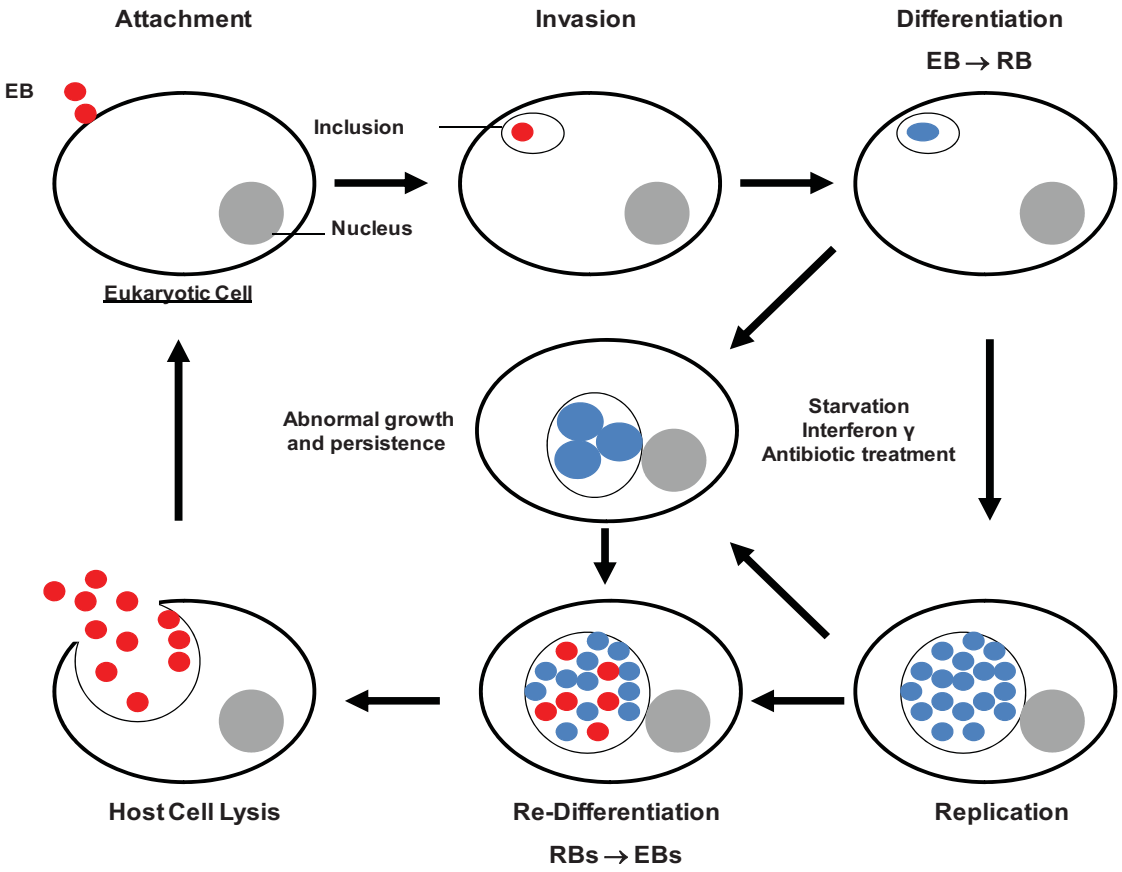

Figure 1-2: A schematic representation of the chlamydial developmental cycle under ideal nutritional conditions or during starvation or antibiotic treatment. The events in the developmental cycle are described in the text. EBs in red, RBs in blue, inclusion and nucleus are indicated.

After EB attachment to the host cell membrane, bound EBs enter the host cell via a process, that has been termed parasite-mediated endocytosis, and stay in a membrane-bound vacuole termed inclusion (Byrne 1978). However, *Chlamydia* have been shown to enter host cells via different mechanisms including clathrin-mediated endocytosis, non-clathrin-mediated endocytosis, actin-dependent phagocytosis and actin-independent pinocytosis (Hodinka and Wyrick 1986; Hodinka, Davis et al. 1988; Prain and Pearce 1989; Wyrick, Choong et al. 1989; Schramm and Wyrick 1995; Escalante-Ochoa, Ducatelle et al. 2000). Therefore, *Chlamydia* probably have evolved multiple mechanisms of entry to guarantee their uptake. So far, no single mechanism for chlamydial entry into the host cells has been identified. Moreover, an additional entry mechanism has been implicated, a lipid raft-mediated uptake, for *C. trachomatis* serovar L2 (Jutras, Abrami et al. 2003). Lipid rafts are microdomains in the cell membranes which contain cholesterol, glycolipids, and sphingomyelin. It is known that they contain many signaling molecules

(Ohkubo and Nakahata 2007). However, further in-depth experiments indicated that pathways that involve lipid rafts are not required for the uptake and development of all *C. trachomatis* serovars tested (Gabel, Elwell et al. 2004).

Like for other pathogenic bacteria, several reports showed that *Chlamydia* entry is associated with the activation of host signaling pathways, including Phosphoinositol 3-kinase (PI3K), Mitogen Activated Protein Kinase (MAPK), as well as the Rho family of GTPases. However, the entry of different chlamydial species is associated with or requires different signaling pathways to be activated. For example, the entry of *C. pneumoniae, C. caviae*, and *C. trachomatis* is associated with the activation of PI3K and the inactivation of PI3K abolishes the uptake of both *C. pneumoniae* and *C. caviae* (Coombes and Mahony 2002). In contrast, the uptake of *C. trachomatis* is not affected by inactivation of PI3K (Carabeo, Grieshaber et al. 2002). Furthermore, both the *C. pneumoniae* and the *C. trachomatis* infection induce the host cell ERK1/2 MAPK pathway. Interestingly, inhibition of ERK1/2 MAPK results in inhibition of *C. pneumoniae* entry. This has been not tested for *C. trachomatis* (Coombes, Johnson et al. 2002; Su, McClarty et al. 2004). In addition to these pathways, the Rho family of GTPases, Cdc42, Rac, and Rho also seems to play a role in *Chlamydia* entry. Cdc42 is required only for *C. caviae*. Rac is activated at the site of *C. caviae* and *C. trachomatis* entry and is required for the entry of these species, but it is not clear if activation of Rac is required for actin recruitment (Carabeo, Grieshaber et al. 2004; Subtil and Dautry-Varsat 2004). The role of specific Rho GTPases has not been investigated in *C. pneumoniae* infected cells. However, general inhibition of Rho GTPases results in inhibition of *C. pneumoniae* entry (Coombes and Mahony 2002). Interestingly, all of these pathways have been shown to also regulate actin dynamics and organization within the eukaryotic cell (Tapon and Hall 1997). Thus, actin dynamics and rearrangements might be relevant for *Chlamydia* entry.

The role of actin has been directly addressed by Carabeo and coworkers (2004) who investigated the mechanism of *C. trachomatis* entry and reported that *C. trachomatis* entry is dependent on a dynamic actin remodeling process forming a pedestal-like structure. It has been also shown that the infection of other chlamydial strains and species such as the infection of *C. trachomatis* (L2 and D), *C. caviae* and *C. pneumoniae* is strongly reduced, but not completely inhibited, when the host actin is disrupted by the actin destabilizing drug cytochalasin D (Ward and Murray 1984; Prain and Pearce 1989; Schramm and Wyrick 1995; Boleti, Benmerah et al. 1999; Escalante-Ochoa, Ducatelle et al. 2000; Coombes and Mahony 2002)

Modulation of the host actin cytoskeleton by pathogens is not only achieved by modulating host signaling pathways. Many gram-negative pathogenic bacteria deliver their effector proteins into the host cell to trigger and modulate host cell mechanisms, including actin

rearrangements directly or indirectly. The Type three secretion system (TIIISS) is the most commonly mechanism used by gram-negative pathogenic bacteria to allow the efficient delivery of effector proteins into the host cell cytoplasm through the use of a syringe-like injectisome (Hueck 1998; Buttner and Bonas 2002). *Chlamydia* encode many proteins with homology to proteins known to be involved in the assembly of TIIISS in other pathogens (Hsia, Pannekoek et al. 1997; Stephens, Kalman et al. 1998; Read, Brunham et al. 2000; Peters, Wilson et al. 2007). In this context, recent studies revealed that the chlamydial translocated actin recruiting protein (Tarp) is implicated in actin rearrangement directly after *C. trachomatis* L2 attachment (Clifton, Fields et al. 2004; Clifton, Dooley et al. 2005; Jewett, Fischer et al. 2006; Elwell, Ceesay et al. 2008; Jewett, Dooley et al. 2008). Interestingly, Tarp encoding genes are found in all sequenced *Chlamydia* genomes. Therefore, it might be that actin modulation by Tarp is a genus-wide property. However, the actin rearrangements during the chlamydial infection are probably not due to Tarp alone. Other pathogens, for example *Salmonella*, secrete at least 6 proteins by its type III secretion system to modulate the host actin and trigger their entry (Cain, Hayward et al. 2008).

Pathogens may also use other strategies, e.g. via the pathogen ligand and host receptor interaction, to induce actin rearrangements and subsequently their uptake (Heise and Dersch 2006). Thus, *Chlamydia* probably secretes or exposes several proteins to trigger its entry by interfering with host signaling pathways and modulating the host actin cytoskeleton. Correspondingly, *C. pneumoniae* infection, but not adhesion could be abrogated in HEp-2 cells pre-incubated with recombinant GroEL1 protein, a *Chlamydia* protein exposed on the surface of EBs and RBs, (Wuppermann, Molleken et al. 2008) suggesting that extra cellular GroEL1 has a role in triggering signaling pathways that are necessary for *Chlamydia* entry. In addition to its adhesion property, Pmp21 is likely implicated in the EBs invasion (Schmidt and Hegemann, not published). However, the host receptor for both GroEL1 and Pmp21 and the processes involved are still unknown.

Upon uptake, EBs begin to differentiate into RBs and replicate by binary fission within the inclusion which is formed by the invagination of the plasma membrane. Soon after uptake, a set of genes is expressed including the inclusion membrane proteins (Incs), which localize to the inclusion membrane and participate in the biogenesis of the nascent inclusion (Rockey, Scidmore et al. 2002). As the infection cycle progresses, the inclusion evolves a variety of properties and interacts with different cellular components through the inclusion membrane. In the *C. trachomatis* infection, inclusions undergo homotypic fusions in a process depending on the inclusion membrane protein IncA. Although *C. pneumoniae* has an IncA protein, *C. pneumoniae* are much less fusogenic (Suchland, Rockey et al. 2000; Wolf, Fischer et al. 2000; Rockey, Scidmore et al. 2002).

In order to gain access to host cell macromolecules, chlamydial inclusions intercept host-derived vesicles via recruitment of Rab GTPases (which regulate host cell fusion) and SNARE molecules (Proteins to mediate fusion of cellular transport vesicle with the cell membrane or lysosome) through the interaction with Inc proteins (Rzomp, Scholtes et al. 2003; Rzomp, Moorhead et al. 2006; Cortes, Rzomp et al. 2007; Delevoye, Nilges et al. 2008). The inclusion expands by receiving components from both the host cell and RBs themselves. For instance, it has been shown that sphingomyelin and cholesterol are cotransported from the Golgi and fuse with the inclusion membrane. In *C. trachomatis*, but not in *C. pneumoniae*, the inclusion uses the host microtubule system to migrate to the centrosome near the nucleus and Golgi (Carabeo, Mead et al. 2003; Grieshaber, Grieshaber et al. 2003).

The *C. pneumoniae* CopN is another TIIIS protein which is required to support the intracellular growth of *C. pneumoniae* and plays an unknown but essential role in infection. Transfected CopN disrupts the spindle apparatus of mammalian cells (Huang, Lesser et al. 2008).

It should be noted that chlamydial effector proteins can also access the cytoplasm of infected cells via TIIISS-independent mechanisms. For example, the chlamydial protease-like activity factor (CPAF) and CT466 have a type 2 secretion signal and are secreted to the inclusion lumen before translocation into the cytoplasm of infected cells. These proteins disable the innate immunity response, block NF-$_k\beta$ signaling and degrade factors important in immunity (Zhong, Fan et al. 2001; Lad, Li et al. 2007; Rupp, Gieffers et al. 2007).

After 9-11 bacterial cell divisions, most of the cytoplasmic space of the host cell is occupied by the inclusion. The RBs differentiate back to EBs that are released from the host cell. The mechanism of chlamydial exit from infected cells is complex with at least two pathways described, cell lysis by the activation of cysteine proteases and by extrusion of the inclusion into the extracellular media by an actin-dependent and myosine-dependent mechanism. The released EBs start to infect new host cells. The developmental cycle lasts from 32-72 h, depending on the *Chlamydia* species and growth conditions (Stephens 1999; Hybiske and Stephens 2007).

1.4. The actin cytoskeleton dynamics are necessary for pathogen entry

The actin cytoskeleton is one of the most dynamic cellular machineries and is important for a variety of cellular processes including migration, polarized growth, division and internalization of receptors, lipids, pathogens and other cargo through the plasma membrane. The actin cytoskeleton is an integral part of the cell cortex and there is convincing evidence that actin filaments play a direct role in the internalization of

extracellular particles including pathogens in a process initiated by pathogen effector proteins (Zhou and Galan 2001; Cossart, Pizarro-Cerda et al. 2003). This section describes how actin dynamics take place and are regulated by the actin related proteins and signaling pathways before the cross-talk between host actin and pathogen effector proteins is discussed.

1.4.1. The actin protein

The actin monomer is a highly conserved 42-44 KDa protein found in all eukaryotic cells, from yeast to mammalian cells. Actin proteins from different eukaryotic cells are very similar with more than 80% identity and about 90% homology in the amino acid sequences. Cellular actin exists in two forms (Figure1-3). The first form is a globular monomeric actin (G-actin) and linking of these monomers to each other results in the other form of actin, filamentous actin (F-actin), which are polar structures as all actin monomers are facing into the same direction (Holmes, Popp et al. 1990). G-actin consists of two major domains that are subdivided into four subdomains (S1-S4), (Kabsch, Mannherz et al. 1990). Every actin monomer has a nucleotide (ATP or ADP) binding site in the cleft between S2 and S4. In the same cleft there is also a divalent cation, either Ca^{2+} or Mg^{2+} (Kabsch and Holmes 1995). On the opposite side of the protein, between S1 and S3, locates a small cleft known to be a target for most acting-binding proteins (ABPs) and it is necessary for actin-actin interaction within the actin filament (Dominguez 2004). Thus, these characteristics of actin proteins make actin a flexible protein with the ability to change its conformation from a closed to a more open one depending on the status of nucleotides, the nature of the cation, the interacting ABPs and the degree of oligomerization (Moraczewska, Wawro et al. 1999; Schuler 2001).

F-actin is a double helical strand structure with a fast growing barbed-end (also called + end) and a slow growing pointed-end (also called – end). The barbed-end is favored for actin polymerization and actin monomers are preferentially added to this end in their ATP form (Wegner 1976). After incorporation into the filaments, ATP is hydrolyzed to ADP and as such the monomers become less stable in the filaments, leading in turn to actin depolymerization at the pointed end. This process is called actin treadmilling (Figure 1-4).

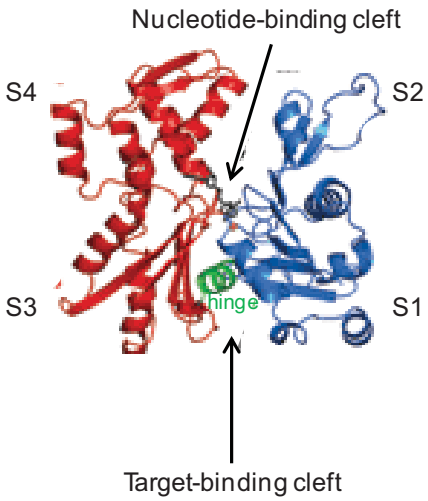

Figure 1-3: Ribbon representation illustrating the "conventional" view of G-actin. Two diametrically opposed clefts, the nucleotide cleft and the target-binding cleft, effectively separate the actin molecule into two large domains. The α-helix between S1 and S3, shown in green, serves as a hinge for inter-domain motions (marked hinge in green). This α-helix lines the target-binding cleft. (taken from (Dominguez 2004).

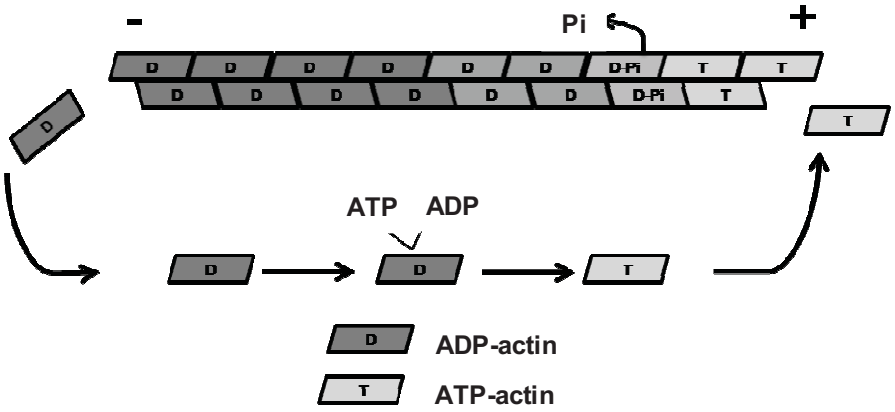

Figure (1-4): Schematic representation of actin treadmilling. Actin filaments grow in a polarized fashion by the addition of ATP–actin monomers to the 'barbed' (+) end. With time, ATP is hydrolyzed (the intermediate phase D-Pi) and phosphate released to yield ADP–actin filament. ADP-actin disassembles by the removal of subunits from the polymer's slow-growing 'pointed' (-) end. The ADP moiety is then exchanged for ATP to ready actin monomers for another round of polymerization (modified after (Carlier, Ressad et al. 1999; Littlefield and Fowler 2002).

F-actin can be assembled spontaneously *in vitro* under physiological ion conditions (Figure 1-5). Actin polymerization can be initiated, in *vitro*, by the addition of a physiological buffer containing magnesium ions to actin monomers. However, spontaneous actin polymerization requires the formation of a trimeric-actin nucleus in a process called nucleation. Spontaneous nucleation is kinetically unfavorable and is the rate-limiting step in polymerization. The lag phase represents the time required for actin nucleation. In the presence of actin nucleation factors (e.g. Arp2/3 complex, formin, and spire), the lag phase becomes shorter and thus actin assembly is enhanced. The rapid

polymerization phase represents the time during which short filaments elongate. Steady state represents an equilibrium between growth of the filaments due to actin monomer addition and shortening of the filaments due to loss of actin monomer (Cooper and Pollard 1982; Goley and Welch 2006; Gunst and Zhang 2008). However, the process can be hundred times faster *in vivo* due to the incorporation of a large number of ABPs in this process. *In vivo*, the differences in actin association at the barbed end and disassociation at the pointed end cause the actin pool never to reach an equilibrium between G-actin and F-actin thus resulting in simultaneous growing and shrinking at the barbed and pointed ends, respectively (Chen, Bernstein et al. 2000).

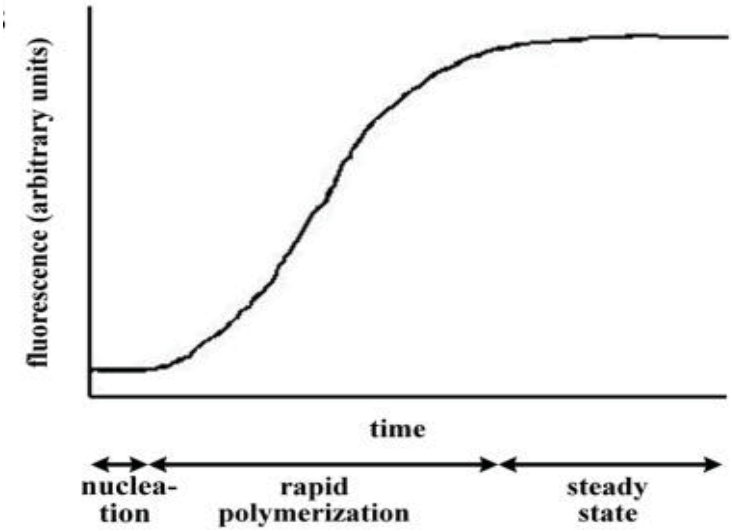

Figure 1-5: Graphical representation of actin filament assembly dynamics *in vitro*. An idealized curve from a pyrene actin assay is shown.
Note: Actin can be modified to contain covalently liked pyrene (a fluorescent dye) at the cysteine 374 residue. The fluorescence of polymerized pyrene-labeled actin is 7-10 times higher than that of monomers (taken from (Cooper and Pollard 1982) and http://www.cytoskeleton.com).

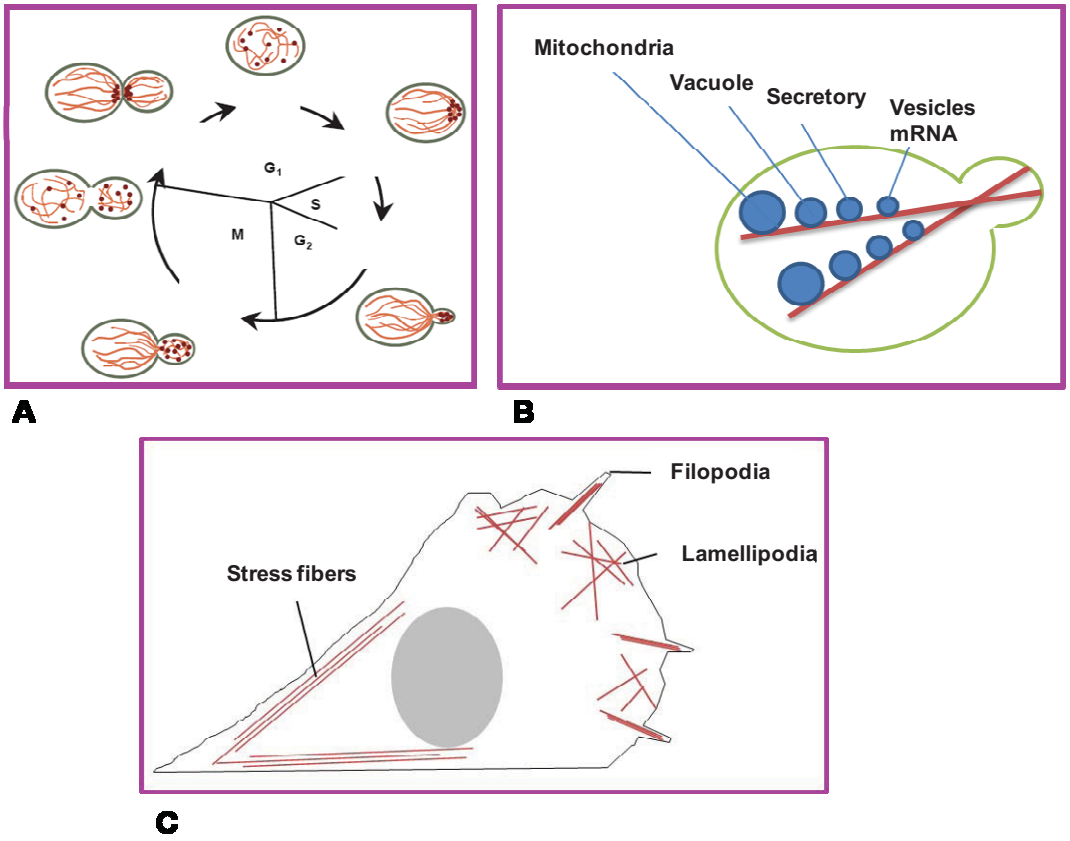

Figure 1-6: Schematic representation of the actin cytoskeleton in eukaryotic cells.
A, the actin cytoskeleton in the budding yeast is highly dynamic throughout the cell cycle. Cortical actin patches are represented by dots and cytoplasmic actin cables are represented by lines. During late G_1-, S- and G_2 phases, actin patches are polarized to the growing bud and actin cables are oriented in this direction. In M-phase, actin patches and cables are symmetrically distributed between mother and bud. After M-phase, actin patches and cables localize to and are oriented toward the bud neck, respectively.
B, yeast actin cables are tracks for movement of cargo from the mother cell to the growing bud.
C, the different organizational forms of actin filaments in mammalian cells consisting lamellipodium, filopodium; stress fibers; and a loose actin network throughout the cell.

1.4.2. Actin dynamics *in vivo*

Actin dynamics is a conserved process among eukaryotes. However, different cells need different structures of the actin cytoskeleton. In *S. cerevisiae*, the actin protein is coded by a single gene, *ACT1*. The actin cytoskeleton in yeast undergoes a highly dynamic process during the cell cycle and consists of two distinct morphological structures; patches and cables (Figure 1-6-A). Cortical patches are biochemically complex and share many of the same components as cortical actin structures in vertebrates. They mediate endocytosis and exocytosis (Moseley and Goode 2006), while actin cables are necessary for polarized growth and serve as tracks for carrying cargo (Figure 1-6-B) (Bretscher 2003). In mammalian cells, F-actin can be assembled further into a wide variety of higher-ordered structures such as stress fibers, structures forming the lamellipodia, filopodia, …etc (Figure 1-6-C) where each of them performs a specific function. However, actin assembly and the proteins and signaling pathways involved are highly conserved in eukaryotic cells

(Chhabra and Higgs 2007).

1.4.2.1. The role of ABPs in regulating actin assembly

Actin assembly is regulated by many other proteins particularly those binding G-actin or F-actin directly. The role of these proteins in actin assembly was nicely reviewed by Pollard (2003) as shown in Figure 1-7. Briefly, actin assembly starts by the initiation of actin polymerization by the Arp2/3 complex which nucleates actin filaments and results in the formation of dense F-actin meshworks. The Arp2/3 complex is activated by WASP as a response to extracellular cues. Once the actin nuclei are available, formin efficiently polymerizes and elongates linear actin filaments at the growing barbed end. Eventually, some proteins such as the barbed capping proteins CapG and Cap2 terminate actin polymerization. By contrast, the capping protein inhibitors such as ENA, VSAP and profilin (which catalyzes the nucleotide exchange that recycles ADP-actin to ATP-actin) promote elongation even in the presence of actin capping proteins. The branching of actin filaments is formed in a process initiated by the Arp2/3 complex. The actin filaments are cross linked and bundled to form actin cables in a process enhanced by actin cross linking proteins such as α-actinins, fimbrins, coronin, …etc (reviewed in (Rafelski and Theriot 2004; Nicholson-Dykstra, Higgs et al. 2005).

To reproduce a continues pool of G-actin, actin filaments disassemble into monomers. Two major actin binding proteins accomplish this task. The first one is the actin severing protein gelsolin, which disrupts the interactions between actin subunits in filaments and tightly caps the barbed end of the severed filaments. Hint, gelsolin is not found in yeast. The second is cofilin (a member of the actin-depolymerizing factors and cofilins “ADF/cofilins” proteins family) which also sever but do not cap the barbed ends of actin filaments. Barbed ends generated by cofilin either serve as initiation sites for new elongation or become capped by the actin interacting protein 1 (Aip1) and subsequently sequester this short filaments into monomers (Okada, Ravi et al. 2006). In higher eukaryotes, cofilin is phosphorylated and regulated by LIM Kinase. The activity of actin depolymerization can be studied in the presence of the actin-depolymerizing drug Latrunculin A (Lat-A) (Morton, Ayscough et al. 2000; Yarmola, Somasundaram et al. 2000; Okada, Ravi et al. 2006).

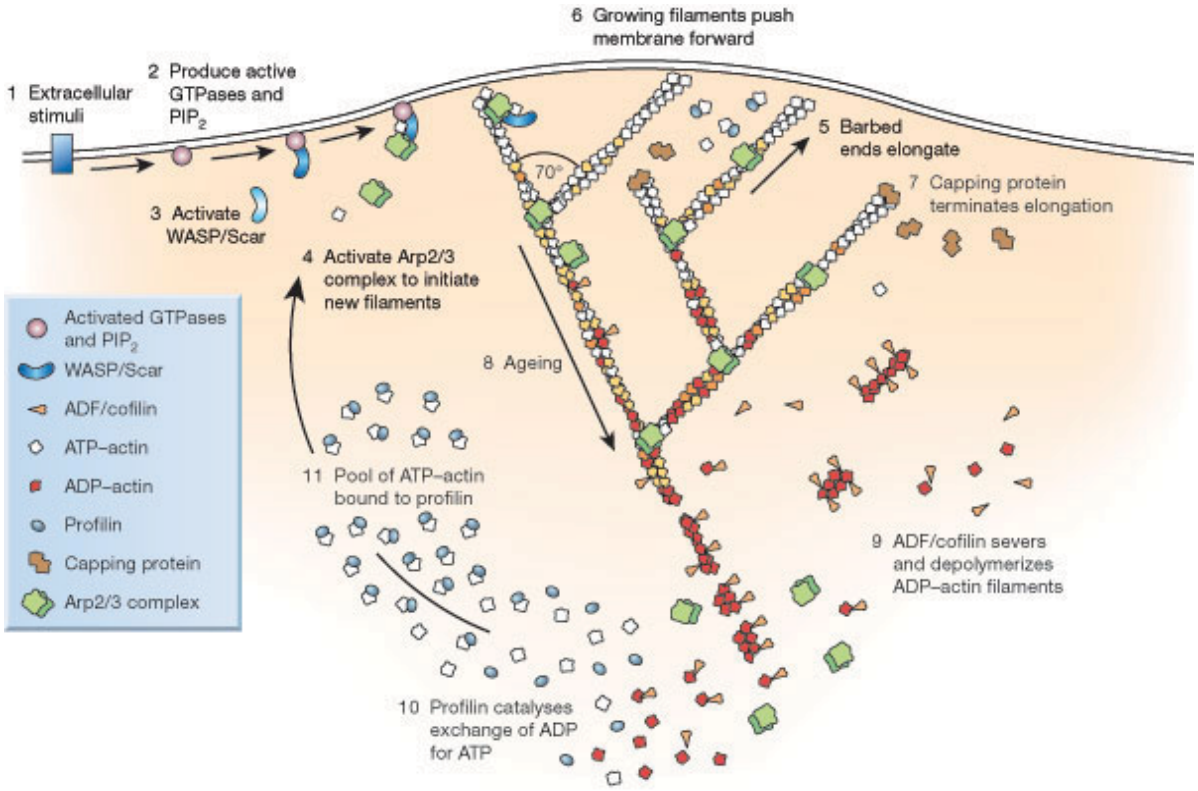

Figure 1-7: The dendritic nucleation model. External cues (step 1) activate signaling pathways that lead to the activation of GTPases (2). These then activate Wiskott–Aldrich syndrome protein (WASP) and related proteins (3), which in turn activate the Arp2/3 complex. The Arp2/3 complex initiates a new filament as a branch on the side of an existing filament (4). Each new filament grows rapidly (5), fed by a high concentration of profilin-bound actin stored in the cytoplasm, and this pushes the plasma membrane forward (6). Capping protein binds to the growing ends, terminating elongation (7). ADF/cofilin proteins family then severs and depolymerizes the ADP filaments, mainly in the 'older' regions of the filaments (8, 9). Profilin re-enters the cycle at this point, promoting dissociation of ADP and binding of ATP to dissociated actin subunits (10). ATP–actin bound by profilin, refills the pool of subunits available for assembly (11) (taken from (Pollard 2003)).

1.4.2.2. The role of signalling pathways in regulating actin assembly

Regulation of the actin cytoskeleton in response to cellular cues is a complex event involving numerous proteins and signaling pathways that allow the cell to respond to different signals. One such pathway involves the Rho family of GTPases including Cdc42, RhoA and Rac1. These small GTPases cycle between GTP-bound active and GDP-bound inactive states. The switch between the two forms is regulated by guanine nucleotide exchange factors (GEFs), which promote GDP→GTP exchange, whereas GTPase activating proteins (GAPs) stimulate GTPases activity and subsequently activate GTP→GDP. The Rho family of GTPases influences the actin cytoskeleton through different and complex signaling cascades resulting in different actin structures. For example, Cdc42 controls formation of filopodia, Rho induces formation of stress fibers, while Rac1 regulates formation of lamellipodia in mammalian cells. Cdc42 also influences actin by signaling to activate N-WASP which in turn induces Arp2/3 complex-directed actin nucleation and branching of actin filaments. Furthermore, Rho induces actin assembly by

activation of formin mDia. Cdc42, Rho and Rac1 also regulate actin dynamics through activation of the LIM kinase which phosphorylates ADF/Cofilin (reviewed in (Bishop and Hall 2000).

Another signaling molecule that affects actin assembly is Phosphatidylinositol (4,5)-bisphosphate (PtdIns(4,5)P2, also called PI(4,5)P2 or PIP2), which is a minor phospholipid component of cell membranes where it is an important substrate for a number of signaling proteins (Strachan T. and Read AP. 1999). Modulation of levels of PtdIns(4,5)P2 affects cortical actin organization, membrane ruffling, and endocytosis. PtdIns(4,5)P2 regulates many of ABPs (Figure 1-8). For example, the binding of actin-bound gelsolin to the lipid bilayers within the cellular membrane containing PIPs results in conformational changes in the gelsolin. Conformational change induces dissociation of gelsolin from actin and allows actin filament assembly at the barbed end (Liepina, Czaplewski et al. 2003).

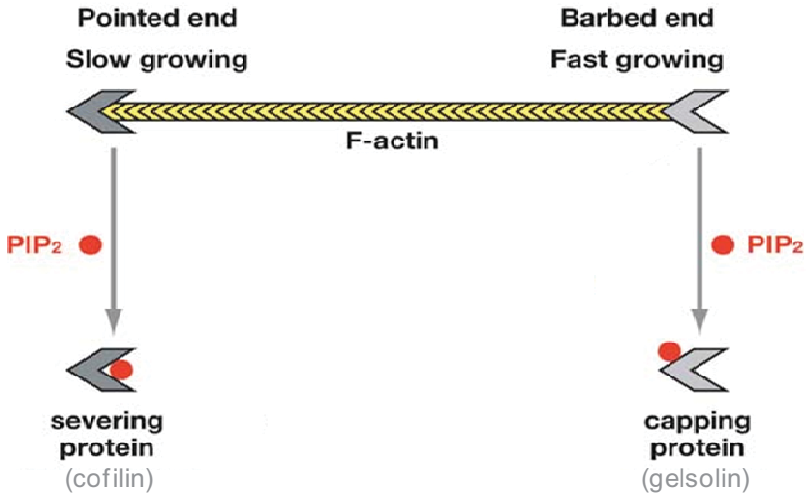

Figure 1-8: Regulation of actin-associated proteins involved in controlling actin assembly by PIP2. Gelsolin severs and caps the severed actin filaments at the barbed end. ADF/Cofilin severs and depolymerizes actin at the pointed end. PIP2 dissociates gelsolin and cofilin from actin and allows actin elongation (modified after Niggli 2005).

In vitro studies showed that, comparable to gelsolin, yeast cofilin binds PI-4,5-P_2 resulting in inhibition of its activity. In yeast, replacement of wild-type cofilin by cofilin with a mutation that disrupts the interaction with PIPs but is not involved in the interaction with actin results in abnormal actin organization, but the cells are viable, indicating that this lipid interaction is not crucial for cell survival, at least in yeast (Ojala, Paavilainen et al. 2001).

1.4.3. Bacterial strategies to manipulate the actin cytoskeleton of the host cell

Pathogens use several strategies to manipulate the host actin cytoskeleton. The first strategy is via the interaction of bacterial adhesins with host receptors. Binding of a bacterial adhesin to an extracellular domain of a host receptor results in receptor

activation and subsequently initiates signaling cascades and actin rearrangements. Usually, this type of host-pathogen interaction results in actin dependent bacterial uptake. For instance, entry of *Listeria monocytogenes* into non-phagocytic cells is mediated by at least two surface proteins, internalin A (InlA) and internalin B (InlB). The host cell surface receptor for InlA is the human E-cadherin which is required for optimal intercellular adherence and adherence junction formation. Actin remodeling resulting from binding of InlA to E-cadherin is promoted by α- and β-catenins, molecules that normally link the receptor to the cytoskeleton fibers present in the adherence junction. Additionally, *Listeria* exploits other host signaling pathways by means of InlB. InlB interacts with at least three host surface molecules: the glycoprotein gC1qR (receptor for C1q, the first component of the complement cascade); the tyrosine-kinase receptor Met, also known as hepatocyte growth factor receptor (HGF-R); and glycosaminoglycans (GAGs). Interaction of InlB with Met (HGF-R) mimics the physiological stimulation of the receptor, leading to a cascade of events, including activation of Phosphoinositide 3-Kinase (PI-3-kinase), release of phosphatidylinositol- 3,4,5 triphosphate (PIP3), and activation of Rho GTPases, that cause actin rearrangements (Cossart, Pizarro-Cerda et al. 2003)

Another strategy to modulate actin is to deliver pathogen virulence proteins directly into host cells to trigger actin rearrangements. The type III secretion system (TIIISS) is the most common secretion system used by bacterial pathogens in which bacteria inject their effectors across both the bacterial and the host cell membrane (Lee 1997). For example, *Salmonella* delivers SigD (also called SopE) via TIIISS into host, cells where it induces rapid disappearance of phosphatidyl-inositol-4,5-bisphosphate (PtdIns (4,5)P2 from invaginating regions of the cytoplasmic membrane and thus subsequently losing the cortical actin cytoskeleton from the membrane. Other *Salmonella* TIIISS proteins (SopE and SopE2) act as guanine-nucleotide-exchange factors (GEFs) that activate either Cdc42 and Rac1 (SopE) or Cdc42 alone (SopE2) resulting in a dramatic rearrangement of actin, which is favored by the other *Salmonella* TIIISS proteins SipC and SipA. SipC nucleates actin polymerization (Hayward and Koronakis 1999), while SipA stabilizes F-actin and suppresses actin depolymerization induced by the host proteins cofilin and gelsolin (Zhou, Mooseker et al. 1999; McGhie, Hayward et al. 2004). Finally, *Salmonella* induces the recovery to the normal actin cytoskeleton via the secretion of SptP, a TIIISS protein that returns Cdc42 and Rac1 to the non-activated form (Zhou and Galan 2001).

Shigella, similar to *Salmonella*, targets GTPases of the Rho subfamily. Functional studies have established that Cdc42 and Rac are required for bacterial uptake. This observation is consistent with the formation of filopodia and lamellipodia, triggered by activated Cdc42 and Rac and Rho, respectively, in the membrane ruffling area containing the invading *Shigella.* This area has also been shown to be depleted of PtdIns(4,5)P2. Bacterial IpaC is

required for activation of these three GTPases, whereas another TIIISS secreted protein, IpaA, down-regulates the extension of the membrane ruffling by binding vinculin. The IpaA-vinculin complex then acts as an actin-depolymerization device, transforming the IpaC-induced extensions into a structure that is productive for bacterial uptake (Tran Van Nhieu, Bourdet-Sicard et al. 2000).

Actin rearrangements are also reported at the site of *Chlamydia* entry and this is at least in part due to the translocated actin-recruiting protein (Tarp) which is likely translocated into the host cell by the TIIISS and tyrosine phosphorylated once exposed to the host cytoplasm (Clifton, Fields et al. 2004).

Recently, Kumar and Valdivia (2008) reported that the *C. trachomatis* inclusion is encased in a scaffold of host cytoskeletal structures made up of a network of F-actin and intermediate filaments (IFs) that act cooperatively to stabilize the inclusion. Formation of F-actin at the inclusion is dependent on RhoA, and its disruption led to the disassembly of IFs, loss of inclusion integrity, and leakage of the inclusion content into the host cytoplasm. The authors proposed that *Chlamydia* has co-opted the function of F-actin and IFs to stabilize the inclusion with a dynamic, structural scaffold while minimizing the exposure of inclusion contents to cytoplasmic innate immune-surveillance pathways. However, the *Chlamydia* proteins triggering the encasing of the inclusion with F-actin and IF are still unknown.

1.5. The *C. trachomatis* protein Tarp

The Tarp gene is found in all known *Chlamydia* species. Tarp was first isolated as a tyrosine phosphorylated protein recruited at the site of *C. trachomatis* entry when an actin like-pedestal is formed. It is likely secreted by TIIISS because it is exported in a *Yersinia* heterologous expression assay. Ectopic expression of Tarp in HeLa cells results in colocalization with and accumulation of actin structures. It is likely that Tarp phosphorylation plays a role in actin accumulation and remodeling via modulation of signaling pathways regulating the actin cytoskeleton (Clifton, Fields et al. 2004). Domain analysis revealed that the phosphorylation of Tarp is independent from its localization with and recruitment of actin. The N-terminal domain of Tarp contains several tyrosin-rich tandem repeats, the number of which differs between serovars. After translocation and exposition to the host cell cytosol, this region undergoes immediate phosphorylation by Src-family tyrosine kinases, a process that precedes actin recruitment (Clifton, Dooley et al. 2005; Jewett, Dooley et al. 2008). Recently, several tyrosine kinases have been shown to modify Tarp phosphorylation including p60-src, Yes, Fyn, Ab1, and Syk kinases. Therefore it is unclear by which kinase Tarp is phosphorylated during infection, however it is possible that Tarp serves as a substrate for multiple host cell kinases (Elwell, Ceesay et

al. 2008; Mehlitz, Banhart et al. 2008). Additionally, it has been found that the Rac-activating guanine nucleotide exchange factors (GEFs) Sos1 and Vav2 associate with crucial tyrosine residues within the Tarp repeat region in a phosphorylation-dependent manner. This initiates a signal transduction cascade activating Rac and the downstream effectors Abi-1 and WAVE2 that trigger Arp2/3 and thus actin remodeling (Lane, Mutchler et al. 2008).

However, Tarp phosphorylation is not essential for *C. trachomatis* entry (Jewett, Dooley et al. 2008). Additionally, Tarp orthologs from *C. muridarum*, *C. psittaci*, and *C. pneumoniae* lack the tandem repeats and do not become tyrosine phosphorylated (Clifton, Dooley et al. 2005). A comparison between the *C. trachomatis* Tarp and the *C. pneumoniae* homolog Cpn0572 is shown in Figure 1-9.

Surprisingly, *in vivo* accumulation of actin and *in vitro* actin nucleation activity by Tarp occurs in an Arp2/3 complex independent manner via two conserved domains within the central and the C-terminal regions. These comprise at least one actin binding helix with sequence similarity to the WH2 domains of WAVE2 capable of binding both G- and F-actin directly, and a proline rich domain that is required for nucleation of F-actin. A proline rich domain promotes Tarp oligomerization. It has been proposed that Tarp oligomerization brings multiple actin binding domains, and thus actin monomers, into close proximity for nucleation (Clifton, Dooley et al. 2005; Jewett, Fischer et al. 2006).

Interestingly, the central and C-terminal region of Tarp is highly conserved among Tarp orthologs. The lack of the tandem repeats in Tarp orthologs from other *Chlamydia* species suggests that they may perform a different function. However, only the *C. trachomatis* L2 Tarp has been analyzed thus far.

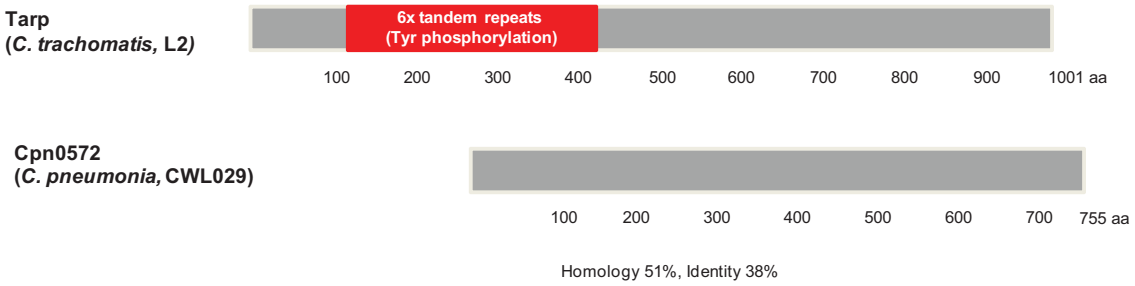

Figure 1-9: Comparison between Tarp (*C. trachomatis*, L2) and Cpn0572 (*C. pneumoniae*, CWL029). Both proteins share significant homology and identity. The tyrosine residues within the tandem repeats region (in red) get phosphorylated upon exposition to the host cytosol. Cpn0572 lacks these repeats and is not tyrosine phosphorylated (Clifton et al., 2005). A detailed comparison between both proteins is shown in the results part.

1.6. The yeast *Saccharomyces cerevisiae* is a powerful model system to study bacterial effector proteins

The unicellular bakers yeast *S. cerevisiae* has been extensively used to unravel and understand basic cellular and molecular processes of eukaryotic cells. For example, most of the fundamental cellular processes such as actin and microtubules dynamics, cell division, cell cycle regulation, vesicle transport, …etc were primarily identified or in depth characterized in yeast. The output of these efforts constitutes the basis of understanding these processes in higher eukaryotes. Indeed, many advantages were accounted to the yeast to accomplish this task. Yeast is genetically well defined: its genome was the first published eukaryotic genome sequence (Goffeau 1996). Furthermore, it is genetically tractable, easily transformed with DNA and undergoes homologous recombination with high precision, which allows an efficient realization of gene disruption, gene tagging, mutation or gene-dosage experiments. Yeast is also cheap and fast to cultivate, as it grows with a doubling time of approximately 90 minutes. Moreover, in contrast to higher eukaryotes that often possess several protein isoforms which complicate functional analysis of a protein, yeast is simple and usually harbors one form of most proteins only, for example, one actin gene (*ACT1*) and one cofilin gene (*COF1*). Therefore, yeast offers a great opportunity for studying the phenotypes of a mutant strain lacking a specific protein, thus revealing information concerning its function. Correspondingly, genome-wide collections of yeast mutation or deletion strains have been constructed and can be easily obtained. Indeed, these strains have greatly contributed to the rebirth of yeast as a powerful system to study genetic interactions and perform screenings. Recently, the yeast system has also been used to analyze bacterial effector proteins (reviewed in (Valdivia 2004).

Microbial pathogens manipulate host cells by delivering their effector proteins into the host cell to gain their own entry and survival. To accomplish this task, effector proteins target host cellular processes such as the cytoskeleton (including actin, microtubules, and intermediate filaments), cell division, vesicular transport, general metabolism, inhibition of endocytosis and phagocytosis, induction of either cytotoxicity or apoptosis and other processes (Hueck 1998). Interestingly, most of these fundamental cellular processes and the proteins involved are highly conserved among eukaryotes, from yeast to human. For example, the human and yeast actin proteins share high homology and identity (89% and 83% respectively).

The first study to analyze bacterial effector proteins in yeast was carried out by Lesser and Miller (2001). In this study, they first localized the *Salmonella* effector protein SipA (also called SspA) to the yeast actin cytoskeleton providing the first evidence that this protein interacts with actin in living cells. Further analysis confirmed that SipA altered cell

polarity and inhibited actin depolymerization confirming the proposed function of SipA in directing the formation of membrane ruffles.

Since then, several reports used the yeast model to analyze or screen for bacterial effector proteins. Here, we just summarize some of these studies in Table 1-1, while three recent studies are described in detail below.

Table 1-1: Summary of studies using the yeast model system to analyze bacterial effector proteins.

Pathogen	**Effector protein**	**Function in yeast cells**	**Function in human cells**	**Reference**
Yersinia pestis	YopE	Disrupts actin polymerization and arrests the cell cycle.	Arrests the cell division cycle. Disrupts actin stress fibers.	(Rosqvist, Forsberg et al. 1991; Lesser and Miller 2001)
Yersinia pestis	YopM	Accumulation in the nucleus, which depends on vesicular transport.	Accumulation in the nucleus, which depends on vesicular transport.	(Skrzypek, Myers-Morales et al. 2003)
Pseudomonas aeroginosa	ExoU	Possesses a lipase activity.	Not applicable (Toxic).	(Sato, Frank et al. 2003)
Eschrichea coli (EPEC)	EspD, EspG and Map	Depolymerize the actin cortical cytoskeleton.	Not tested.	(Rodriguez-Escudero, Hardwidge et al. 2005)
Shigella	OspF	Inhibits mitogen activated protein Kinase signaling.	Inhibits mitogen activated protein Kinase signaling, which is associated with attenuation of the host innate immune response to *Shigella* infection.	(Kramer, Slagowski et al. 2007)

Recently, in an interesting study, Alto et al., (2006) assembled several bacterial TIIISS effectors into a single family. Members of this family subvert host cell function by mimicking the signaling properties of Ras-like GTPases. For example, the *Shigella* effector IpgB2 stimulates cellular responses analogous to GTP-activated RhoA and therefore induces the formation of actin stress fibers. These effectors do not bind guanine nucleotides or have sequences corresponding to the conserved GTPase domain, suggesting that they are functional but not structural mimics. Therefore, the mechanisms how these effector proteins stimulate host signaling pathways was unclear. To investigate

that, the authors analyzed IpgB2 in the yeast system. Expression of IpgB2 in yeast is toxic and thus causing lethality. Therefore, they expressed IpgB2 in a yeast knock out library (about 5000 viable gene-deleted strains) and screened for viable cells. Only gene deletions in *BCK1*, *SLT2* or *RLM1* resulted in a robust growth phenotype. Remarkably, each of these genes encodes a member of the Rho1p/MAP kinase (MAPK) signaling module (Figure 1-10-A). While yeast carrying deletions in *BCK1*, *SLT2*, and *RLM1* grow well in the presence of IpgB2, deletion of genes encoding components of other MAPK signaling modules continue to result in cell toxicity. Thus, yeast system can be used to investigate the signaling pathways involved during bacterial infection (Alto, Shao et al. 2006).

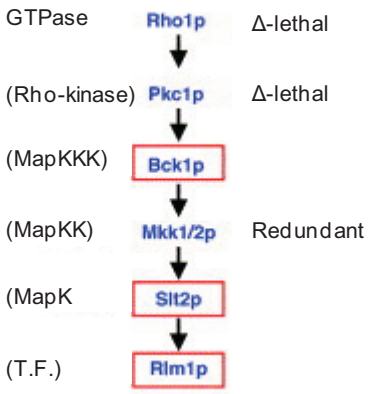

Figure 1-10: Diagram of the Rho1p-activated Pkc1p/MAPK pathway. The function of each protein is given in parenthesis (T.F. denotes transcription factor). Gene deletions that allow IpgB2 expressing yeast cells to survive are boxed in red. *Δ*-lethal denotes the deletion of gene encodes an essential protein (taken from Alto, Shao et al. 2006).

(Sisko, Spaeth et al. 2006) used the yeast model as a first step to identify some of *C. trachomatis* virulence proteins that are translocated into the host cell during infection. In this study, about 235 *C. trachomatis* hypothetical proteins or protein domains were expressed in the yeast *S. cerevisiae* and those proteins which showed growth phenotypes in yeast were selected for further analysis. To identify which of these proteins are secreted into the host cell, an intelligent approach was performed by testing these proteins for reactivity toward antisera raised against vacuolar membranes purified from infected mammalian cells. Further analysis in yeast showed that these proteins impact yeast cellular function or are tropic for a range of eukaryotic organelles including mitochondria, nucleus and cytoplasmic lipid droplets. Many of these finding were subsequently confirmed in infected mammalian cells demonstrating how yeast system biology can facilitate the identification and functional characterization of pathogenic bacterial effector proteins. For example, among these potential effector proteins, 4 proteins were found associated with lipid droplets in yeast. During *C. trachomatis* infection, 3 of these proteins have been shown to be secreted into the mammalian host and associated with

mammalian lipid rich structures. Additionally, they found that inhibition of lipid droplets negatively impact *C. trachomatis* infection (Kumar, Cocchiaro et al. 2006). In a follow-up study, they showed that lipid droplets are translocated from the host cytoplasm into the inclusion lumen and at least one of those proteins identified above in the yeast screen are implicated in this process (Cocchiaro, Kumar et al. 2008).

Recently, the yeast model system was also used to identify an inhibitor for the *C. pneumoniae* effector protein CopN. In this study, CopN was cloned and expressed in yeast and yeast cells expressing CopN showed a severe growth defect indicating that CopN disrupts at least one of the major cellular processes. Further analysis revealed that expression of CopN in yeast resulted in a cell cycle arrest and that this is probably due to alterations in the microtubule cytoskeleton. Indeed, the authors could confirm that CopN led to disruption of the spindle apparatus in both yeast and mammalian cells. Because *Chlamydia* cannot be genetically manipulated, the authors circumvented this limitation by screening a library of 40,000 small molecules and looking for those which alleviated the yeast growth inhibition induced by CopN. Successfully, two compounds were found to significantly restore growth of CopN-expressing yeast cells. These compounds were used to alternatively perform ‘functional knockouts’ of CopN during infection of mammalian cultured cells with *C. pneumoniae*. Interestingly, cells treated with these small molecules showed a strong reduction in *C. pneumoniae* replication demonstrating that CopN is required to support the intracellular growth of *C. pneumoniae* and plays an essential virulence role in a *C. pneumoniae* infected cell (Huang, Lesser et al. 2008).

1.7. Aims of the study

At the beginning of this study, the *C. trachomatis* Tarp was one of the few known chlamydial secreted proteins. It is secreted 5 minutes post of infection and directly gets phosphorylated. Tarp colocalizes with actin filaments accumulated at the site of EB entry in infected HeLa cells. However, the molecular mechanism of how Tarp interacts with actin was not known (Clifton, Fields et al. 2004). Although several studies have been carried out to analyze the protein function, the understanding of the role of Tarp in modulating and interacting with the host actin cytoskeleton was not complete. In particular, almost all studies analyzed the biochemical activities of Tarp but its function in living eukaryotic cells has not been analyzed until today (Clifton, Dooley et al. 2005; Jewett, Fischer et al. 2006; Elwell, Ceesay et al. 2008; Jewett, Dooley et al. 2008; Mehlitz, Banhart et al. 2008).

Other chlamydial species contain Tarp orthologs (for example the *C. pneumoniae* Cpn0572), but they have not been analyzed yet. In this study, we used the well established eukaryotic system *S. cerevisiae* to characterize the function of the *C. pneumoniae* protein Cpn0572. Therefore, this study was carried out to achieve the following goals:

- To reveal the expression and the translocation of Cpn0572 protein in the host cell by *C. pneumoniae* during infection.
- To dissect the molecular mechanisms by which Cpn0572 protein modulates the host actin cytoskeleton.
- To identify interacting partners of the Cpn0572 protein.
- To map the binding sites of actin on Cpn0572 protein.

2. MATERIALS AND METHODS

2.1. Materials

Table 2-1: Materials and equipments used in this work.

Materials/ Devices	Source
µMACS separator	MACS Molecular
Avanti Centrifuge J-25	Beckman
Axiovert 200 microscope	Carl Zeiss
Balance	Sartorius
Biofuge Pico R	Heraeus
Biofuge Primo R	Heraeus
Cell Scraper	Nunc
Conical Disposable Centrifugation Tubes (15 and 50 ml)	Sarstedt
Cryo Tube Vials (1,8 ml)	Nunc
Dialysis Tube , MWCO 12000-15000, Diameter 16 mm	Serva
DU 800 Spectrophotometer	Beckman
Electrophoresis Chamber	Amersham Biosciences
Eppendorf Tube, 1.5 and 2 ml	Eppendorf
Filter Discs for Lat-A Test (diameter, 6 mm), Sterile	Oxoid
Gene Pulse Controller	BIO-RAD
Gene Pulser Cuvette	BIO-RAD
Glass beads (diameter, 1µm)	Sigma
Glass Coverslips for Tissue Culture Plates	Roth
Isopropanol Freezing Box	Roth
Megafuge 1.0 R	Heraeus
Mini-vertical Gel Electrophoresis Unit	Hoefer
PCR-Thermocycler: Gene Amp 9700	MJ Research
pH Meter	inoLab
Polystyrene Round Bottom Tube, 5 ml, 12x75 mm Style	Falcon
Rotana 460R centrifuge	Heraeus
Round Bottom Centrifugation Tubes, 14 ml: PP-tube, sterile	Greiner
Sonopuls	Bandelin
Speed-Vac Vacuum-Concentrator	Savant
Tissue Culture Plasticware: Polystyrol-Flasks, 25 cm² and 80 cm², sterile	Nunc
Tissue culture plates (24 wells)	Corsa
Ultracentrifuge TL-100	Beckman
Vibrax VXR	IKA
Western Blotting Machine	Biometra
Whatman Paper for Western-Blot Analysis: Sheet of 58×58 cm	Schleicher & Schuell

2.2. Chemicals

Table 2-2: Chemicals used in this work

Chemicals	Source
2-(N-Morpholino)ethanesulfonic acid 4-Morpholineethanesulfonic acid, MES ($C_6H_{13}NO_4S$)	Sigma
5-Bromo-4-chloro-3-Indolyl-Phosphate (BCIP)	Sigma
Acetic acid	Riedel-deHaën
Acrylamid solution (30 %: 0,8 % Bisacrylamid)	Roth
Adenin	Roth
Adenosine 5'-triphosphate Disodium Salt (ATP)	Cytoskeleton
Agar	Invitrogen
Agarose: SeaKem LE	FMC Bioproducts
Ammonium persulfate	Merck
Ammonium sulfat	Sigma
Ampicillin	Bayer
Arginin	Roth
Bacto Pepton	Difco
Bacto Trypton	Difco
Boric Acid (H_3BO_3)	Sigma
Bovines Serumalbumin (BSA)	Serva
Bradford Reagent	Biorad
Bromphenol Blue	Fluka
Calcium chloride ($CaCl_2$)	Roth
Coomassie Brilliant Blue R250	Serva
Cycloheximide	Invitrogen
Deoxynucleoside-5'-Triphosphate (dNTPs)	MBI Fermentas
Dimethyl Sulfoxid (DMSO)	Sigma
Dimethylformamide (DMF)	Roth
Di-Sodium hydrogen phosphate (Na_2HPO_4)	Merck
Dithiothreitol (DTT)	Serva
Ethanol (96 %)	Riedel-deHaën
Ethanolamine ($NH_2CH_2CH_2OH$)	Sigma
Ethidium Bromide, 1% solution	Roth
Ethylenediaminetetraacetic acid (EDTA)	Roth
Galactose	Roth
Gastrographin	Schering
Glucose	Merck
Glutamic acid	Serva, Sigma
Glutathione-Agarose	Sigma
Glycerol	Roth
Glycin	Roth
HEPES	Sigma
Histidin	Roth
Hydrochloric Acid (HCl)	Riedel-deHaën
Imidazol	Sigma
Isoleucin	Roth
Isopropanol	Merck
Isopropyl-b-D-thiogalactopyranoside (IPTG)	Biomol
Leucin	Roth

Chemicals	**Source**
L-Glutathione reduced	Sigma
Lithium acetate (LiOAc)	Roth
Lysin	Roth
Magnesium chloride ($MgCl_2$)	Roth
Methanol	Riedel-deHaën
Methionin	Roth
Milk powder	Roth
Mounting fluid	Vectashield
N,N-Bis(2-hydroxyethyl)-2-aminoethanesulfonic acid, BES($C_6H_{15}NO_5S$)	Sigma
Nickel-NTA Agarose	Qiagen
Nitro Blue Tetrazolium (NBT)	Sigma
Paraformaldehyde	Fluka
Phenylalanin	Roth
Phenylmethylsulfonylfluoride (PMSF)	Sigma
Polyethylenglycol 3350 (PEG)	Sigma
Potassium Acetate (KAc)	Prolabo
Potassium chloride (KCl)	Merck
Potassium dihydrogen phosphate (KH_2PO_4)	Merck
Protease inhibitor Cocktail	Roche
Sodium Deoxycholate ($C_{24}H_{39}NaO_4$)	Sigma
Sodium Dodecyl Sulfate *(*SDS)	Serva
Sodium hydroxide (NaOH)	J.T.Baker
Sorbitol	Roth
Sucrose Monohydrate	Roth
TEMED	Roth
Threonin	Roth
Trisma base	Sigma
Triton X-100	Merck
Tryptophan	Roth
Tween-20	Merck
Tyrosin	Roth
Valin	Roth
Vectashield (Anti-fade, mounting fluid)	Linaris
Xylene Cyanol	Serva
Yeast extract	Difco
Yeast Nitrogen Base (YNB)	Difco

2.3. Oligonucleotides

All oligonucleotides were synthesized by Sigma-Genosys and delivered as purified desalted stocks and routinely resuspended at a final concentration of 50 µM. The forward and revere oligonucleotides used for cloning experiments by homologous recombination in yeast were designed as 40-45 bases homologous to the both ends of the linear plasmid followed with 20-23 bases homologous to the DNA fragment that can be used for homologous recombination in yeast. Sequencing oligonucleotides were designed as 20-23 bases homologous to the region upstream (about 100 bp) of the region to be sequenced. The oligonucleotides used in this work are listed below.

Table 2-3: Oligonucleotides used in this work

Oligonucleotide Nr.	Name of the oligonucleotide	Sequence (5`→3`)
C-341	Cpn0572-1	TATGGATGAATTGTACAAATCTAGAACTAGTGGATC CCCCATGGCAGCTCCTATCAACCA
C-342	Cpn0572-2	CGACGGTATCGATAAGCTTGATATCGAATTCCTGCA GCCCCTATTTTCTTCGTGGACTTGTCTATTTTCTTCG TGGACTTG
C-375	Cpn0572_3	CTATTACCCCCATCCATACTCTAGAACTAGTGGATC CCCCATGGCAGCTCCTATCAACCA
C-417	Tet1	CGCAATTAACCCTCACTAAAGGGAACAAAAGCTGGA GCTAATTCCTCGATCGAGTTTAC
C-418	Tet2	TTAGCTTTTGTTCACCGTTAATTAACCCGGGGATCC GCATCGAATTGATCCGGTAATTTA
C-419	Myc1	GCAAACACAAATACACACACTAAATTACCGGATCAA TTCGATGCGGATCCCCGGGTTAA
C-420	Myc2	TCGATGGTTGGTTGATAGGAGCTGCGGGGGATCCA CTAGTGTGATTGATTAATTTTTGTTCAC
C-441	Cpn0572_5 rev	CGACGGTATCGATAAGCTTGATATCGAATTCCTGCA GCCCCTAGTTCAAGGACGCATTCGAAA
C-442	DUF1547-1 for	CTATTACCCCCATCCATACTCTAGAACTAGTGGATC CCCCATGCAAGTCTTACAGAATGTCCGA
C-495	E-Cpn0572	GGATGAGCTCTACAAAAGCGGTTCCGGACCGGTGC TAGCG GCAGCTCCTATCAACCAACC
C-496	E-Cpn0572 rev	GAATTCCACCACACTGGACTAGTGGATCCGAGCTC GGTACCTATTTTCTTCGTGGACTTGTT
C-542	pAH0572 for	TGCTGCTGGTATTACCCATGGTATGGATGAATTGTA CAAAACTAGTGGATCCCCCATGGCAGCTCCTATCAA CCAA
C-543	pAH0572 rev	ATGTAAGCGTGACATAACTAATTACATGATGCGGCC CTCCCTATTTTCTTCGTGGACTTGTT
C-546	pAC0572 for	GGTGTTTTCACGAGCACTTCACCAACAAGGACCATA GATTATGAGAGGATCGCATCACCATCACCATCACAT GGCAGCTCCTATCAACCA
C-625	pAC0572-2	GCCAAGCTTGCCTGCAGGTCGACTCTAGAGGATCC GAATTCTATTTTCTTCGTGGACTTGT
C-628	AMP W297:A	GCTCAGCATGAAATTTAAAACTGCTGTAGTCTACGG TCCTGCT AATGCTAAAGAATCTAGTAGTG
C-629	AMP E301:A	GCTCAGCATGAAATTTAAAACTGCTGTAGTCTACGG TCCTTGGAATGCTAAAGCGTCTAGTAGTGGATATAC ACCC
C-630	AMP-His-Rev	GGTCGACGGTATCGATAAGCTTGATATCGAATTCCT GCAGCTAGTGATGGTGATGGTGATGTTTTCTTCGTG GACTTGTTGG

C-631	DUF-His-Rev	GGTCGACGGTATCGATAAGCTTGATATCGAATTCCT GCAGCTAGTGATGGTGATGGTGATGTGCTTGACCG GATGGATCTG
C-632	WSTAE for	TGAAGCCAGAAGTAGTTTCATTTTTGTCCGCAATGG TGACGCCTCAACTGCTGAGTCTATAAAAGTT
C-634	Ala stretch for	TTGACGATCCTGGTCAGGGAGAGGATGATAACGCA ATTCCCGGCACAAACACAGCAGCAGCAGCAGCAGC AGCAGCA AATCTAAGCAGTTCTCGCTTG
C-678	L1 rev	TATTACGGATATGACCGCCGCCTTCAGTGACTCCTC CGGTGTTCAAGGACGCATTCGAAAT
C-679	L2(For)	ACCGGAGGAGTCACTGAAGG
C-725	Cpn0572_J rev	CGACGGTATCGATAAGCTTGATATCGAATTCCTGCA GCCCCTAATGGTGATGGTGATGGTGGATTGTAGCA ACATGCCTGGT
C-726	Cpn0572_K rev	CGACGGTATCGATAAGCTTGATATCGAATTCCTGCA GCCCCTAATGGTGATGGTGATGGTGCCCCATATTCT GTGTTCCAGT
C-727	DUF-ZM for	TATGGATGAATTGTACAAATCTAGAACTAGTGGATC CCCCATGCAAGTCAATCAGAATAATCGACAACATAA TAATACGGCTTATGATTCGAATG
C-728	DUF-gfp-ZM for	TATGGATGAATTGTACAAATCTAGAACTAGTGGATC CCCCCAAGTCAATCAGAATAATCGACAACATAATAA TACGGCTTATGATTCGAATGGTA
C-729	Cpn0572-I for	CTATTACCCCCATCCATACTCTAGAACTAGTGGATC CCCCATGCAGGGAGAGGATGATAACGC
C-731	ABDM for	GCAGGCCAGGCAGCAAAAAACAGTGAAAACGGAGT GA
C-732	ABDM rev	AGTTCACTCCGTTTTCACTGTTTTTTGCTGCCTGGC CTGC ATCCTGATTGAGATCTGAGAC
C-733	GST-AMP for	TCCTCCAAAATCGGATCTGATCGAAGGTCGTGGGAT CCCCCTGGAAGTTCTGTTCCAGGGGCCCCTGGGAT CCATGGCAGCTCCTATCAACCAA
C-734	GST-AMP rev	ACGCGCGAGGCAGATCGTCAGTCAGTCACGATGAA TTCCC CTATTTTCTTCGTGGACTTGTT
C-735	GST-AMP-I for	TCCTCCAAAATCGGATCTGATCGAAGGTCGTGGGAT CCCCCTGGAAGTTCTGTTCCAGGGGCCCCTGGGAT CC CAGGGAGAGGATGATAACGC
C-737	GST-AMP-C for	TCCTCCAAAATCGGATCTGATCGAAGGTCGTGGGAT CCCCCTGGAAGTTCTGTTCCAGGGGCCCCTGGGAT CC ATGCAAGTCTTACAGAATGTCCGAC
C-754	Cpn0572_D-His rev	CGACGGTATCGATAAGCTTGATATCGAATTCCTGCA GCCCCTAATGGTGATGGTGATGGTGCGTCGTAGCT ACTTGTGGTT
C-755	Cpn0572_ERev-His	CGACGGTATCGATAAGCTTGATATCGAATTCCTGCA GCCCCTAATGGTGATGGTGATGGTGCGTAGTTGGT GTCCCTACGC
C-756	Cpn0572_A-His rev	CGACGGTATCGATAAGCTTGATATCGAATTCCTGCA GCCCCTAATGGTGATGGTGATGGTGGTTCAAGGAC GCATTCGAAA
C-443	DUF1547_2 rev	CGACGGTATCGATAAGCTTGATATCGAATTCCTGCA GCCCCTATGCTTGACCGGATGGATCTG
C-473	Cpn0572_D rev	CGACGGTATCGATAAGCTTGATATCGAATTCCTGCA GCCCCTACGTCGTAGCTACTTGTGGTT
C-1031	Cpn0572_G2 for	TATGGATGAATTGTACAAATCTAGAACTAGTGGATC CCCCACCGGAGGAGTCACTGAAGG
C-698	Cpn-ZM rev	TCATAAGCCGTATTATTATGTTGTCGATTATTCTGAT TGACTTGGTTCAAGGACGCATTCGAAAT
C-1033	CEN/ARSH-URA for	CTCGACCCCAAAAAACTTGATTAGGGTGATGGTTCA CGTA GGTCCTTTTCATCACGTGCT
C-1034	CEN/ARSH-	GTCAAAGGGCGAAAAACCGTCTATCAGGGCGATGG

	URA rev	CCCACTTAGTTTTGCTGGCCGCATC
C-735	GST-AMP-I Rev	ACGCGCGAGGCAGATCGTCAGTCAGTCACGATGAA TTCCCCTATGCTTGACCGGATGGATCTG
C-1035	n1for	TCCTCCAAAATCGGATCTGATCGAAGGTCGTGGGAT CCCCGGGCTGGAAGTTCTGTTCCAGGGGCCCCTGG GATCCTCCTTTATAAATGAAACTCCAG
C-1036	P-rep-del for	AACTCCAGGTGGAGGGGCTCACTCGACGTCTCATA CAGGTAATGTGAATGTCAACTTGGGA
C-1037	P-rep-del rev	ACTCGACGTCTCATACAGGT
C-1038	Pro-cut for	CAGGGAGAGGATGATAACGCAATTCCCGGCACAAA CACAAATCTAAGCAGTTCTCGCTTG
C-1039	Pro-cut rev	TGTGTTTGTGCCGGGAATTGCGTTA
C-1040	GST-AMP-C-zm	TCCTCCAAAATCGGATCTGATCGAAGGTCGTGGGAT CCCCCTGGAAGTTCTGTTCCAGGGGCCCCTGGGAT CCATGCAAGTCAATCAGAATAATCGAC

2.4. Plasmids

Table 2-4: Plasmids used or constructed in this work

Name	Serial Number	Construction	Genetic markers
pUG34	848	Lab collection	Amp/HIS3
p426MET25	235	Lab collection	Amp/URA3
pAH4	911	Lab collection	Amp/URA3
pcDNA3.1/NT-GFP	1349	Invitrogen	Amp
pRZ1	1205	Full length Cpn0572 was amplified by the oligonucleotides #C-341 and #C-342 and integrated in pUG34 at *SmaI* site by homologous recombination	Amp/HIS3
pRZ2	1206	Full length Cpn0572 was amplified by the oligonucleotides #C-375 and #C-630 and integrated in p426MET25 at *SmaI* site by homologous recombination	Amp/URA3
pRZ4	1207	Full length Cpn0572 was amplified by the oligonucleotides #C-375 and #C-630 and integrated in p426MET25 at *SmaI* site by homologous recombination	Amp/URA3
pRZ2-A	1208	A domain of Cpn0572 (nt: 1-1431) was amplified by the oligonucleotides #C-375 and #C-756 and integrated in p426MET25 at *SmaI* site by homologous recombination	Amp/URA3
pRZ2-B	1209	B domain of Cpn0572 (nt: 1432-2268) was amplified by the oligonucleotides #C-442 and #C-630 and integrated in p426MET25 at *SmaI* site by homologous recombination	Amp/URA3
pRZ2-C	1343	C domain of Cpn0572 (nt: 1432-1608) was amplified by the oligonucleotides #C-1030 and #C-631 and integrated in p426MET25 at *SmaI* site by homologous recombination	Amp/URA3
pRZ2-D	1249	D domain of Cpn0572 (nt: 1432-1794) was amplified by the oligonucleotides #C-1030 and #C-754 and integrated in p426MET25 at *SmaI* site by homologous recombination	Amp/URA3
pRZ2-G	1251	G domain of Cpn0572 (nt: 1609-2268) was amplified by the oligonucleotides #C-1031 and #C-630 and integrated in p426MET25 at *SmaI* site by homologous recombination	Amp/URA3

pRZ2-H	1348	H domain of Cpn0572 (nt: 1-1608) was amplified by the oligonucleotides #C-341 and #C-631 and integrated in p426MET25 at *SmaI* site by homologous recombination	Amp/URA3
pRZ2-I	1518	I domain of Cpn0572 (nt: 1312-1608) was amplified by the oligonucleotides #C-729 and #C-631 and integrated in p426MET25 at *SmaI* site by homologous recombination.	Amp/URA3
pRZ2-J	1367	J domain of Cpn0572 (nt: 1432-2037) was amplified by the oligonucleotides #C-442 and #C-725 and integrated in p426MET25 at *SmaI* site by homologous recombination	Amp/URA3
pRZ2-K	1368	K domain of Cpn0572 (nt: 1432-2142) was amplified by the oligonucleotides #C-442 and #C-726 and integrated in p426MET25at *SmaI* site by homologous recombination	Amp/URA3
pRZ2-L	1520	L domain of Cpn0572 (Full length lacking C domain) was constructed by triple homologues recombination; A domain was amplified by the oligonucleotides (#C-375,#C-678) and the G domain was amplified with (#C-442 and #C-725) and integrated in p426MET25 at *SmaI* site by homologous recombination	Amp/URA3
pRZ2-ALA	1363	The coding nucleotides for the proline stretch (nt: 1360-1383) was substituted with the coding nucleotides of alanine by homologues recombination using the oligonucleotides (#C-375, #C-441)for the first fragment and (#C-634,#C-630) for the second fragment. The fragment was integrated in p426MET25 at *SmaI* site by triple homologous recombination	Amp/URA3
pRZ2-H-ALA	1364	H domain of Cpn0572 (nt: 1-1608) amplified by the oligonucleotides #C-375 and #C-631 using pRZ2-ALA as a DNA template. The fragment was integrated in p426MET25 at *SmaI* site by homologous recombination	Amp/URA3
pRZ2-M1	1521	The coding nucleotides for 3 amino acids were substituted with the coding nucleotides of alanine by amplifying 2 parts of Cpn0572 using the oligonucleotides (#C-375, #C-698) for the first fragment and (#C-727, #C-630) for the second fragment. The fragment was integrated in p426MET25 at *SmaI* site by triple homologues homologous	Amp/URA3
pRZ2-M2	1372	The coding nucleotides for 3 amino acids were substituted with the coding nucleotides of alanine by amplifying 2 parts of Cpn0572 using the oligonucleotides (#C-375, #C-732) for the first fragment and (#C-727, #C-731) for the second fragment. The fragment was integrated in p426MET25 at *SmaI* site by triple homologous recombination	Amp/URA3
pRZ1-A	1252	A domain of Cpn0572 (nt: 1-1431) was amplified by the oligonucleotides #C-341 and #C-441 and integrated in pUG34 at *SmaI* site by homologous recombination	Amp/HIS3
pRZ1-B	1253	B domain of Cpn0572 (nt: 1432-2268) was amplified by the oligonucleotides #C-1030 and #C-342 and integrated in pUG34 at *SmaI* site by homologous recombination	Amp/HIS3
pRZ1-C	1248	C domain of Cpn0572 (nt: 1432-1608) was	Amp/HIS3

		amplified by the oligonucleotides #C-1030 and #C-443 and integrated in pUG34 at *SmaI* site by homologous recombination	
pRZ1-D	1344	D domain of Cpn0572 (nt: 1432-1794) was amplified by the oligonucleotides #C-1030 and #C-473 and integrated in pUG34 at *SmaI* site by homologous recombination	Amp/HIS3
pRZ1-G	1246	G domain of Cpn0572 (nt: 1609-2268) was amplified by the oligonucleotides #C-1031 and #C-342 and integrated in pUG34 at *SmaI* site by homologous recombination	Amp/HIS3
pRZ1-H	1247	H domain of Cpn0572 (nt: 1-1608) was amplified by the oligonucleotides #C-341 and #C-443 and integrated in pUG34 at *SmaI* site by homologous recombination	Amp/HIS3
pRZ1-I	1253	I domain of Cpn0572 (nt: 1312-1608) was cut out of pRZ2-I with *SpeI* and *XhoI* and cloned in pUG34 at the same cutting sites by ligation.	Amp/HIS3
pRZ1-J	1367	J domain of Cpn0572 (nt: 1432-2037) was cut out of pRZ2-J with *SpeI* and *XhoI* and cloned in pUG34 at the same cutting sites by ligation.	Amp/HIS3
pRZ1-K	1368	K domain of Cpn0572 (nt: 1432-2142) was cut out of pRZ2-K with *SpeI* and *XhoI* and cloned in pUG34 at the same cutting sites by ligation	Amp/HIS3
pRZ1-L	1719	L domain of Cpn0572 (Full length lacking C domain) was cut out of pRZ2-L with *SpeI* and *XhoI* and cloned in pUG34 at the same cutting sites by ligation	Amp/HIS3
pRZ1-ALA	1365	Full length Cpn0572 carrying the alanine stretch mutation instead of wt proline atretch was cut out of pRZ2-ALA with *SpeI* and *XhoI* and cloned in pUG34 at the same cutting site by ligation	Amp/HIS3
pRZ1-H-ALA	1366	H domain of Cpn0572 carrying the alanine stretch mutation instead of wt proline atretch was cut out of pRZ2-H-ALA with *SpeI* and *XhoI* and cloned in pUG34 at the same cutting site by ligation	Amp/HIS3
pRZ1-M1	1522	Full length Cpn0572 carrying the M1 was cut out of pRZ2-M1 with *SpeI* and *XhoI* and cloned in pUG34 at the same cutting site by ligation.	Amp/HIS3
pRZ1-M2	1373	Full length Cpn0572 carrying the M2 was cut out of pRZ2-M2 with *SpeI* and *XhoI* and cloned in pUG34 at the same cutting site by ligation.	Amp/HIS3
pRZ3	1361	Full length of Cpn0572 was amplified using the oligonucleotides #C-546 and #C-625 and integrated in pAC2 at *BglII and EcoRI* sites by homologous recombination.	Amp/URA3
pRZ5CON	1330	The MET25 promoter in p414MET25 was cut out with SacI and SmaI. *tetO* promoter (amplified with oligonucleotides #C-417, 'C-418) and c-myc (amplified with the.#C-419, #C-1032). The amplified fragments were integrated in the linear plasmid by homologous recombination.	Amp/TRP1
pRZ5	1143	The MET25 promoter in pRZ4 was cut out with *SacI* and *NcoI*. *tetO* promoter (amplified with oligonucleotides (#C-417, 'C-418) and c-myc (amplified with the.(#C-419, #C-420). The amplified fragments were integrated in the linear plasmid by homologous recombination.	Amp/TRP1
pRZ6	1360	Full length Cpn0572 fragment was amplified with oligonucleotides. (#C-542, #C-543) and integrated into pAH4 at *PstI* site by homologous	Amp/URA3

		recombination.	
pBYE	1353	The CEN6/ARSH4-URA region was amplified from p416MET25 using the oligonucleotides (#C1033-#C-1034) and integrated in pcDNA3.1/NT-GFP at *DraIII* site by homologous recombination.	Amp/URA3
pBYE1	1354	Full length Cpn0572 was amplified using the oligonucleotides #C-495 and #C-496 and integrated in pBYE at *Acc65I* site by homologous recombination.	Amp/URA3
pBYE1-ALA	1523	Full length Cpn0572 was amplified from pRZ2-ALA using the oligonucleotides #C-495 and #C-496 and integrated in pBYE at *Acc65I* site by homologous recombination.	Amp/URA3
pBYE1-M1	1524	Full length Cpn0572 was amplified from pRZ2-M1 using the oligonucleotides #C-495 and #C-496 and integrated in pBYE at *Acc65I* site by homologous recombination.	Amp/URA3
pBYE1-M2	1525	Full length Cpn0572 was amplified from pRZ2-M2 using the oligonucleotides #C-495 and #C-496 and integrated in pBYE at *Acc65I* site by homologous recombination.	Amp/URA3
pBYE1-L	1526	Full length Cpn0572 was amplified from pRZ2-L using the oligonucleotides #C-495 and #C-496 and integrated in pBYE at *Acc65I* site by homologous recombination.	Amp/URA3
p413GAL1	479	Lab collection	Amp/HIS3
p423GAL1	480	Lab collection	Amp/HIS3
pRZ9	1527	The coding region of $Cpn0572_{6His}$ was cut out pRZ2 with *SpeI* and *XhoI* and integrated at the same sites into p423GAL1 by ligation.	Amp/HIS3
pRZ10	1528	The *gfp* coding region was cut with XbaI from pUG34MET25 and integrated at *Xbai* site in p413GAL1 by ligation.	Amp/HIS3
pRZ11	1529	The coding region of Cpn0572 was cut out pRZ1 with *SpeI* and *SalI* and integrated at the same sites into pRZ10 by ligation.	Amp/HIS3
pRZ11-B	1530	The coding region of Cpn0572-B was cut out pRZ1 with *SpeI* and *SalI* and integrated at the same sites into pRZ10 by ligation.	Amp/HIS3
pRZ11-C	1531	The coding region of Cpn0572-C was cut out pRZ1 with SpeI and SalI and integrated at the same sites into pRZ10 by ligation.	Amp/HIS3
pRZ11-I	1532	The coding region of Cpn0572-I was cut out pRZ1 with *SpeI* and *SalI* and integrated at the same sites into pRZ10 by ligation.	Amp/HIS3
pKM36	1644		Amp/TRP1
pRZ13	1533	Cpn0572 full length fragment was amplified by the oligonucleotides #C-733 and #C-734 and integrated into pKM36 at *SmaI* site by homologous recombination	Amp/TRP1
pRZ13-B	1534	B domain of Cpn0572 (nt: 1432-2268) was amplified by the oligonucleotides #C-737 and #C-734 and integrated in pKM36 at *SmaI* site by homologous recombination	Amp/TRP1
pRZ13-C	1535	C domain of Cpn0572 (nt:1432-1608) was amplified by the oligonucleotides #C-737and #C-736 and integrated in pKM36 at *SmaI* site by homologous recombination	Amp/TRP1
pRZ13-I	1536	I domain of Cpn0572 (nt: 1312-1608) was amplified by the oligonucleotides #C-735and #C-	Amp/TRP1

		736 and integrated in pKM36 at *SmaI* site by homologous recombination	
pRZ13-N1	1537	I domain of Cpn0572 (nt: 1027-1608) was amplified by the oligonucleotides #C-1035 and #C-736 and integrated in pKM36 at *SmaI* site by homologous recombination	Amp/TRP1
pRZ13-DPR	1538	Cpn0572 full length fragment was amplified as a two fragments to delete the coding region of proline repeats using the oligonucleotides (#C-733, #C-1037) for the first fragment and (#C-1036, #C-734) for the second fragment. The fragment was integrated in and the fragments was integrated into pKM36 at *SmaI* site by triple homologous recombination	Amp/TRP1
pRZ13-DPS	1539	Cpn0572 full length fragment was amplified as a two fragments to delete the coding region of proline stretch using the oligonucleotides (#C-733, #C-1039) for the first fragment and (#C-1038, #C-734) for the second fragment. The fragment was integrated in and the fragments was integrated into pKM36 at *SmaI* site by triple homologous recombination	Amp/TRP1
pRZ13-CM1	1540	C domain of Cpn0572 (nt: 1432-1608) containing M1 mutation was amplified by the oligonucleotides #C-1040 and #C-736 and integrated in pKM36 at *SmaI* site by homologous recombination	Amp/TRP1
pRZ13-CM2	1541	C domain of Cpn0572 (nt:1432-1608) containing M1 mutation was amplified from pRZ2-M2 by the oligonucleotides #C-737and #C-736 and integrated in pKM36 at *SmaI* site by homologous recombination	Amp/TRP1
pRZ13-DM	1542	C domain of Cpn0572 (nt: 1432-1608) containing M1 and M2 mutations was amplified from pRZ2-M2 by the oligonucleotides #C-1040 and #C-736 and integrated in pKM36 at *SmaI* site by homologous recombination	Amp/TRP1

2.5. Enzymes

Table 2-5: List of enzymes used in this work

Enzyme Name	Source
RNase A	Qiagen
Taq Polymerase	Produced by Frau Volfson
Platinum *PFX* DNA Polymerase	Invitrogen
Trypsin/EDTA	Invitrogen
Lysozyme	Sigma
Quick T4 DNA Ligase	BioLabs
Zymolase-20T	ICN Biomedicals
Calf Intestine Alkaline Phosphatase (CIAP)	Fermentas

2.6. Antibodies

Table 2-6: List of primary antibodies used in this work

Primary Antibody	Origin	Dilutions	Producer
Pathfinder	Mouse	1:4 IF	Bio-Rad
DnaK	Rabbit	1:50 IF 1:500 WB	(Birkelund, Lundemose et al. 1990)
Anti-MOMP	Mouse	1:50 IF	Dako
Penta His	Mouse	1:2500	Qiagen
Anti-Cof1 antibody	Chicken	1:250 IF 1:2500 WB	(Okada, Ravi et al. 2006)
Anti-GST antibody (Z-5)	Rabbit	1:1000	Santa Crutz biotechnology
Anti-Gfp (clone: A11122)	Rabbit	1:1000	Molecular Probes
Anti-Cpn0572 (Affinity purified from rabbit 3090)	Rabbit	1:50 WB	This work
Anti-Cpn0572 (Adsorbed serum from rabbit 3091)	Rabbit	1:10 IF	This work

Table 2-7: Secondary antibodies used in this work

Secondary Antibody	Origin	Dilutions	Producer/Reference
Cy3-Anti-Maus	Rabbit	1:200 IF	Sigma
Cy3-Anti Rabbit	Mouse	1:200 IF	Sigma
AP-Anti Mouse	Rabbit	1:7500 WB	Promega
AP-Anti Rabbit	Mouse	1:7500 WB	Promega
Anti- Chicken-FITC	Goat	1:100 IF	Santa Crutz biotechnology
Anti- Chicken-TR	Goat	1:100 IF	Santa Crutz biotechnology
Anti- Mouse-FITC	Rabbit	1:20 IF	Dako
Anti- Rabbit-FITC	Pig	1:40 IF	Dako

2.7. Kits (Company)

µMACS c-myc Tagged Protein Isolation Kit (MACS Molecular)

QIAEX II Gel Extraction Kit (QIAGEN)

QIAGEN Plasmid Midi Kit (QIAGEN)

Quick Ligation Kit (New Englands, Bio Labs)

2.8. Proteins

Protein Name	Source
rCpn0572/ rCpn0572 derivatives	This work
Purified Rabbit Muscle Actin/ pyrene labeled	Cytoskeleton, USA
Human Cofilin Protein (Isotype 1)	Cytoskeleton, USA

2.9. Cells, strains and cell lines

2.9.1. Prokaryotic cells and strains

- ***Chlamydia pneumoniae***

Chlamydia pneumoniae (GiD); isolated from a patient who suffered from acute bronchitis (Jantos, et al., 1997).

- ***Escherichia coli* (*E. coli*)**

E. coli strains used in this work are listed below:

Strain	Genotype	Source
XL1-blue	supE44 hsdR17 recA1 endA1 gyrA96 thi relA1 lac- [F´proAB lac1q ZΔM15 Tn10(Rodal, Tetreault et al.)]	Stratagene
BL21(DE3)	F- *ompT hsdS*(rB- mB-) *dcm*+ Tetr *gal* l(DE3) *endA* Hte (pLysSCamr)	Stratagene

2.9.2. Eukaryotic cell lines and strains

- **Human cell lines**

Human cell lines used in this work are listed below:

Cell line	Description
HEp-2 cells	Epithelial cervix carcinoma cell line, human origin, HeLa morphology (ECACC: # 86030501; ATCC: # CCL-23)
HEK-293 cells	Human embryonic kidney epithelial cell line (ATCC: # CRL-11268)

- ***Saccharomyces cerevisiae* (S. *cerevisiae*)**

Yeast strains used in this work are listed below:

Strain	Genotype	Reference
CEN.PK 2	*MATa ura3-52 trp1-289 leu2-3,112 his3-Δ1* *MATá ura3-52 trp1-289 leu2-3,112 his3-Δ1*	(Entian and Kötter 1998)
yUG37	*MATa ura3-52 trp1-63 leu2-Δ1: LEU2 pCM149*	(Guldener, Koehler et al. 2004)
yRZ1	*MATa ura3-52 trp1-63 leu2-Δ1: LEU2 pCM149 His3:His3 TRP1 tetO-p cpn0572*	This work

BY4741	*MATa; his3D1; leu2D0; met15D0; ura3D0*	EUROSCARF Acc. Nr Y00000
aip1Δ	*BY4741; Mat a; his3Δ1; leu2 Δ0; met15 Δ0; ura3 Δ0; YMR092c::kanMX4*	EUROSCARF Acc. Nr Y06227
crn1Δ	*BY4741; Mat a; his3Δ1; leu2 Δ0; met15 Δ0; ura3 Δ0; YLR429w::kanMX4*	EUROSCARF Acc. Nr Y06032

2.10. Media

2.10.1. Medium for *E. coli*

E. coli cells were grown in/on Luria-Bertani (LB) broth or agar plates supplemented with ampicillin. The medium was prepared as following:

10 g Bacto Tryptone
5 g Yeast extract
5 g NaCl
13,5 g Agar (only for plates)

Components were dissolved in one liter of deionized water and autoclaved. The media was then cooled down (~45 °C) and ampicillin was added to a final concentration of 50 mg/l.

2.10.2. Medium for *S. cerevisiae*

- **Yeast Extract Peptone Dextrose (YPD^+ or $YEPD^+$)**

10,0 g Yeast extract
20,0 g Bacto Peptone
13,5 g Agar (only for plates)
2 ml Adenine stock solution (2 mg/ ml)
4 ml Tryptophan stock solution (5 mg/ ml)

Components were dissolved in 894 ml of deionized water and autoclaved. 20 g of glucose/dextrose in 100 ml of deionized water was prepared separately and autoclaved. Both components were combined to a final volume of 1000 ml.

- **Synthetic Defined Minimal media (SD)**

20,0 g Glucose
20,0 g Agar (only for plates)
1,7 g Yeast Nitrogen Base (YNB)
5,0 g Ammonium Sulfate
2,0 g amino acids mixture (lacking the desired amino acids, stored at 4°C)

Components were dissolved in one liter of deionized water and the pH was adjusted to 6 before autoclaving.

2.10.3. Cell culture medium and components

- **Media and solutions used for cell culture**

Components	Source
Minimal Essential Medium (MEM) + HEPES (25 mM) + „Earle's salts" (1X)	Invitrogen
Inactivated fetal calf serum (FCS)	Invitrogen
Sterilized glucose solution, (100 g/ml)	Merck
L-glutamine (200 mM, 100X)	Invitrogen
Vitamine mix (MEM), (100X)	Biochrom
Nonessential amino acids (MEM), (100X)	Invitrogen
Amphotericin B 250, (µg/ml)	Invitrogen
Gentamycin, (50 mg/ml)	Invitrogen
Hank's saline solution (HBSS), (1X)	Invitrogen
Trypsin-EDTA, (10X)	Invitrogen

- **Storage and preparation of stocks solutions and components**

1- Heat inactivated FCS: FCS was incubated at – 70 °C. To prepare portions, CFS was dissolved over night at room temperature. Next, the dissolved CFS was incubated in a water bath (56 °C) for 60 min. Then portions of 50 ml were made and frozen at – 20 °C till used.

2- 100% glucose: 100 g of glucose was dissolved in 100 ml ddH_2O. The solution was autoclaved. Then, portions of 5 ml were made and frozen at – 20 °C till used.

3- L-glutamine, Vitamine mix, Amphotericin and Gentamycin: all of these components were frozen at – 20 °C. Portions were also made by dissolving 1 bottle of each and filled in 5 ml portions. The portions were also frozen at – 20 °C till used.

4- Trypsin-EDTA: Trypsin-EDTA was frozen at – 20 °C. Portions were made in 5 ml and also frozen at – 20 °C. Working solution was made by adding 5 ml of Trypsin-EDTA to 95 ml sterilized ddH_2O. The solution was stored at 4 °C.

- **Preparation of Medium for cell culture**

HEp-2 cells or HEK-293 were cultured in 15 ml of MEM+7 medium: Minimal Essential Medium (MEM) + HEPES (25 mM) + „Earle's salts"; supplemented with the following additives:

Components and volume	Final concentration
500 ml minimal essential medium (MEM) + HEPES (25 mM) + „Earle's salts"	1X
50 ml heat inactivated fetal calf serum	10%
5 ml sterilized glucose solution	1%
5 ml L-glutamine	2 mM
5 ml Vitamine mix (MEM)	1%
5 ml Nonessential amino acids (MEM)	1X
5 ml Amphotericin B	2.5 µg/ml
0.5 ml Gentamycin	50 µg/ml

2.11. General molecular biology methods

2.11.1. Restriction enzymes and DNA digestion

All restriction enzymes used in this work were purchased from Fermentas. Digestion was carried out in a volume of 20 μl containing 1x of the corresponding buffer, 1-10 μg of DNA and 1-5 units of the restriction enzyme. Double digestions were carried out as recommended by the manufacturer.

2.11.2. Polymerase chain reaction (PCR)

PCR was performed using either *Taq* or *Pfx* polymerases. The PCR mixture and the PCR programs are as described below:

- **PCR mixture:**

Amplification of DNA using *Taq*		**Amplification of DNA using *Pfx***	
Oligonucleotide 1 (50 μM)	0.5 μl	Oligonucleotide 1 (50 μM)	0.5 μl
Oligonucleotide 2 (50 μM)	0.5 μl	Oligonucleotide 2 (50 μM)	0.5 μl
25 mM MgCl2	5 μl	50 mM $MgSO_4$	4 μl
4 mM dNTP's (dATP, dCTP, dGTP, dTTP)	2.5 μl	4 mM dNTP's (dATP, dCTP, dGTP, dTTP)	2.5 μl
Taq amplification buffer (10x)	5 μl	*Pfx* amplification buffer (10x)	5 μl
Taq polymerase	0.5 μl	*Pfx* polymerase (2.5 U/μl)	0.5 μl
DNA template (0.1-1 μg/μl)	1 μl	DNA template (0.1-1 μg/μl)	1 μl
ddH_2O	to 50 μl	ddH_2O	to 50 μl

- **PCR Programs**

	Amplification using *Taq*	**Amplification using *Pfx***
1- Initial denaturation	94°C, 5 min	94°C, 5 min
2- Denaturation	94°C, 1 min.	94°C, 1 min.
3- Annealing	46-52°C, 1 min	46-52°C, 1 min
4- Elongation	72°C, 1-3 min	68°C, 1-3 min
5- Cycles (steps 2-4)	39	39
6- Final elongation	72°C, 7 min.	68°C, 7 min

2.11.3. Agarose gel electrophoresis

The agarose gel (0.7 %-1 %) was prepared by melting agarose in 1x TBE buffer (89 mM Tris/HCl, 89 mM boric acid, 2 mM EDTA) using a microwave. The solution was cooled down before adding the ethidium bromide to a final concentration of 0.5 µg/ml. Each DNA sample was mixed with 1/5 volume of the 6 x loading buffer (0.25% bromophenol blue, 0.25% xylene cyanol and 30% glycerol). After electrophoresis at 100 volts in 1x TBE buffer, the DNA was visualized on a UV Transilluminator. For checking the quality of oligonucleotides, 3% agarose gel was used.

2.11.4. Extraction of DNA from agarose gel

Extraction of DNA from agarose gel was performed using Qiagen Gel Extraction Kit. The procedure was used as described by the manufacturer.

2.11.5. Cloning strategies

Most of the constructs were made via homologous recombination in yeast. Mutants or deletion fragments were also generated by homologous recombination. Other constructs were made by Ligation.

- **Homologous recombination in yeast and yeast transformation via the lithium acetate method**

- 5 ml of liquid YPD was inoculated with one colony of the appropriate yeast strain and incubated with shaking overnight at 30 ^{o}C.
- 500 µl of the overnight culture were used to inoculate a 50 ml YPD liquid medium and incubated with shaking at 30 ^{o}C for 4-5 h until the culture contained approximately 2x10^{7} cells/ml.
- The culture was harvested in a sterile 50 ml centrifuge tube at 1210 x g (3500 rpm on Heraeus Megafuge 1.0 R) for 5 min.
- The medium was removed and the pellet containing yeast cells was resuspended in 25 ml of sterilized ddH_2O and centrifuged again.
- The water was removed and cells were resuspended in 1 ml 100 mM LiAc and transferred to a 1.5 ml microfuge tube.
- Cell pellets were obtained at top speed for 15 sec and the LiAc was removed with a micropipette.
- The cells were resuspended to a final volume of 500 µl (about 2 x 10^{9} cells/ml) by adding about 400µl of 100 mM LiAc.
- ss-DNA was boiled at 100 °C for 5 min. and quickly chilled on ice.

- 50 µl of cell suspension were transferred into labeled microfuge tubes and the cells pellet was obtained by centrifugation at top speed for 15 sec. The LiAc was removed with a micropipette.
- The basic "transformation mix" consists of (The ingredients was carefully added in the following order):

  240 µl Sterile PEG (50% w/v)
  36 µl 1.0 M. Sterile LiAc
  50 µl ss-DNA (2.0 mg/ml)
  X µl (about 0.1 - 10 µg) Plasmid DNA OR linearized plasmid and a DNA fragment at ratio of 1:3, respectively OR no DNA as a negative control.
  34-X µl sterile ddH_2O
  360 µl TOTAL

- The tubes were vigorously vortexed until the cells pellet was completely mixed.
- The tubes were incubated at 30 ^oC for 30 min, then at 42 ^oC for another 30 min.
- The tubes were centrifuged at 8000 rpm (Heraeus Biofuge Pico R) for 15 sec and the transformation mix was removed with a micropipette.
- The cells were resuspended in 200 µl of sterile ddH_2O.
- Different portions (20%-80% of the cells) from each suspension were plated on the desired SD agar plates.
- The plates were incubated at 30 °C for 2-3 days.
- Single colonies were isolated and streaked on agar plates and subsequently used for either further experiments or for preparing cultures for plasmid extraction.

➢ **Ligation**

- The plasmid and the DNA fragments to be integrated were cut with the appropriate enzyme(s).
- The linear plasmid and the DNA fragment were separated from uncut vector and other DNA fragments, respectively, by gel electrophoresis and extracted from the agarose gel.
- The extracted vector was dephosphorylated by the Calf Intestinal Alkaline Phosphatase (CIAP) in a mixture buffered with CIAP buffer (Fermentas) as follows:

DNA	5-10 µg
5 x CIAP buffer	5 µl
CIAP	1 µl (1u)
H2O	to 50 µl

Incubation at 37 ^oC for 30 minutes before extraction using Qiagen Gel Extraction Kit.

- The ligation was performed using the Quick ligation kit as follows:

DNA fragment	150 ng
Linear plasmid	50 ng

Quick Ligase buffer (2 x)	10 µl
Quick T4 DNA Ligase	1 µl
H_2O	to 20 µl

- Mixtures were incubated at room temperature for 5-10 min followed on ice for 5 min.
- 1-10 µl of the ligation mixture was used for transformation into *E. coli* via electroporation.

2.11.6. Plasmid DNA extraction

➢ **DNA extraction from yeast (Mini-Prep)**

- 1-2 colonies of yeast cells carrying the desired plasmid were used to inoculate a 5 ml of the selective liquid medium (shaken overnight at 200 rpm and 30 °C).
- Culture was transferred into 15 ml falcon tube and centrifuged at 1210 x g (3500 rpm on Heraeus Megafuge 1.0 R) for 5 min.
- The pellet was resuspended into 700 µl P1 buffer (50 mM Tris-HCl pH 8.0, 10 µM EDTA, 100 µg/ ml RNase) and vortexed until the pellet was resuspended.
- 700 µl of P2 buffer (200 µM NaOH and 1 % SDS) and an equal volume to 700 µl of sterilized glass beads were added to the suspension to break the cells with strong vibrating (IKA Vibrax) at max speed, 4 °C for 20 min.
- The tube was centrifuged at 250 x g (1200 rpm on Heraeus Megafuge 1.0 R) for 1 min and the supernatant was collected.
- 1 ml of the supernatant was transferred to a 1.5 ml microfuge tube and mixed gently with 0.5 ml of P3 buffer (3M KAc pH 5.5) and placed on ice for 15 min.
- The tube was centrifuged at top speed for 10 minutes and the supernatant was obtained and transferred into a new microfuge tube.
- 750 µl of the supernatant was mixed with an equal volume of Isopropanol and vortexed well before the DNA was predicated by centrifugation at top speed, 4 °C for 30 min (Biofuge Primo R).
- The supernatant was removed and the pellet was washed with 300 µl of 70% ethanol vortexed well and centrifuged at top speed, 4 °C for 5 min.
- The supernatant was removed and the pellet containing the plasmid was dried down using the speed-vac for 5-10 min and the dried pellet was resuspended into 20 µl of cold sterilized ddH_2O.
- 2 µl of this suspension was used for electroporation.

➢ **Plasmid isolation from *E. coli* (Miniprep)**

- A single bacterial colony carrying the desired plasmid was cultured into 2 ml of LB+Amp liquid medium (incubated overnight at 250 rpm and 37 °C).
- The culture was transferred into 1.5 ml microfuge and centrifuged at top speed for 1

min.

- The pellet was resuspended into 300 µl P1 buffer (50 mM Tris-HCl pH 8.0, 10 µM EDTA, 100 µg/ ml RNase) and vortexed until the pellet was resuspended.
- 300 µl of P2 buffer (200 µM NaOH and 1 % SDS) was added to the suspension, mixed gently and placed on a rack at room temperature for 5 min.
- 300 µl of P3 buffer (3M KAc pH 5.5) was added to the suspension, mixed gently and centrifuged at top speed, 4 °C for 10 min.
- The supernatant was removed into new microfuge tube and mixed vigorously with 450 µl isopropanol. The tube was then centrifuged at top speed, 4 °C for 20-30 min.
- The supernatant was removed and the pellet was washed with 300 µl 70% ethanol.
- The tube was centrifuged at top speed, 4 °C for 5 min.
- The supernatant was removed and the pellet containing the plasmid was dried down using the speed-vac for 5-10 min
- The dried pellet was resuspended into 200 µl of cold sterilized ddH_2O.

➢ **Plasmid isolation from *E. coli* (Midiprep)**

The plasmid extraction from *E. coli* (Midi-prep) was carried out using the Qiagen Midi-DNA extraction kit. The procedure was used as described by the manufacturer.

2.11.7. Plasmid transformation into *E. coli*

Plasmid transformation into *E. coli* was performed using the standard methods as following:

➢ **1 Minute transformation:**

- DMSO *E. coli* cells (stored at – 70 °C, made regularly by the lab members as described in Maniatis et al., 1989) was thawed on ice.
- 1-2 µl of the desired plasmid (~100 µg/ml) or sterilized ddH_2O (for negative control) was mixed to the thawed *E. coli* cells and incubated at 41 °C for 1 min.
- The cells were then incubated on ice for 5 minute before adding 100 µl of LB medium containing ampicillin (50 mg/L) and platted on LB+ ampicillin agar plate.
- The plate was incubated at 37 °C for 14-16 h till colonies were can be visualized and easily picked up.

➢ **Electroporation:**

- Sterilized electroporation cuvette was incubated on ice for 30 min before use.
- Electrocompetent *E. coli* cells (stored at -70 °C) was thawed on ice for 20 min.
- 2-3 µl of the desired vector (extracted from yeast) was placed on the bottom of the

pre-cooled electroporation cuvette. A 40 µl of the thawed Electrocompetent *E. coli* cells (diluted in ddH_2O as 1:1) or ddH_2O alone (for negative control) were added to the cuvette.

- The electroporation was performed using Bio-Rad Gene Pulser (2.1 KV, 200 Ohm and 25µF).
- Electroporated cells were resuspended with 1 ml LB liquid medium and incubated at 250 rpm, 37 °C for 45 min.
- Cells suspension was centrifuged at 13000 for 1 min and about 80% of the supernatant was removed.
- The pellet was resuspended in the rest of the supernatant (about 200 µl) LB+Amp liquid medium.
- 20% and 80% portions were platted on LB+Amp agar plates and incubated for 16-20 h till colonies were can be visualized and easily picked up.

2.11.8. DNA sequencing

Sequencing was carried out by the biomedical research center (BMFZ) at the Heinrich-Heine University of Duesseldorf or GATC Biotech (Germany).

2.12. Other yeast methods

2.12.1. Serial dilution patch test

- 2-3 colonies of the yeast cells harboring the empty plasmid or the specific plasmid were grown in 5 ml of the selective liquid medium under inducing conditions (e.g. no methionine or Dox.), shaken overnight on the wheel at 30°C.
- 150-200 µl of the overnight culture were used to inoculate a new 5 ml of the same medium and incubated on the wheel at 30°C for 4-6 h, or until the culture density reached OD_{600} 0.8-1.
- Cells were counted and dilutions from each culture were prepared in water.
  Note: the dilutions were: $2x10^6$, $2x10^5$, $2x10^4$ and $2x10^3$ cells/ml.
- The selective medium agar plates that induced or suppressed the expression of the protein were dried under the laminar flow.
- 5 µl of the cells dilutions were dropped on the top of the agar plates and incubated at the desired temperature(s) for 2-3 days.

2.12.2. Latrunculin-A (Lat-A) halo assay

The Latrunculin-A (Lat-A) halo assay was performed as described by (Fiedler, Karpova et al. 2002) with the following modification:

- 2-3 colonies of the yeast cells harboring the empty vector or the vector expressing Cpn0572 were grown in 5 ml of the selective liquid medium which also induced the expression of the protein (shaken overnight on the wheel at 30 °C).
- Note: the selective medium is SD medium lacking the amino acids which are encoded by the plasmid transformed into the yeast cells.
- 50-100 µl of each culture were used to inoculate two new 5 ml of the same medium and incubated on the wheel at 30 °C for 4-6 h, until the culture density is ~ OD_{600}:0.8.
- Cells of each culture were counted and 10^6 cells were mixed with 2 ml of SD (lacking the desired marker of the plasmid) and 2 ml of molten 0.8% agar.
- Each cell suspension was quickly poured onto the surface of SD plates.
- Sterile filter disks (ø 6 mm) were placed on the top of agar plates.
- Lat-A was diluted in DMSO appropriately (0, 0.25, 0.5 or 1 mM), and 6 µl of each dilution was pipetted onto the center of a sterile filter disk.
  Note: Lat-A was purchased from Invitrogen as a 100 µg lyophilized powder. The stock solution was prepared by resuspending the 100 µg in 47.6 µl DMSO to give a concentration of 5 mM.
- Plates were incubated at 30 °C until a halo was clearly visible (24-48 h).

2.12.3. Lat-A treatment of cells in culture

The Lat-A treatment of cells in culture was performed as described by (Ayscough, Stryker et al. 1997) with the following modifications:

- 2-3 colonies of the yeast cells harboring the empty vector or the vector expressing Cpn0572 were grown in 5 ml of the selective liquid medium which also induced the expression of the protein (shaken overnight on the wheel at 30 °C).
- Note: the selective medium is SD medium lacking the amino acids that are coded by the plasmid transformed into the yeast cells.
- 100 µl of the overnight culture were used to inoculate a new 5 ml of the same medium and incubated on the wheel at 30°C for 2-3 h, until the culture density is ~ OD_{600}:0.6.
- DMSO alone or Lat-A diluted in DMSO was added into the culture to a final concentration of 2.5 µM and cultures were incubated further on the wheel at 30 °C.
- Portions of the cells were taken at different time points and directly fixed with formaldehyde and stained with rhodamine-phalloidin as described in section 2.12.5.
- Cells expressing GFP or GFP-Cpn052 fusion proteins were analyzed for the presence of actin cables or structures induced by Cpn0572/fragments and counted.

2.12.4. Growth and fixation of *S. cerevisiae* cells for fluorescence microscopy analysis

- 2-3 colonies of the yeast strain were inoculated into 5 ml of the corresponding liquid media and incubated over night on the wheel at 30 ˚C.
- 50-100 µl of the grown cells were used to reinoculate a new 5 ml from the same media to a final OD_{600}: 0.15-0.2, and incubated at the same condition for 4-6 h.
- When the cells reached the proper density, cells were fixed by adding 555 µl of 37% formaldehyde solution directly to the culture medium to get the final concentration of 3.7% formaldehyde.

  Note: 37% formaldehyde stock was prepared by dissolving 0.37 g of paraformaldehyde into 1 ml of 1M KPi buffer pH 7.0 (61.5% of 1M K_2HPO_4 and 38.5% of 1M KH_2PO_4). The sample was incubated at 56 ˚C and vortexed every 1 min till it became clear and paraformaldehyde completely dissolved. The formaldehyde solution was always freshly prepared.
- The culture medium containing formaldehyde was incubated on the wheel at 30 ˚C for 10 min.
- Culture was then transferred to a 15 ml falcon tube and centrifuged at 1210 x g (3500 rpm on Heraeus Megafuge 1.0 R) for 5 min. The pellet was taken and resuspended in 5 ml of 0.1 M KPi buffer pH 7 containing 3.7% formaldehyde and incubated on the wheel for another 1 h at room temperature.
- The tube containing the resuspended cells was then centrifuged at 1210 x g (3500 rpm on Heraeus Megafuge 1.0 R) for 5 min.
- To quench residual formaldehyde, the pellet was resuspended into 10 ml of 0.1M KPi buffer pH 7 containing 10 mM ethanolamine and incubated on the wheel for 10 min at room temperature.
- The cell pellet was then obtained at 1210 x g (3500 rpm on Heraeus Megafuge 1.0 R) for 5 min and resuspended into 1 ml of 0.1 M KPi buffer pH 7 and transferred to 1.5 ml eppendorf tube.
- Cells were sonicated briefly (1 min) and centrifuged in a table centrifuge at 13000 rpm (Heraeus Biofuge Pico R) for 10 sec.
- The cell pellet was washed 3 times in 0.1 M KPi buffer pH 7 and then resuspended in final volume of 200 µl of the same buffer.
- Cells were used directly or stored for 2-3 days at 4 ˚C for rhodamine-phalloidin staining or further methanol/acetone fixation and permeabilization for indirect immunofluorescence staining.

2.12.5. Actin staining of *S. cerevisiae* cells

- 30 µl of fixed yeast cells were centrifuged at 13000 rpm (Heraeus Biofuge Pico R) for 10 sec and the cell pellet was collected.
- The supernatant was removed and the pellet was resuspended into 30 µl of 6.6 µM rhodamine-phalloidin (Invitrogen). The cells were incubated in the dark at 4 °C with gentle agitation for 45-50 min.

  Note: the stock solution of rhodamine-phalloidin (6.6 µM) was prepared by dissolving 300 U of rhodamine-phalloidin into 1.5 ml methanole and frozen at – 20 °C. 30 µl of the stock was down using the speed-vac for 5 min and the pellet was redissolved into 30 µl 0.1 M KPi buffer pH 7.
- Cells were then washed 3 times with 0.1 M KPi buffer pH 7 and then adhered to a polylysine-coated coverslip for 2 min, washed with water and aspirated.

  Note: polylysine stock solution (25 mg/ml) was diluted to 1 mg/ml and 50 µl was placed on a cover slip for 20 sec, then aspirated and washed with 50 µl ddH_2O. The coverslip was left until it dried before it can be used.
- A drop of mounting medium was added to a slide to mount the coverslip. The edges were dried and the coverslip was fixed with fingernail polish.
- Actin structures were visualized using Axiovert 200 system and red filter supported.

2.12.6. Cofilin staining of *S. cerevisiae* cells

- 50 µl of fixed yeast cells were centrifuged at 13000 rpm (Heraeus Biofuge Pico R) for 10 sec to collect the cells.
- Cells in the pellet were washed 2 times with 1.2 M sorbitol, 0.1 M KPi buffer pH7.
- The cells were resuspended in 0.5 ml of the same buffer with 1 µl of β-mercaptoethanol and 20 µl of 1 mg/ml of zymolyase-20T (stored in freezer). Cell suspension was incubated at 37 °C for 30 min.
- Cells were centrifuged at 13000 (Heraeus Biofuge Pico R) for 10 sec in table centrifuge and the supernatant was removed. The cell pellet was resuspended in the same buffer and 15 µl of the suspension was placed on a polylysine-coated well for 15 min to settle the cells before aspiration.
- The cells adhering to the slide were permeabilized with ethanol (- 20 °C for 6 min) followed with acetone (- 20 °C for 30 sec).
- The slide was air dried thoroughly to get maximum flattening and therefore resolution of cell structures.
- The well was washed 5 times with 1 mg/ml of BSA (dissolved in PBS) before incubation with 15 µl of the primary antibody (α-Cof1 antibody diluted 1:500) for 1 h in a wet dark chamber at room temperature.

- Cells were washed 5 times with 1 mg/ml of BSA (dissolved in PBS) and incubated afterwards with 15 µl of the secondary antibody (Goat anti-chicken TR or FITC conjugated diluted 1:100) for 1 h in a wet dark chamber at room temperature.
- Cells were washed 5 times with PBS and a drop of the mounting solution was added before fixing the coverslip with fingernail polish.
- Cofilin structures were visualized using the Axiovert 200 system and the filters supported.

2.12.7. Live cell fluorescence imaging of GFP/GFP fusion proteins expressed in *S. cerevisiae* cells

Living cells expressing GFP/GFP Fusion Proteins or fixed cells were visualized using the Axiovert 200 system and the FITC filters.

2.13. Cultivation of human cell lines

HEp-2 cells, HEK-293 cells were taken out of -70 °C and thawed at room temperature.
15 ml of the corresponding media was added into big flask and the thawed cells were then added. Flask was then placed on a shelf in 37 °C, humidified CO_2 incubator for 24 h. Unattached cells were removed after washing with PBS and new media were added to the cells. Cells were incubated till a confluent cells layer was achieved and used for subculturing.

2.13.1. Subculturing of human cells

- A Flask (80 cm²) of actively growing cells that are 80-90% confluent was taken from the CO_2 incubator for harvesting.
- The old medium was removed using a sterile pipette before washing the adhering cells with 5 ml of Hank's saline.
- The cells were trypsinized by adding 5 ml of 0.1% trypsin solution for 5-10 min.
- 5 ml of the medium were added and detached cells were collected into a sterile centrifuge tube.
- Cells were harvested by spinning at 500 rpm for 10 min using a Rotana 460R centrifuge and the cell pellet was resuspended in 5 ml medium and gently vortexed.
- Empty flask was filled with 15 ml of medium and 1.5-2 ml of the cells suspension was added.
- Caps on flask was left slightly loosened and placed on a shelf in a 37 °C, humidified CO_2 incubator.
- The culture was examined daily and subculturing was carried out as required.

2.13.2. Transient transfection of HEK-293 cells

Transient transfection of HEK-293 cells was carried out using the calcium chloride method as described in Maniates et al, 1989 with the following modification:

- Cells were platted at the indicated concentration on the table 24h before transfection.

Dish Size	Number of Cells	Amount of media (Ford, Gemmell et al.)	2x BES (pH 6.95)	1M $CaCl_2$	DNA µg	dH_2O
24- well	6.0 x 10^5	1-1.25	62.5	15	1	To 125
100 mm dish	3.0 x 10^6	9	400	80	16	To 800

The following ingredients were added and vortexed well in a 5 ml polystyrene sterilized tube in the following order: DNA → $CaCl_2$ → ddH_2O.

- While the mixture was vortexed, the 2x BES (10.7 g/L BES, 1632 g/L NaCl, 0.27 g/L Na_2HPO_4, pH 6.95) buffer was added dropwise.
- The mixture was left on a rack for 10-15 min at room temperature.
- The mixture was added dropwise to the cells. The plate was swirled during this step.
- The plate was placed and incubated in a humidified CO_2 incubator at 37 °C.
- The medium was changed after 5 h.
- The cells were allowed to grow under the same condition for 16-24 h. The transfected cells were either fixed and stained for microscopic analysis or lysed for western blot analysis.

2.13.3. Immunofluorescence of human cells

➢ Fixation of human cells

- Cells grown on coverslips were washed twice with 1 ml prewarmed Hank's solution.
- The cells were then fixed with freshly made 3.7 % formaldehyde in 1x PBS for 10-15 min at room temperature.
- Formaldehyde was removed by washing the cells 3x with 1 ml 1x PBS.
- Cells were permeabilized with 0.1 % Triton X-100 in PBS for 2-3 minutes.
- Cells were blocked with 3% filtered BSA/PBS for 1 h at room temperature.
- Cells were washed 3-5 times with 1x PBS.

➢ Indirect Immunofluorescence

- Fixed cells incubated with 3 % filtered BSA/PBS were washed 3-5x with PBS.
- The primary antibody was diluted to the appropriate dilution in 1% BSA/PBS and 40-50 µl were added to the fixed cells followed by an incubating for 1-1.5 h at room temperature in a wet chamber.
- To remove the unbound primary antibody, the cells were washed 3-5x with PBS.

- The secondary antibody was diluted to the appropriate dilution in 1% BSA/PBS and 40-50 µl was added to the cells. Incubated for 1 h at room temperature in a wet dark chamber.
- The cells were washed 3-5x with PBS and the coverslips containing cells were dried.
- A drop of mounting medium was added to a slide to mount the coverslip. The edges were dried and the coverslip was fixed with fingernail polish.

➢ **Actin staining of human cells**

- Rhodamine-phalloidin stock (6.6 µM) was diluted 1:40 in PBS.
- Formaldehyde-fixed cells were stained with 50 µl of the diluted stain and incubated in the dark at room temperature for 20-30 minutes.
- Cells were washed 3x with PBS (1 ml each).
- A drop of mounting medium was added to a slide to mount the coverslip. The edges were dried and the coverslip was fixed with fingernail polish.

2.14. Propagation of *C. pneumoniae* in HEp-2 cells

2.14.1. Seeding of HEp-2 cells and infection with *C. pneumoniae* EBs

- HEp-2 cells in MEM+7 medium were grown on wells plate or 25 cm^2 flasks 1-2 days prior to infection till a confluent monolayer has been achieved.
- 1 ml of the *C. pneumoniae* EBs pool (IFU, 10^6-10^7) was thawed on ice.
- The old medium was removed and the cells were washed with 5 ml of Hank's solution.
- The EBs were mixed with 25 ml of MEM+7 medium, and 6 ml were added into each flask containing HEp-2 cells (or 1 ml into each well).
- The flasks (or wells plate) were centrifuged at 4000 x g (2890 rpm on Rotana 460R centrifuge) and 30°C for 1h.
- The flasks (or well plates) were incubated in a humidified CO_2 incubator for 1h at 37 °C.
- The media was then removed and fresh media containing cycloheximide (final concentration 1.2 µg/ml) was added.
- Flasks were placed on a shelf in a 37 °C, humidified CO_2 incubator for 2-4 days, depending on the purpose of the infection.
- The culture was examined daily.

2.14.2. Passaging of *C. pneumoniae*

- After 4 days, medium was removed from the flasks containing infected cells by aspiration.

- 6 ml of fresh medium (MEM+7) was added to the flask and attached infected cells were gently disrupted with a plastic scraper.
- Suspensions (from each 4 flasks) were collected into 50 ml falcon tubes.
- Cells were broken by sonication (two times: 40%, 45 sec).
- Materials obtained from the broken cells were centrifuged 2 times at 1560 x g (2900 pm on Rotana 460R centrifuge) for 10 minutes.
- The supernatant (from 1 flask) was used to infect new monolayer cells (of 4 flasks) or further preceded for preparation of a *Chlamydia* pool.

2.14.3. Preparation of a *C. pneumoniae* pool

- The supernatant containing *C. pneumoniae* cells was placed into ultracentrifugation tubes and ultracentrifuged at 30000 x g (16000 rpm on Beckmann J2-21), 4 °C for 1h.
- The pellet containing *C. pneumoniae* particles was resuspended into 1 ml SPG buffer (75 g/l sucrose, 0,52 g/l KH_2PO_4, 1,53 g/l Na_2HPO_4, 0,72 g/l glutamic acid; pH 7,5) and dissolved by gentle sonication.
- The suspension was either subsequently used for further purification or aliquots were prepared (*C. pneumoniae* Pool) by adding 10-20 μl of the suspension to 1 ml SPG buffer (75 g/l sucrose, 0,52 g/l KH_2PO_4, 1,53 g/l Na_2HPO_4, 0,72 g/l glutamic acid; pH 7,5) in Cryo tube vials and frozen at - 80 °C.

2.14.4. Purification of *C. pneumoniae* EBs

- The suspension of the *Chlamydia* pool was further centrifuged at 22000 x g (15000 rpm on Heraeus Biofuge primoR with Sepatech rotor # 7593) for 30 min.
- The supernatant was removed and the pellet was resuspended into 100 μl of Hank's solution before sonication in a water bath sonicator. If dissolving the pellet took a long time, the samples were placed every 3 minutes on ice for 1 minute.
- 10 ml of gastrografin solution (30% of gastrografin in sterilized ddH_2O) was placed into a cortex tube and the *C. pneumoniae* suspension was added into the top of the gastrografin solution.
- The *C. pneumoniae* EBs were centrifuged through a discontinuous gradient of gastrografin at 30000 x g (16000 rpm on Beckmann J2-21) at 4 °C for 1h and the supernatant was removed.
- The pellet was resuspended into 10 ml Hank's solution and recentrifuged at 30000 x g (16000 rpm on Beckmann J2-21) and 4 °C for 30 min.
- The supernatant was removed and the pellet was resuspended into 500 μl of Hank's solution and placed into a new Eppendorf tube. Another 500 μl of Hank's solution was added to the cortex tube to collect the residual particles and combined to the first 500

µl.

- The suspension was centrifuged at 22000 x g (15000 rpm on Heraeus Biofuge primoR with Sepatech rotor # 7593) and 4 °C for 30 min.
- The supernatant was removed and the pellet was resuspended into 100 µl of SPG buffer (75 g/l sucrose, 0,52 g/l KH_2PO_4, 1,53 g/l Na_2HPO_4, 0,72 g/l glutamic acid; pH 7,5). The suspension was diluted (1:10) and divided into portions in Cryo tube vials.
- Purified EBs were frozen using the Isopropanol freezing box at – 80 °C.

2.15. Immunofluorescence of *C. pneumoniae* and *C. pneumoniae* infected cells

2.15.1. Fixation of infected HEp-2 cells

HEp-2 infected cells were fixed for immunofluorescence staining in two different ways; either using formaldehyde fixation (as described in section 2.13.2) or methanol fixation as follows:

➢ **Methanol fixation**

- Growth media of infected cells (grown in plate wells) was aspirated and the cells washed with 1 ml of Hank's solution.
- Infected cells were covered with methanol and incubated at room temperature for 10-15 min.
- The cells washed 3 x with PBS (1 ml each).
- Fixed cells were incubated with PBS at 4 °C or used directly for immunofluorescence staining.

2.15.2. Staining of fixed HEp-2 infected cells

Indirect immunofluorescence staining of fixed HEp-2 infected cells was carried out as described in section 2.13.2 using antibodies specific for *C. pneumoniae* antigens with the corresponding labeled secondary antibody.

2.15.3. Microimmunofluorescence assay (MIF)

The MIF assay recognizes conformational epitopes on intact unfixed EBs as follows:

- 20 µl of purified EBs were placed on multi-well slide and the slide was incubated at 37 °C to dry and immobilize the EBs.
- 20 µl of the primary antibody diluted in PBS as indicated was placed on the top of EBs and incubated for 45 min at 37 °C.
- Unbound primary antibody was removed by washing with 20 µl PBS.
- 20 µl of the proper secondary antibody diluted in PBS was placed on the top of EBs

and incubated for 45 min at 37 °C.

- Unbound secondary antibody was removed by washing with 20 µl PBS.
- The slides were dried before adding 1-2 µl of mounting solution and the coverslips were sealed with finger nail polish.

2.16. Biochemical assays

2.16.1. Expression and purification of the recombinant proteins

Recombinant proteins were produced in the *E. coli* strain BL21 using standard methods. All proteins produced in this work were induced by addition of Isopropyl-β-D-1-thiogalactopyranoside (IPTG) and expressed at 37 °C for 3-5h. The expression and purification of recombinant proteins were carried out as follows:

➢ **Preparation of the cells**

- An *E. coli* clone bearing the plasmid of interest was used to inoculate a 50 ml overnight starter culture in LB+Amp. The culture was shaken at 225 rpm, 37 °C overnight.
- About 20 ml of the starter culture was used to inoculate 1L of LB+Amp and incubated under the same condition for 2-3 h (until OD_{600}: 0.4).
- Protein expression was induced by the addition of IPTG (final concentration 1 mM) and incubated for further 3-5 h under the same condition.
  - The cells were harvested by centrifugation at 1210 x g (3500 rpm on Heraeus Megafuge 1.0 R), 4 °C for 12 min.
- The pellet was washed with 20 ml of 1x PBS and the cells were again harvested by centrifugation (6240 x g, 6000 rpm Heraeus Megafuge 1.0 R, 4 °C for 5 min).
- The pellet was weighted and resuspended in 2 ml 1 x PBS before freezing at - 20°C.

➢ **Cell breakage and preparation of cells lysates**

1. GST-fusion protein

Purification of GST-fusion proteins was carried out under native conditions. The cells were broken and the lysate was obtained as follows:

- Cells were pelleted, dissolved and resuspended in 40 ml of the digestion buffer (0.5 mg/ml lysozyme, 1 mM PMSF, 25 mM Protease inhibitor cocktail and 1% Triton X-100 in PBS).
- The cell suspension was subjected to sonication, on ice (40%, 10 x 10 sec, Bandelin sonopuls).
- Cells debris was removed by centrifugation (26000 x g, 15000 rpm on Beckman Avanti J-25 JA Rotor, 20 minutes, and 4 °C) and the supernatant was collected.

2. His-tagged protein

Purification of His-tagged proteins was carried out under denatured condition, the cells were broken and the lysate was obtained as follows:

- The cells were pelleted was dissolved on ice and 5 ml of buffer B (8 M Urea, 0.1 M NaH_2PO_4, 10 mM Tris-HCl pH 8.0) gram pellet was added and cells resuspended.
- The suspension was shaken on the wheel for 1-2 h at room temperature.
- Cell debris was removed by centrifugation (17000 x g, 12000 rpm on Beckman Avanti J-25 JA Rotor, 10 minutes, and 20 °C) and the supernatant was collected.

➢ **Protein purification schemes**

1. GST-fusion protein

The supernatant containing the cells lysate was used for protein purification using the AKTA prime unit with a GSTTrap HP column using the GST purification program installed in the machine. 1X PBS was used as a binding buffer and proteins were eluted using cold elution buffer (50 mM Tris-HCl, 10 mM reduced glutathione, pH 8). The eluted fractions were collected and subjected for SDS-PAGE and western blot analysis before they were dialyzed.

2. His-tagged protein

- The supernatant containing the cells lysate was collected into 2 x 15 ml falcon tubes.
- 1 ml of Ni-NTA was added to each tube and filled completely with buffer B.
- The mixture was shaken on the wheel for 1-2 h at room temperature.
- Preparation of the column: a polystyrene column containing a porous polyethylene disc was fixed in a holder and washed with 3 ml of buffer B.
- The protein mixture (2x 15 ml) was applied to the column and the flow throw solution was collected.
- The solution was applied again on the column.
- The column was washed with 20 ml buffer B, and the eluted fractions (2 ml each) were collected into 2 ml Eppendorf tubes.
- The column was washed with 15 ml of buffer C (8 M Urea, 0.1 M NaH_2PO_4, 10 mM Tris-HCl pH 6.3) containing 10 mM Imidazol (a 1 M stock solution was prepared and 150 µl of the stock were use for 15 ml buffer C) and the eluted fractions were collected into 2 ml Eppendorf tubes.
- The column was washed with 10 ml of buffer E (buffer C containing 250 mM Imidazol, 2.5 ml of the stock were used for 7.5 ml buffer C) and the column was kept closed from the bottom for 5 min before starting the collection of fractions into 2 ml Eppendorf tubes.

- The column was washed with 5 ml of buffer TE (buffer C containing 500 mM Imidazol (use 2.5 ml of the stock for 2.5 ml buffer C) and the eluted fractions were collected into 2 ml Eppendorf tubes.
- The collected fractions were subjected for SDS-PAGE and western blot analysis before dialyzing them.

2.16.2. Renaturation of eluted His-tagged proteins

The eluted proteins were filled in a pre-boiled dialysis tube and dialyzed three times against 1 liter of 1x PBS, (12 h each).

2.16.3. GST-fusion protein pull-down assay

➢ **Preparation of HEp-2 cell lysates**

- HEp-2 cells were grown in a 80 cm^2 flask 1-2 days prior to infection till a confluent monolayer has been achieved.
- The medium was removed and cells were washed with 5 ml of Hank`s solution.
- Cells were detached using a cell scraper and resuspended in 20 ml of pre-cooled fresh lysis buffer (100 mM KCl, 10 mM HEPES (pH 7.5), 2 mM MgCl2 and 2 mM ATP).
- Cells were ultrasonicated, on ice (40%, 10 x 10 sec, Bandelin sonopuls).
- Insoluble materials were removed by centrifugation (12 000 g, 20 min, 4 °C, Avanti J-25 JA Rotor).
- The Supernatant containing the soluble cell lysate was used for the pull-down experiments.

➢ **Pull-down assay**

- 50 µL Glutathione Sepharose beads (50% slurry, prepared as described by the manufacturer) were added to the column and washed 3 times with 5 ml PBS.
- The beads were incubated with 1 ml PBS or 30 µg (in 1 ml PBS) GST or GST-fusion proteins and columns were shaken on the wheel for 1 h at 4°C.
- The beads were then blocked by adding 50 µg of BSA and incubated for another 30 min.
- The beads (binding GST or GST-fusion protein) were washed 2 x with 5 ml PBS and 1 X with 5 ml of the lysis buffer
- About 1 ml of the cell lysate (250 µg) was added to the GST-fusion protein-coated beads and the column containing the mixture was incubated again on the wheel for 2 h at 4°C.
- The beads were then washed 3x with 1 ml of the lysis buffer and the binding proteins

were eluted with 200 µl of the elution buffer (50 mM Tris-HCl, 10 mM reduced glutathione, pH8).

- The eluted samples were mixed with 100 µl of 4x Laemmli sample buffer and boiled at 100 °C for 10 minutes before analyzing on SDS-PAGE gels.

2.16.4. Protein immunoprecipitation from yeast cell extract

The immunoprecipitation experiment was carried out using µMACS^{TM} Epitope Tag Protein Isolation Kits as follows:

➢ **Preparation of the Lysis Buffer:**

The lysis buffer was prepared every time fresh. The ingredients and the concentration of chemicals used for preparation of the lysis buffer are listed follows:.

For 1x	**For 5 ml**
50 mM HEPS-KOH ph7.5	250 µl of 1 M
140 mM NaCl	140 µl of 5 M
1 mM EDTA	10 µl of 500 µl of 10%
1% Triton x-100	500 µl of the 10%
0.1% Na-deoxycholate	100 µl of 5%
1 mM PMSF	50 µl of 100 mM
100 mM Protease inhibitor cocktail	200 µl of 25x
Cold dH_2O	To final volume 5 ml

➢ **Preparation of yeast cells**

- The starting cultures were prepared by inoculating 5 ml of inducing media (SD –TRP) with 2-3 colonies of the yeast cells harboring the empty vector (pRZ5CON) or expressing Cpn0572 (pRZ5), incubated at 30 °C on the wheel overnight.
- The starting culture was used to inoculate 50 ml of the same type of liquid media, starting OD_{600}=0.1-0.2, shaken at 220 rpm, 30 °C, for 4-6 h
- When the cultures reached OD_{600}= 0.8-1, they were transferred into a 55 ml Falcon tube and harvested by centrifugation (1360 x g, 2800 rpm on Heraeus Megafuge 1.0 R, 4 °C, 5 minutes).
- The pellet was washed once with pre-cooled 40 ml TBS (140mM NaCl, 2.5 mM KCl, 3.5 mM Tris-HCl, pH 7.4) by inversion until the cells were resuspended.
- The cell suspension was centrifuged again as indicated above. The pellet was collected and resuspended in 1 ml of pre-cooled TBS buffer and transferred into 1.5 Eppendorf tube.
- The cells were centrifuged (22000 x g, 15000 rpm Heraeus Biofuge Primo R, 4 °C, 1 minute) and the supernatant was removed.
- The Cell pellet was snap frozen in liquid nitrogen and stored at -80 °C till the next day.

➢ **Cell lysis and immunoprecipitation**

- The cells were taken from -80 °C and thawed on ice.
- The thawed cells were centrifuged and resuspended in 700 µl lysis buffer and mixed with an equivalent volume to 0.5 ml of sterilized glass beads.
- The cells were broken by 1h vibration on a vibrating device (IKA Vibrax) at 4 °C and max speed.
- The suspension was centrifuged (22000 x g, 15000 rpm Heraeus Biofuge Primo R, 4 °C, 5 minutes) to separate lysed cells and debris from the clear supernatant.
- The supernatant was transferred into new tube and placed on ice.
- 150 µl of the cell extract was mixed with 50 µl of Anti-c-myc coated magnetic beads and incubated on ice for 1 h.
- The column was placed in the magnetic field of the µMACS separator and the column was calibrated with 200 µl lysis buffer lacking the protease inhibitors and PMSF.
- The mixture of beads and cell extract was added to the column and subsequently washed 4x with 200 µl of wash buffer 1 (W1, supplemented with kit).
- The column was washed with 200 µl of wash buffer 2 (W2, supplemented with kit).
- To remove the washing buffer, 20 µl of the pre-heated elution buffer (95 °C for 5 minutes) was applied to the column.
- After 5 minutes, the proteins were eluted with 50 µl of pre-heated elution buffer.
- Eluted fractions were analyzed by SDS-PAGE and western blot analysis.

2.16.5. Separation of proteins by SDS-polyacrylamide gel electrophoresis

➢ **Preparation of the SDS-PAGE gel**

SDS-PAGE was run as described by (Laemmli 1970) with the following modifications:

- The Separation gel components were mixed just prior to use and assembled within a glass/aluminum sandwich unit. The composition and quantities of separating gel and running buffer are listed below,

Table 2-8: Composition of running gels:

Running gels	Acrylamide monomer	4x Separation buffer *	10% Ammonium-persulfate	TEMED	ddH_2O
10%	13.3 ml	10 ml	200 µl	40 µl	16.5 ml
12%	16.0 ml	10 ml	200 µl	40 µl	13.8 ml
14%	18.6	10 ml	200 µl	40 µl	11.2

***Separating buffer**: 1,5 M Tris/HCl pH 8.8; 0.4 % SDS

- Once the separating gel was polymerized, the stalking gel components were mixed just prior to use and loaded on top of the separating gel within the sandwich unit. The composition and quantities of stalking gel and buffer are listed below,

Table2-9: Composition of stalking gel:

Stalking gels	Acrylamide monomer	4x Stalking buffer *	10% Ammonium-persulfate	TEMED	ddH_2O
6%	1.5 ml	2.5 ml	100 µl	20 µl	5.8 ml

***Stalking buffer** 0,5 M Tris/HCL pH 6.8; 0.4 % SDS

- The comb was directly placed on top of the stalking gel solution.
- Once the stalking gel was polymerized, the comb was removed and the sandwich unit containing the gel was placed into the electrophoresis chamber.

➢ **Preparation of protein samples**

A volume of cells corresponding to OD_{600} = 1 was microcentrifuged for 30 sec. The pellet was resuspended in 32,5 ìl ddH_2O, 12,5 ìl of 4x SDS-PAGE sample buffer (50 mM Tris pH 6,9; 2 % SDS; 0,1 % Bromphenol blue; 5 % Glycerin) and 5 ìl of 1 M DTT. The Sample was boiled at 100 °C for 5-10 min and followed on ice for 10 min. Samples were then subjected for SDS gel or frozen at – 20 °C. Purified proteins were treated the same, but 32,5 ìl protein sample was used instead of water.

➢ **Loading the samples and running the gel**

- The gel were submerged in the running buffer (0,05 M Tris/HCL pH 8.3; 0.2 M Glycin; 0.2 % SDS) and the electrophoresis chamber was filled to a level of two-thirds of its height.
- 10 ìl or 15 ìl of the sample was loaded on the gel for SDS gel separation unless somewhere mentioned.
- The proteins were migrated at 100 volts for 2.5-4 h.

➢ **Fixation and Staining of Proteins**

Proteins are fixed and stained at the same time by agitating the gels in a staining solution (45% ddH_2O, 45% methanol, 10% acetic acid, 0.25 % w/v CBB R-250) for 1 h at room temperature. Excess dye is then removed by destaining solution (45% ddH_2O, 45% methanol, 10% acetic acid) for 1-2 h.

2.16.6. Immunoblotting

- Samples were subjected to SDS-PAGE on Tris-Glycin gels.
- 6 whatman paper (7 cm x 9 cm) were merged in transfer buffer (48 mM Tris/HCL, 39 mM Glycin, 0,037 %(v/v) SDS, 20 % Methanol) for 10-15 minutes.
- The proteins in the gels were electrotransferred to immobile PVDF membranes (prewashed with methanol followed by ddH_2O) at 300 mAmb for 40 minutes.

- Membranes were then blocked for 1h in the blocking solution (3% milk powder, 1.25 ml 20 Tween 20 in 500 ml 1x sterilized PBS).
- The membranes were incubated with 5 ml of the blocking solution containing the first antibody for 2h.
- The membranes were washed 3 times (3 x 10 minutes) with 1x PBS at room temperature.
- The membranes were incubated with 5 ml of the blocking solution containing the secondary antibody for 1h at room temperature.
- The membranes were washed 3 times (3 x 10 minutes) with 1x PBS.
- To detect reactive bands, 66 µl of both BCIP and NBT solutions were mixed with 20 ml of detection buffer (100 mM Tris-HCl pH 9.5, 100 mM NaCl, 50 mM $MgCl_2$).
- Mixture was applied to the membrane and incubated till bands could be visualized.
  Note: BCIP stock solution (500 mg in 20 ml of 100% DMF). NBT stock solution (500 mg in 10 ml of 70% DMF).

2.16.7. *In vitro* actin polymerization

2.16.7.1. Reconstitution and storage of actin protein

Pyrene-labeled rabbit muscle actin protein was purchased as a 1 mg white lyophilized powder (Cytoskeleton, USA). The actin protein was reconstituted to 20 mg/ml with 50 µl of cold ddH_2O and aliquots of 5 µl were made in 1.5 ml Eppendorf tubes. The actin protein was then snap-frozen in liquid nitrogen and stored at – 80 °C. The biological activity of pyrene muscle actin can be determined by its ability to efficiently polymerize into filaments *in vitro* which can be measured by the increase in fluorescence.

2.16.7.2. Solutions for actin polymerization assay

General actin buffer (0.2 mM calcium chloride, 5 mM Tris-HCl pH8.0) and actin polymerization buffer (100 mM Tris HCl, 20 mM $MgCl_2$, 500 mM KCl, 10 mM ATP, 0.05 M guanidine carbonate pH 7.5) were purchased as a lyophilized powder (Cytoskeleton, USA). The buffers were reconstituted and stored as recommended by the manufacturer.

2.16.7.3. Actin polymerization assay

- Aliquot of pyrene muscle actin (about 100 µg in 5 µl volume), 100 mM ATP and 1 M DTT were thawed on ice.
- The pyrene muscle actin was diluted into 880 µl of general actin buffer supplemented with 0.2 mM ATP (0.88 µl of 100 mM ATP) and 1 mM DTT (0.44 µl of 1 M DTT). The sample was left on ice for 1 h to depolymerize actin oligomers.
- The protein sample was centrifuged at 19000 x g (14000 rpm on Heraeus Biofuge

Primo R), 4 °C for 30 min to remove any residual nucleating actin oligomers.

- About 400 µl of the supernatant was collected carefully and divided into 2 Eppendorf tubes and placed on ice.
- 20 µl of the 10x actin polymerization buffer was added to one of the tubes containing actin (reference sample). The reference sample was incubated at room temperature for 1 h.
- Once F-actin is assembled, both samples were placed into 2 wells of a black assay 96 well plate.
- The well plate was placed into the fluorescence spectrophotometer (excitation wavelength of 355 and emission 405) and the reference sample was chosen for gain adjustment. The machine was programmed to read the fluorescence intensity for 5 min to establish a baseline fluorescence measurement.
- After 5 minutes, 10x actin polymerization buffer was mixed with general actin buffer 1:1 (v/v) and 20 µl of the mixture was added to the second sample, mixed and placed into the spectrophotometer to read the increase in fluorescence for 1 h.
- In the presence of GST or GST-fusion proteins, the volume of diluting actin was reduced depending on the concentration of fusion proteins, to have the same final concentration of actin used above.

2.16.8. F-Actin spin-down assay

The biological activity of pyrene actin can be determined by its ability to efficiently polymerize into filaments *in vitro*, which can be separated from unpolymerized components in a spin down assay at 100,000 x g (Ultracentrifuge TL-100, TLA45 rotor, Beckmann) for 30-60 min. The pellet and 90% of the supernatant were added into two different tubes and mixed with 4x SDS-PAGE sample buffer and boiled for 5 min at 100 °C. The samples were then subjected for SDS-PAGE analysis.

2.16.9. Actin binding activity of cofilin

Recombinant human cofilin was purchased as a white lyophilized powder (100 µg, Cytoskeleton, USA) and reconstituted to 5 mg/ml with 20 µl of ddH_2O. Aliquots of 4 µl were made in 1.5 ml Eppendorf tubes and snap-frozen in liquid nitrogen before storing at – 80 °C. The biological activity of cofilin can be determined from its ability to bind or sever F-actin *in vitro* as following:

- 5 µl of the rabbit muscle actin stock was thawed on ice and diluted to 2 mg/ml with 45 µl general actin buffer.
- 5 µl of 10x actin polymerization buffer was added and the sample was incubated to 30 min to polymerize actin at room temperature.

- Equal molar amounts of F-actin, cofilin and GST-fusion proteins were combined at 2 different pH as follows:

	1st control	**2ed control**	**pH 8 cofilin severs F-actin**	**pH 6.8 cofilin binds F-actin**	**Actin binding (Cofilin/Cpn0572) pH 6.8**
F-actin (Final concentration: 1.6 µM)	12 µl	12 µl	12 µl	12 µl	12 µl
MES buffer pH 6.2	-	36 µl	-	36 µl	36 µl
10 mM Tris-HCl pH 8	36 µl	-	36 µl	-	-
GST-fusion proteins in PBS (Final concentration: 1.6 µM)	250 µl PBS	250 µl PBS	250 µl PBS	250 µl PBS	250 µl GST-fusion protein
Cofilin (Final concentration: 1.6 µM)	-	-	2 µl	2 µl	2 µl
Final volume	300 µl	300 µl	300 µl	300 µl	300 µl

- The experimental and control tubes were incubated for 30 min at room temperature.
- The samples were centrifuged at 100000 x g for 1 h to pellet F-actin and any associated proteins.
- The supernatant and pellet were separated and mixed with 150 µl of 4x SDS-PAGE sample buffer, boiled 5 min at 100 °C and subjected for SDS-PAGE analysis.

3. RESULTS

3.1. Expression of Cpn0572 induces a severe phenotype in yeast

3.1.1. Cpn0572 can be expressed heterologously in *S. cerevisiae*

Cpn0572 is the homologous protein of the *C. trachomatis* Tarp which is secreted into the host cell where it modulates the host actin cytoskeleton (Clifton, Fields et al. 2004). Both proteins share regions of high homology and identity (see figure 1-9 in the introduction chapter). However, Cpn0572 has not been characterized so far. Because many molecular host cell mechanisms that are affected during a bacterial infection are conserved from yeast to mammals, we used the yeast *S. cerevisiae* as an eukaryotic model system to investigate the role of Cpn0572 in modulating host cell processes. Therefore, we cloned the coding region of Cpn0572 fused to a N-terminal His-tag into the yeast high copy number vector p426MET25. The resulting vector pRZ2 allows regulatable expression of $Cpn0572_{6His}$. Subsequently, the vector was transformed into yeast and expression of Cpn0572 was confirmed by western blot analysis (Figure 3-1) indicating that this *C. pneumoniae* protein can be heterologously expressed in the yeast *S. cerevisiae*.

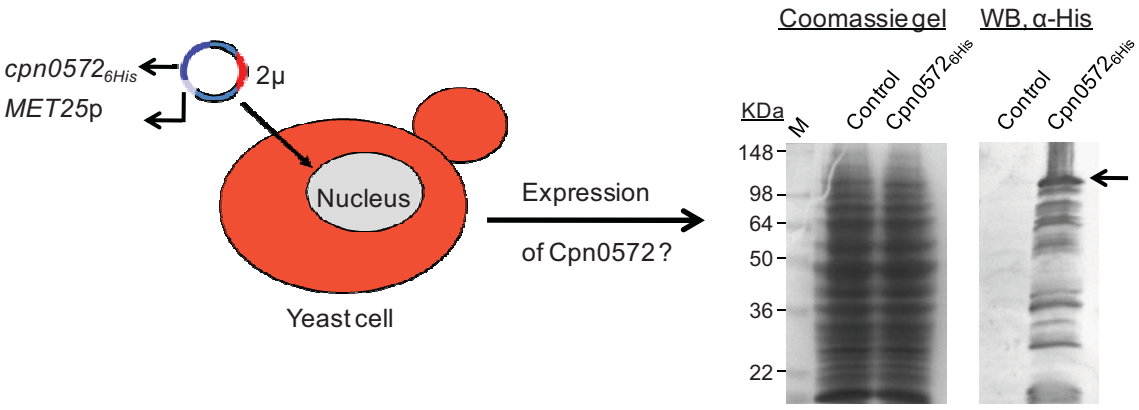

Figure 3-1: The *C. pneumoniae* protein Cpn0572 is expressed in yeast.
Expression of empty vector or *cpn0572*$_{6His}$ were for 20 h. Expression of $Cpn0572_{6His}$ fusion protein was detected with α-His antibody followed by a secondary antibody and the bands were visualized using the alkaline phosphatase method. Arrow indicates the corresponding band of the $Cpn0572_{6His}$ fusion protein.

3.1.2. Expression of Cpn0572 in yeast cells induces an increased lethality

To study the consequences of the expression of Cpn0572 in yeast, growth of control yeast cells or cells expressing the $Cpn0572_{6His}$ fusion protein was tested via the serial dilution patch test. In this test, different cell numbers (harboring the empty vector or pRZ2) were dropped on promoter non-inducing or inducing agar plates (Figure 3-2-A). After growth for 2-3 days at different temperatures colony size and colony numbers were compared (Figure 3-2-B). Control cells harboring the empty vector showed regular growth at all media and temperatures tested. Cpn572-expressing cells grown at non-inducing condition showed also normal growth compared to the control cells. In contrast, Cpn572-expressing

cells grown at inducing condition showed a severe growth defect indicating that Cpn0572 altered (an) essential process(es) in yeast cells.

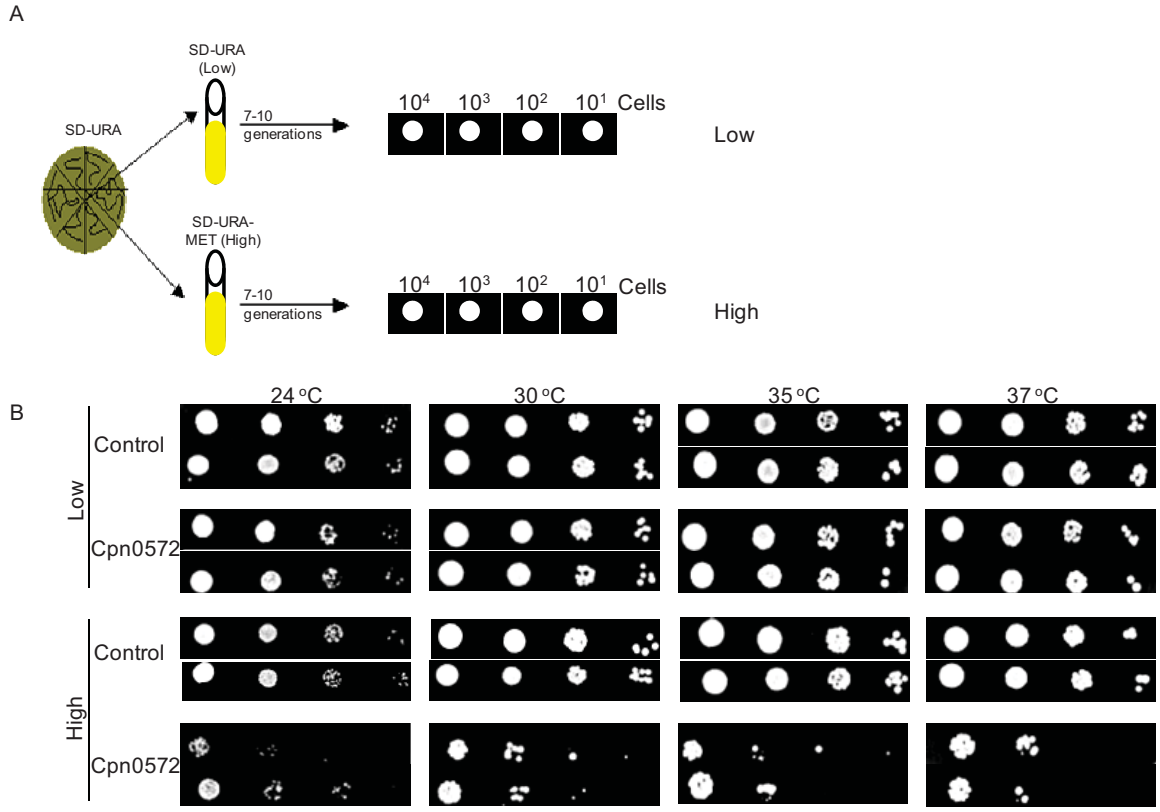

Figure 3-2: Expression of Cpn0572 in yeast cells induced a severe growth defect.
A, schematic representation of the set up of the serial dilution patch test experiment. Yeast cells were grown for 7-10 generations in either non-inducing or inducing selective liquid media (SD-URA or SD-URA-MET) indicated as Low or High, respectively. Suspensions of 10^4 exponentially growing cells and 10-fold serial dilutions of cells were dropped on the top of the same type of medium (either inducing or non-inducing) agar plates (left to right).
B, serial dilution patch test of yeast cells carrying the empty vector (Control) or the pRZ2 vector expressing $Cpn0572_{6His}$ (Cpn0572). Expression of Cpn0572 is low or high (indicated as Low or High). Colony growth was observed after incubating the plates for 2 days at different temperatures as indicated. The experiment was performed in duplicate.

The yeast growth phenotype induced by $Cpn0572_{6His}$ is either due to a reversible or irreversible defect. To test this directly, we performed a yeast viability assay (Figure 3-3-A). High expression of Cpn0572 reduced the viability of the yeast cells down to 5 % compared to 75 % of control cells grown under the same condition, while 55 % viability was found for the yeast cells expressing Cpn0572 at low level due to unknown reasons (Figure 3-3-B, see bars for HH and LL). To check if the decrease in Cpn0572 expression will alleviate the growth phenotype in Cpn0572-expressing yeast cells, the cells were grown for several generations in inducing selective media and finally plated on non-inducing selective media to suppress $Cpn0572_{6His}$ expression as schematically shown in Figure 3-3-A. Yeast cells expressing Cpn0572 at high level for 7-10 generations were unable to resume growth when they were shifted to media mediating a low expression level (Figure 3-3-B, see bars for HL). These results indicate that expression of

Cpn0572$_{6His}$ fusion protein is lethal for the yeast cells and that defect is irreversible.

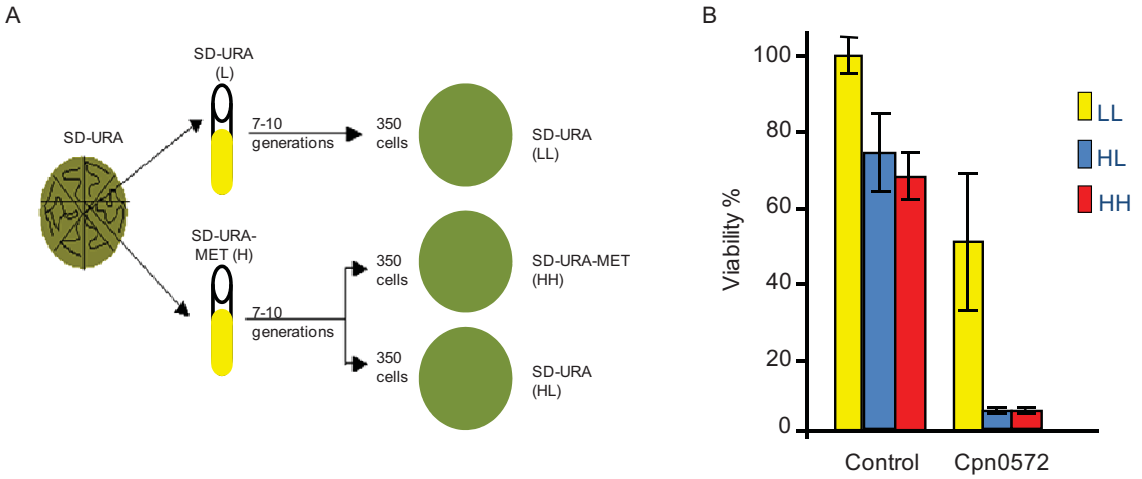

Figure 3-3: Expression of Cpn0572 in yeast cells is lethal.
A, schematic representation of the set up of the viability assay. Yeast cells were grown for 7-10 generations in either non-inducing selective liquid media (L, for low expression) or inducing selective liquid media (H, for high expression). 350 cells from each culture were plated on non-inducing selective media agar plates (LL and HL). Additionally, cells from the inducing selective liquid media were plated onto inducing selective media agar plates (HH).
B, viability assay of yeast cells carrying the empty vector (Control) or pRZ2 vector (Cpn0572) as described in A. Colony growth was observed after incubating the plates for 2 days at 30 °C. 5 individual transformants for each were tested. Colonies were counted and the number of colonies of control cells grown at LL conditions was set to 100%. Bars represent the standard deviation.

3.1.3. Expression of Cpn0572 in yeast interferes with the actin cytoskeleton

The *C. trachomatis* Tarp modulates the host actin cytoskeleton (Clifton, Fields et al. 2004). Therefore we studied the possible effect of Cpn0572 on the yeast actin cytoskeleton. Cpn0572 was expressed in actin mutant strains to test if *cpn0572* genetically interacts with actin mutant alleles (Figure 3-4-A). The actin mutant strains alone showed only a slight growth phenotype when grow at 30 ºC compared to the wild type strain (Figure 3-4-B). Low expression of Cpn0572 in the wild type strain did not affect growth compared to the control wild type cells harboring the empty vector. However, actin mutant strains expressing low levels of Cpn0572 showed already a reduced growth compared to the actin mutant strains harboring the empty vector. Additionally, the wild type strain expressing high level of Cpn0572 showed a severe growth defect compared to wild type cells harboring the empty vector. The actin mutant strains expressing high levels of Cpn0572 did not show any growth at all. These results reveal that *cpn0572* genetically interacts with actin mutant alleles.

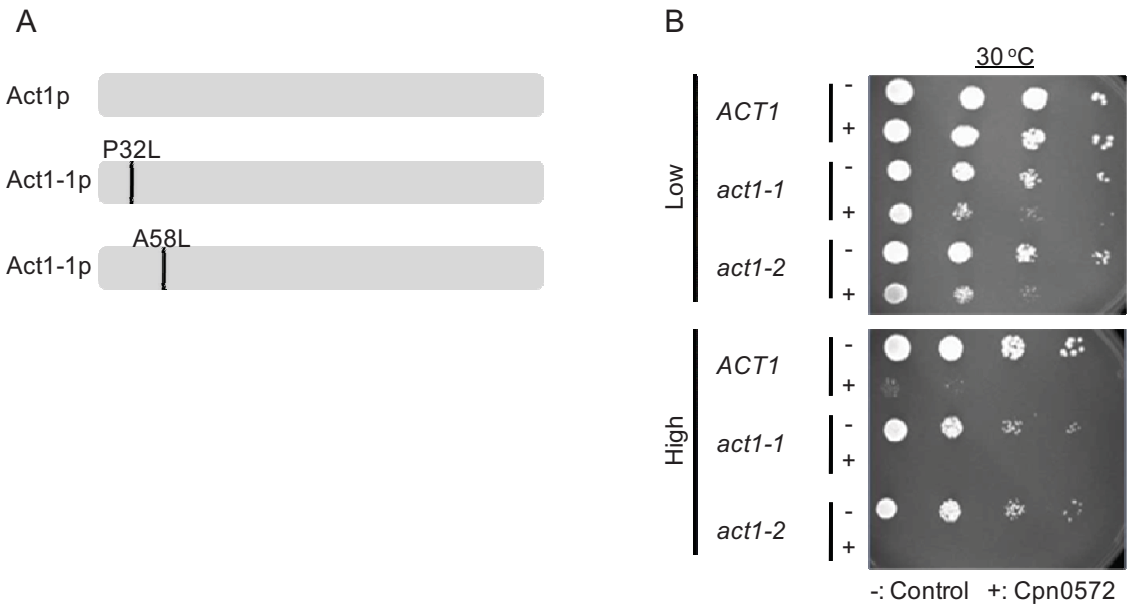

Figure 3-4: *cpn0572* interacts genetically with actin mutant alleles.
A, schematic representation of wild type Act1p and mutant proteins Act1-1p and Act1-2p. Sites of mutations are indicated.
B, serial dilution patch test of wild type (*ACT1*) and actin mutant strains harboring the empty vector p426-MET25 (-) or the vector expressing Cpn0572, pRZ2 (+). Yeast cells were primarily grown for 7-10 generations in inducing medium (SD-URA-MET) and then dropped on either non-inducing media (Low) or inducing media (High) to suppress or induce high expression of Cpn0572, respectively. Colony growth was observed after incubation of the plates for 2 days at 30 °C.

To further confirm that Cpn0572 interferes with the yeast actin cytoskeleton, we tested the sensitivity of Cpn0572-expressing yeast cells to the actin destabilizing drug Latrunculin-A (Lat-A). Lat-A binds G-actin and prevents their association and assembly into F-actin. As a result, Lat-A reduces or blocks actin dynamics depending on its concentration (Morton, Ayscough et al. 2000; Yarmola, Somasundaram et al. 2000). Due to that, yeast cells containing Lat-A will be unable to grow properly as it can be detected experimentally by the halo assay (Figure 3-5-A). Using this approach, control yeast cells harboring the empty vector showed a moderate sensitivity to a low Lat-A concentration, while higher concentrations resulted in a gradual increase in sensitivity (a in Figure 3-5-B). Compared to the control cells, Cpn0572-expressing yeast cells showed a high sensitivity to Lat-A at all concentrations tested. This sensitivity significantly increased in a dose-dependent manner (b in Figure 3-5-B and -C). Thus, these results further revealed that Cpn0572 interferes with the yeast actin cytoskeleton.

A

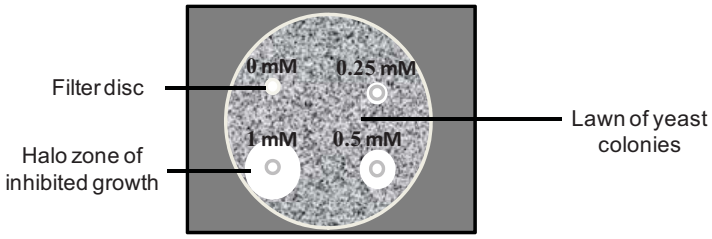

B

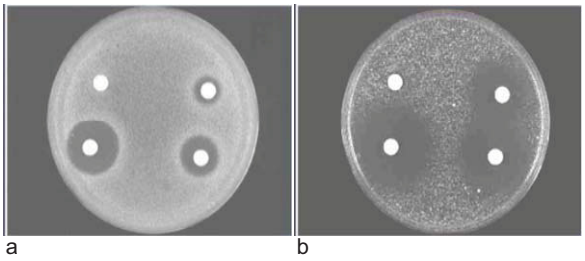

C

Yeast cells	Diameters of halo zones of inhibited growth (cm) Control	Cpn0572
0.0 mM Lat-A	0.0	0.0
0.25 mM Lat-A	1.3	2.6
0.5 mM Lat-A	1.5	3.2
1 mM Lat-A	2.2	3.8

Figure 3-5: In a halo assay Cpn0572-expressing yeast cells show high sensitivity against the actin destabilizing drug Lat-A.
A, schematic representation shows the experimental set-up and the different concentrations of Lat-A used in this experiment. Cells were grown in inducing selective liquid media until mid-log phase. About 10^6 cells were mixed with 2 ml of inducing selective liquid media and 2 ml of 0.8% molten agar and plated out. Filter discs were placed on each plate and 6 µl of different concentrations of Lat-A diluted in DMSO were applied to the discs as indicated. The plates were incubated at 30°C for 48 h.
B, sensitivity of yeast cells harboring the control empty vector (a) or expressing Cpn0572 (b) to Lat-A.
C, diameters of halo zones of inhibited growth obtained in typical experiments as shown in (B) were measured and presented in the table.

3.1.4. Expression of Cpn0572 in yeast transforms the wild type actin into clumps

Cpn0572 genetically interacts with *act1* mutant strains and Cpn0572-expressing yeast cells showed high sensitivity to the Lat-A. These results prompted us to study the morphology of the actin cytoskeleton in yeast cells expressing Cpn0572. To do so, we performed actin staining and subsequently microscopical analysis to visualize the actin cytoskeleton of Cpn0572-expressing cells. Control cells harboring the empty vector (p426MET25 is a 2µ vector, presumably 50-100 plasmids per cell) showed a wild type actin cytoskeleton consisting of both actin patches (10-20 patches) accumulating dominantly in the bud and actin cables (2-5 cables) directed toward the bud neck in parallel to the mother-bud cell axis (Figure 3-6-A). In contrast, Cpn0572-expressing yeast cells did not show actin cables, but instead the cells mainly carried 1-2 actin clumps and showed a significant decrease in the number of actin patches (5-11 patches), (Figure 3-6-B). These results suggest that Cpn0572 transforms actin cables and some of actin patches into clumps. We next analyzed the subcellular localization of Cpn0572 protein in

yeast cells. For this purpose, Cpn0572 was integrated into a vector containing N-terminally the *gfp* gene (pUG34 which is a CEN/ARS vector, presumably 1-2 vector copies per cell). The fusion protein GFP-Cpn0572 was expressed in yeast and cells were subjected to actin staining and examined using fluorescence microscopy. As expected, *gfp*-expressing control yeast cells exhibited the GFP protein throughout the entire cell and showed normal actin patches and cables (Figure.3-6-C, upper panel). In contrast, *gfp*-Cpn0572-expressing cells showed actin clumps with a significant decrease in the number

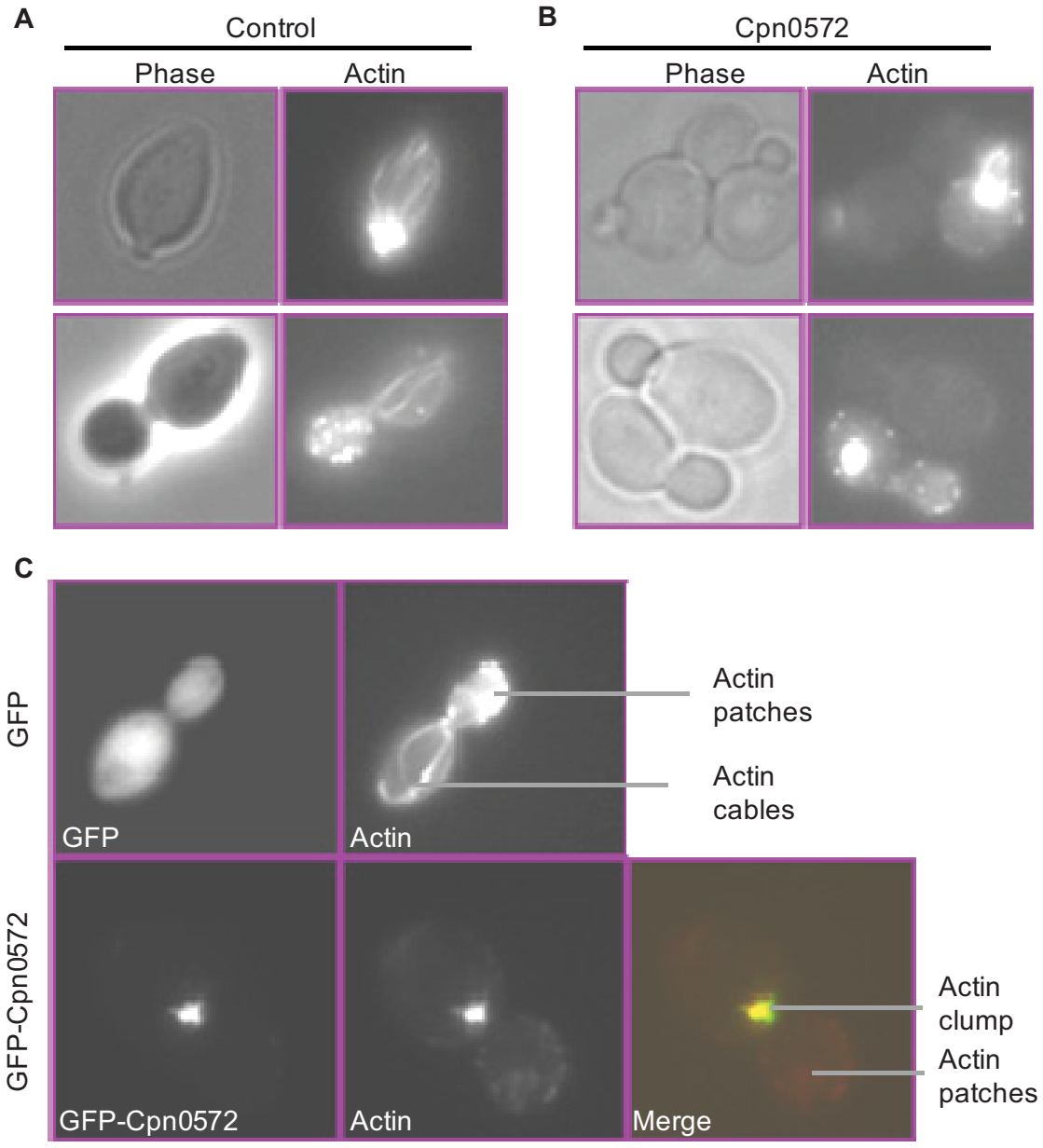

Figure 3-6: Expression of Cpn0572 in yeast cells induces an actin phenotype.
Yeast cells were grown in inducing selective media for about 20 h and in mid-log phase, cells were fixed using 3,7% paraformaldehyde and stained with rhodamine-phalloidin.
A, actin staining of yeast cells expressing the empty vector (Control). Two examples are presented.
B, Cpn0572 transforms the wild type actin into clumps. Actin staining of yeast cells expressing pRZ2 (Cpn0572). Two examples are presented.
C, GFP-Cpn0572 colocalizes with actin clumps. Actin staining of yeast cells expressing pUG34 (GFP) or pRZ1 (GFP-Cpn0572).

of actin patches (Figure 3-6-C, lower panel), similar to that phenotype obtained in cells carrying and expressing the 2µ vector containing *cpn0572*$_{6His}$. Interestingly, the GFP-Cpn0572 fusion protein formed big aggregates that were exclusively colocalized with the actin clumps. Collectively, the results revealed that Cpn0572 interferes with the yeast actin cytoskeleton by transforming the wild type actin cytoskeleton into clumps, thus resulting in a disruption of the actin cytoskeleton and subsequently inducing a severe growth phenotype in yeast.

3.1.5. Cpn0572 structures aggregate before transforming actin structures into clumps

Yeast cells expressing the fusion protein GFP-Cpn0572 for more than 20 h showed distinct clump like structures of the fusion protein completely colocalize with actin. In order to analyze how these clumps are formed, time course experiments were performed focusing on the first subcellular localization pattern of the fusion protein (in mother, bud, or bud neck) and the colocalization of the fusion protein with different actin structures at different positions in the budding cells (patches or cables). *cpn0572* was integrated into a vector containing the *gfp* gene under control of the regulatable *tetO* promoter yielding pRZ6. Yeast cells were then transformed with a control vector (pAH4) for expression of GFP alone or pRZ6 for the expression of the fusion protein GFP-Cpn0572. The expression was under the control of *tetO* promoter, which is inactive in the presence of doxycycline (Dox) and active in the absence of Dox. Microscopical imaging showed that the control cells or cells harboring pRZ6 did not show a detectable green fluorescence signal during the first 4 h after induction of expression. Both cells showed a normal actin cytoskeleton (Figure. 3-7-A). After 5 h of induction, about 3% or 2.7% of the cells expressing GFP or GFP-Cpn0572 showed a detectable fluorescence signal, respectively (Figure 3-7-B). Control cells showed a diffuse cytosolic GFP staining and wild type actin structures. Notably, cells expressing *gfp-cpn0572* showed distinct GFP-Cpn0572 structures or a weak diffuse cytosolic and distinct GFP-Cpn0572 structures (a or b in Figure 3-7-C, respectively). Detailed analysis revealed that these distinct structures of the fusion protein were detected as small punctuate structures in about 78% or clumps in about 22% of cells expressing the fusion protein (1-5 or 9 in Figure 3-7-B, respectively). Like the control cells, cells carried the small punctuate structures showed wild type actin structures. Often, these punctuate GFP-Cpn0572 structures localized close to actin cables or overlaps with both actin cables and patches (a and b in Figure 3-7-C). In contrast, cells carrying clumps of the fusion protein showed clumps of actin with a reduced number in actin cables and the fusion protein was exclusively colocalized with big or small actin clumps (c in Figure 3-7-C). Furthermore, our analysis revealed that the GFP-Cpn0572

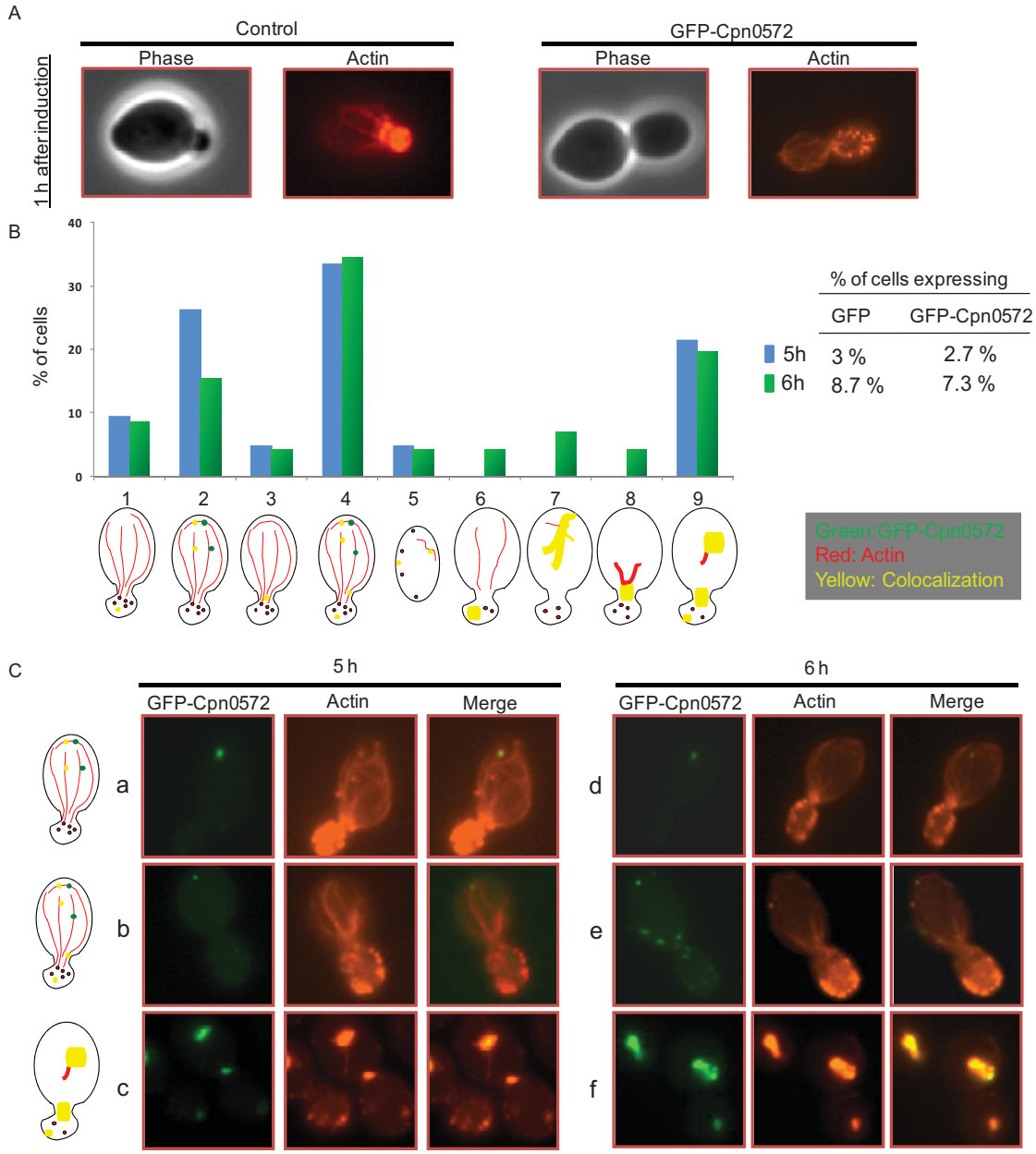

Figure 3-7: Cpn0572 recruits before clumping actin at early time points of expression in yeast cells. Cells harboring the empty vector pAH4 (control) or pRZ6 vector (GFP-Cpn0572) were grown in non-inducing selective liquid media until mid-log phase. Cells were then washed 3 times and 1/3^{ed} of the cells was used to inoculate fresh inducing selective media. Portions of cells were taken every 1 h for fixation and actin staining.
A, actin staining of yeast cells harboring the empty vector or pRZ6 encoding GFP-Cpn0572 vector after 1 h of induction. No GFP signals were detected for both cells.
B, expression of the GFP-Cpn0572 fusion protein was detected first after 5 to 6 h of induction. Actin staining was performed and cells were categorized based on the localization of the fusion protein (green) and the actin cables and patches (red) as indicated by the schematic representation shown below the graph. Colocalization of Cpn0572 and actin in yellow.
C, examples of fluorescence images representing the major categories identified in B.

fusion protein was not restricted to the mother cells or buds since more than 50% of the cells showed GFP-Cpn0572 structures in both mother cells and buds at the same time (see 4 and 9 in Figure 3-7-B and the examples b and c in Figure 3-7-C).

After 6 h of induction about 8.7% or 7.3% of the cells expressing GFP or GFP-Cpn0572 showed a detectable fluorescence signal, respectively. The cells showed the GFP-Cpn0572 fusion protein either as small punctuate structures in about 66% or clumps in about 34% of cells expressing the fusion protein (1-5 or 6-9 in Figure 3-7-B, respectively). Cells carrying the small punctuate structures showed also wild type actin structures and they localized close to actin cables or overlapped with both actin cables and patches (d and e in Figure 3-7-C), while cells carrying clumps of GFP-Cpn0572 showed clumps of actin with almost no actin cables and patches and the fusion protein was exclusively colocalized with big actin clumps (f in Figure 3-7- C).

Collectively, the results imply that the aggregation of the fusion protein is probably a prerequisite for transforming actin structures into clumps. The results also indicate that the fusion protein is not specifically limited to the bud or mother cells and interacts with both actin structures. However, wild type actin cables disappear faster than actin patches. Thus actin clumps are probably a mixture of actin cables and patches or a new structure of actin.

3.2. Immunoprecipitation assay identifies actin and actin binding proteins as potential Cpn0572-interacting partners

We addressed the question, how Cpn0572 interacts with and transforms actin structures into clumps, e.g. does it interact with actin directly or indirectly by interacting with actin binding proteins (ABPs). Most of ABPs are associated with both actin structures, for example Abp140p binds actin filaments and localizes to actin patches and cables (Asakura, Sasaki et al. 1998). However, some of them are associated with one actin structure only. For example the major isoform of Tpm1p binds to and stabilizes actin cables while Sla2p is present in the actin cortical patch of the emerging bud tip (Liu and Bretscher 1989; Yang, Cope et al. 1999). The detection of Cpn0572 structures at early time of expression revealed that Cpn0572 is not specifically limited to one actin structure (as shown previously in Figure 3-7).

In order to identify Cpn0572 interaction partners in yeast, immunoprecipitation (IP) assays were performed. We expressed the protein tag c-myc alone or a c-myc-Cpn0572 fusion protein in yeast. Western blot analysis of eluted proteins from anti-c-myc antibody coated beads revealed that the beads were able to immunoprecipitate c-myc and c-myc-Cpn0572 proteins (Figure 3-8-A). Correspondingly, SDS-PAGE analysis of these eluted proteins identified at least 4 protein bands that were not detectable in the eluted proteins of the c-

myc control (Figure 3-8-B). These proteins bands are not degradation products of the c-myc-Cpn0572 fusion protein (Figure 3-8-C). The proteins were identified by mass spectrometry (biomedical research center (BMFZ) at Heinrich-Heine University of Duesseldorf) and turned out to be actin (Act1p) and the actin-related proteins coronin (Crn1p), the translation elongation factor 1 alpha (Tef1p: the mammalian eEF1α homologue), and the hypothetical protein YRF016C. The Crn1 protein cross-links actin filaments and negatively regulates Arp2/3 nucleation activity (Goode, Wong et al. 1999; Humphries, Balcer et al. 2002). In addition to its role in protein translation, Tef1 protein bundles F-actin *in vitro* (Owen, DeRosier et al. 1992). However, these proteins bind actin directly (Goode, Wong et al. 1999; Munshi, Kandl et al. 2001). Therefore, it could be that they were immunoprecipitated due to their direct interaction with actin and not due to specific interaction with the c-myc-Cpn0572 fusion protein.

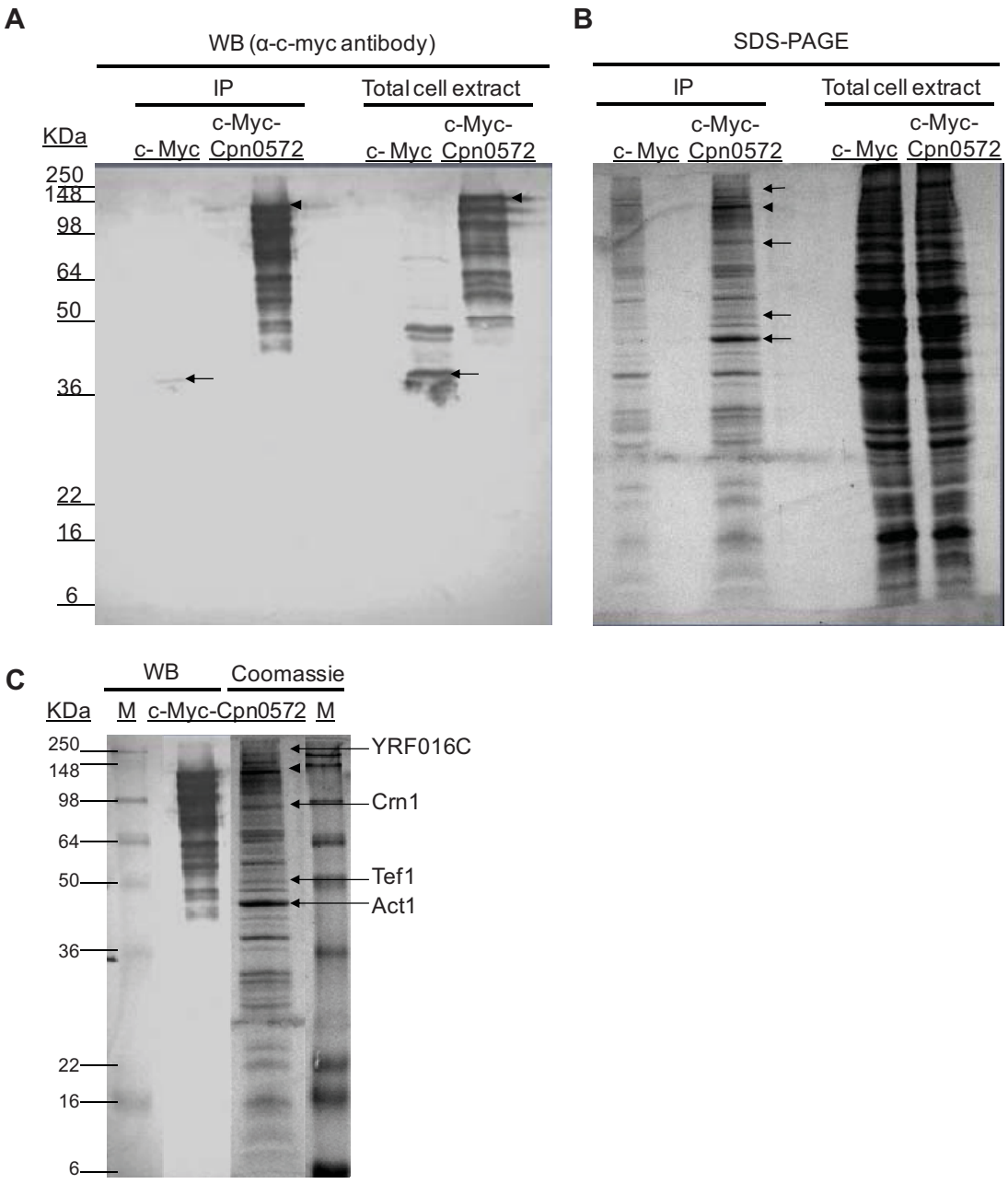

Figure 3-8: Act1, Crn1 and Tef1 are immunoprecipitated with c-myc-Cpn0572 expressed in yeast. Total protein extracts from cells expressing c-myc alone or the c-myc-Cpn0572 fusion protein were incubated with α-c-myc antibody coated beads. Beads were washed and bound proteins were eluted and subjected to SDS-PAGE and western blot analysis.

A, western blot analysis of the eluted proteins and total cell extracts from c-myc- or c-myc-Cpn0572-expressing cells. The membrane was incubated with an α-c-myc antibody followed with α-mouse antibody and visualized using the alkaline phosphatase method. Arrows and arrow heads indicate the c-myc and c-myc-Cpn0572 bands, respectively. Proteins sizes are indicated in KDa.

B, coomassie staining of SDS-PAGE of the eluted proteins and total cell extracts from c-myc- or c-myc-Cpn0572-expressing cells. Arrow head and arrows indicate the bands corresponding to c-myc-Cpn0572 and potential interacting partners, respectively.

C, a direct comparison of western blot and coomassie staining showed that the bands on the coomassie gel are not degradation products of c-myc-Cpn0572. The lanes containing the protein marker (M) from the coomassie gel and western blot membrane were also compared to verify that similar protein bands are migrated equally in both gels.

To investigate if these proteins bind Cpn0572 protein directly or the interaction is mediated by actin, the diploma student B. Koehnen performed a two hybrid protein-protein interaction analysis and the results revealed that a protein fragment of Cpn0572 protein interacts physically with actin and Crn1 but not with Tef1 (Benjamin Koehnen Diploma thesis, 2007).

To test if Crn1p is necessary for Cpn0572 activity in inducing growth phenotype in yeast, we expressed Cpn0572 in a *crn1Δ* strain and performed a serial dilution patch test. As shown previously, wild type cells expressing the empty vector showed normal growth, while *Cpn0572*-expressing cells showed a reduced growth (Figure 3-9). However the *crn1Δ* strain expressing the empty vector grew also normal, the *crn1Δ* cells expressing Cpn0572 did not rescue the effect of Cpn0572 and exhibited a reduced growth almost similar to wild type cells expressing Cpn0572. Thus, the results indicate that Crn1p is not crucial for Cpn0572 activity and probably does not mediate Cpn0572-actin interaction. Collectively, the results suggest that Cpn0572 interacts directly with actin.

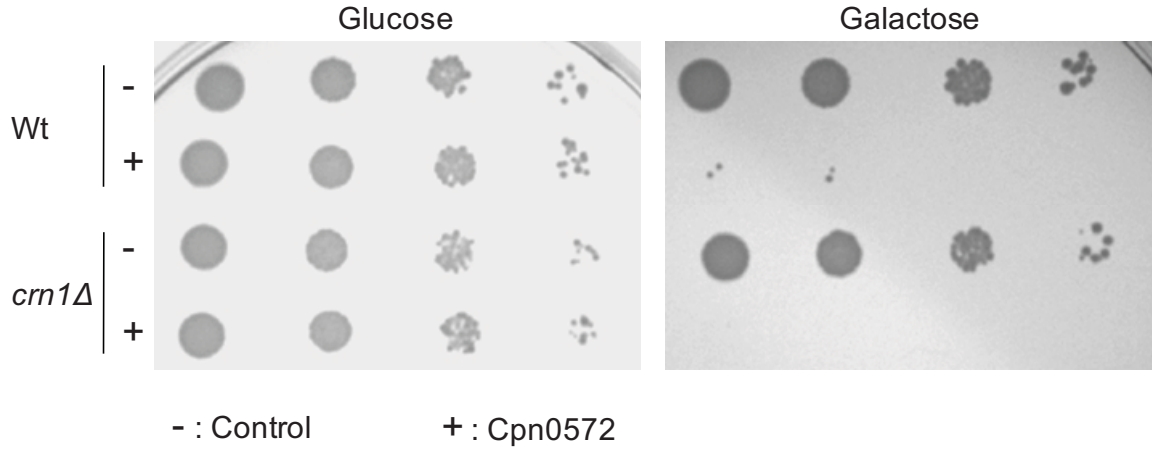

Figure 3-9: The *crn1Δ* does not alleviate the growth phenotype induced by Cpn072 in yeast.
Serial dilution patch test of wild type and the *crn1Δ* strains harboring the empty vector p423GAL1 (-) or the vector expressing *Cpn0572*, pRZ9 (+). Yeast cells were primarily grown for 7-10 generations in a non-inducing medium containing glucose and then dropped on either non-inducing media (glucose) or inducing media (Galactose) to suppress or induce high expression of Cpn0572, respectively. Colony growth was observed after incubation of the plates for 2 days at 30 ^{o}C.

3.3. Domain analysis of the Cpn0572 protein in yeast

3.3.1. Computer based analysis of the Cpn0572 protein identified a conserved domain of unknown function (DUF)

Cpn0572 is relatively a large protein with 755 amino acids. Often large proteins are built from domains, which may represent relatively independent structural units. To facilitate the functional characterization of Cpn0572 protein, we dissected the Cpn0572 protein. A bioinformatic analysis using PFAM web site (http://pfam.sanger.ac.uk/) identified a domain of unknown function (DUF1547, called DUF in this thesis) which is only found in Cpn0572 and its homologous proteins from different *Chlamydia* species suggesting that DUF may play a role in the function of these proteins (Figure 3-10). Remarkably, Cpn0572 contains only one DUF, while the homologous proteins contain more than one DUF. Furthermore, the C-terminal part following DUF in Cpn0572 is significantly longer compared to the other Cpn0572 homologous proteins. Therefore, DUF was used as a basis for dissecting Cpn0572 into shorter domains.

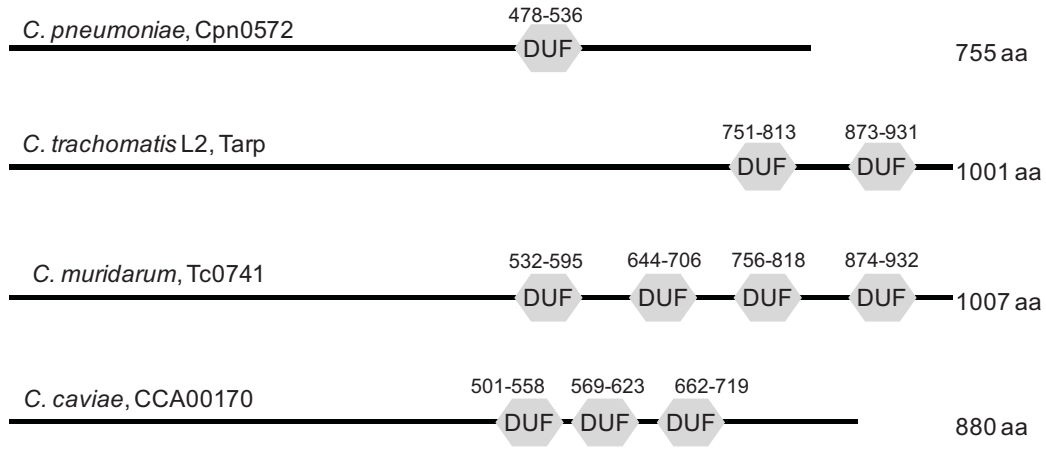

Figure 3-10: Cpn0572 and its homologous proteins from different *Chlamydia* species have a conserved domain of unknown function (DUF). Schematic representation of the primary structures of Cpn0572 and its homologous proteins is shown. The position of DUF in each protein is indicated by the number of the first and last amino acid in each DUF. The length of each protein is indicated at the right side.

3.3.2. DUF is necessary for inducing the severe growth defect and for colocalization with actin structures in yeast cells

To facilitate the functional characterization of Cpn0572 protein, we expressed several domains of Cpn0572 in yeast and tested their ability to induce a growth phenotype using the serial dilution patch test. Initially, to determine the role of the N- terminal and the C-terminal parts of the protein, we expressed domains that are lacking DUF (A and G) or containing DUF (B and H) (Figure 3-11- A). At low level of expression, all cells grew normal and similar to the control cells. At high level of expression, cells expressing A or G

domains grew similarly to control cells. In contrast, cells expressing B or H domains showed a severe growth phenotype, almost similar to that induced by the full length Cpn0572 protein (Figure 3-11-B). These results suggest that DUF is the growth phenotype-inducing domain. The microscopical analysis of yeast cells expressing GFP-Cpn0572-A or GFP-Cpn0572-G fusion proteins revealed that the cells diffused these proteins in the cytosol and showed a normal actin cytoskeleton (Figure 3-12).

Cells expressing either GFP-Cpn0572-H or GFP-Cpn0572-B lost their normal actin structures and cells expressing GFP-Cpn0572-H fusion protein showed clump structures that colocalized with actin clumps but were smaller than those induced by the full length protein. Interestingly, GFP-Cpn0572-B expressing cells showed a completely different pattern with distinct thick cables of the fusion protein that colocalized with thick and long actin cables (Figure 3-12). These results imply that DUF is necessary for interaction of Cpn0572 with actin.

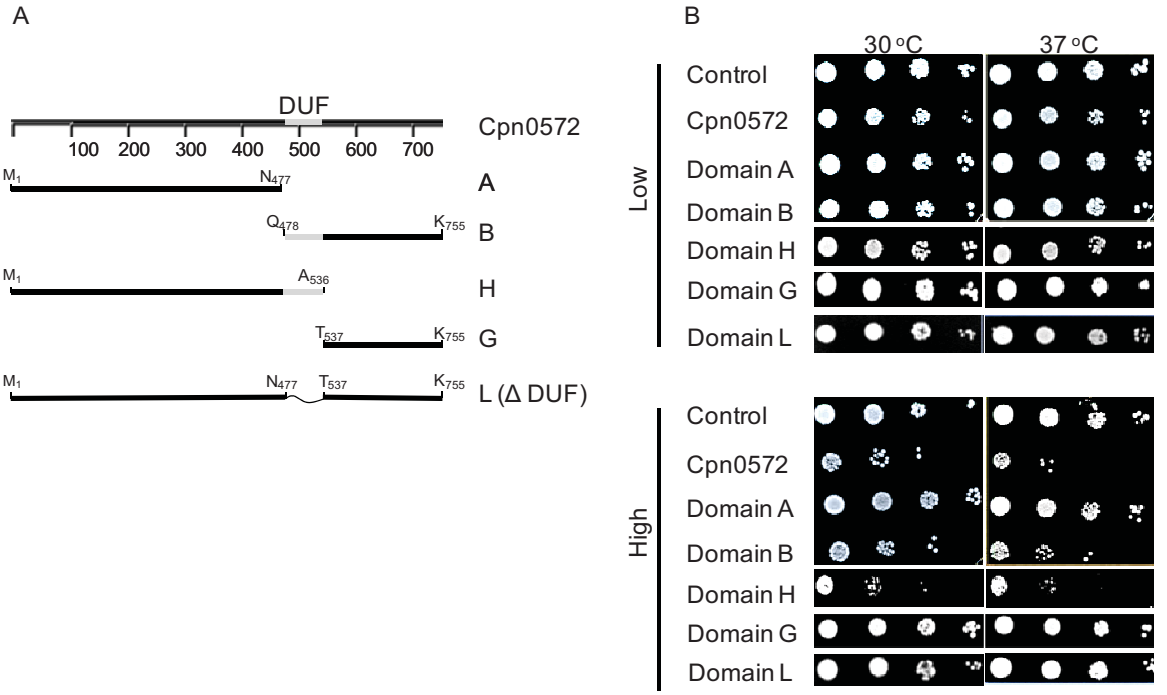

Figure 3-11: DUF is essential to induce a severe growth defect in yeast cells.
A, schematic representation of Cpn0572 domains tested. The dissection of the protein was based on the presence or the absence of DUF with other parts of the protein.
B, serial dilution patch test of cells expressing the domains indicated in (A). DNA fragments encoding the domains were integrated into the p426MET25 vector and transformed into yeast cells. Subsequently, transformants were subjected to serial dilution patch tests. “Low” and “High” indicate conditions mediating low and high expression, respectively.

To further confirm that, we deleted DUF from the full length protein to yield the L domain (Figure 3-11-A) and tested its ability to induce growth and actin phenotypes in yeast. As expected, this domain was unable to induce growth or actin phenotypes in yeast (Figure 3-11-B and Figure 3-12). Collectively, the results suggest that DUF is the only actin-binding region in the protein. The results also show that the C-terminal part of Cpn0572

including DUF can bundle actin raising the possibility that a part of Cpn0572 function is to bundle actin filaments. Furthermore, the N-terminal part of Cpn0572 protein is necessary to induce the formation of actin clumps, however the actin clumps induced by GFP-Cpn0572-H are smaller than those induced by the full length protein. Thus, neither the N-terminal nor the C-terminal parts is sufficient for proper modulation of actin achieved by the full length protein.

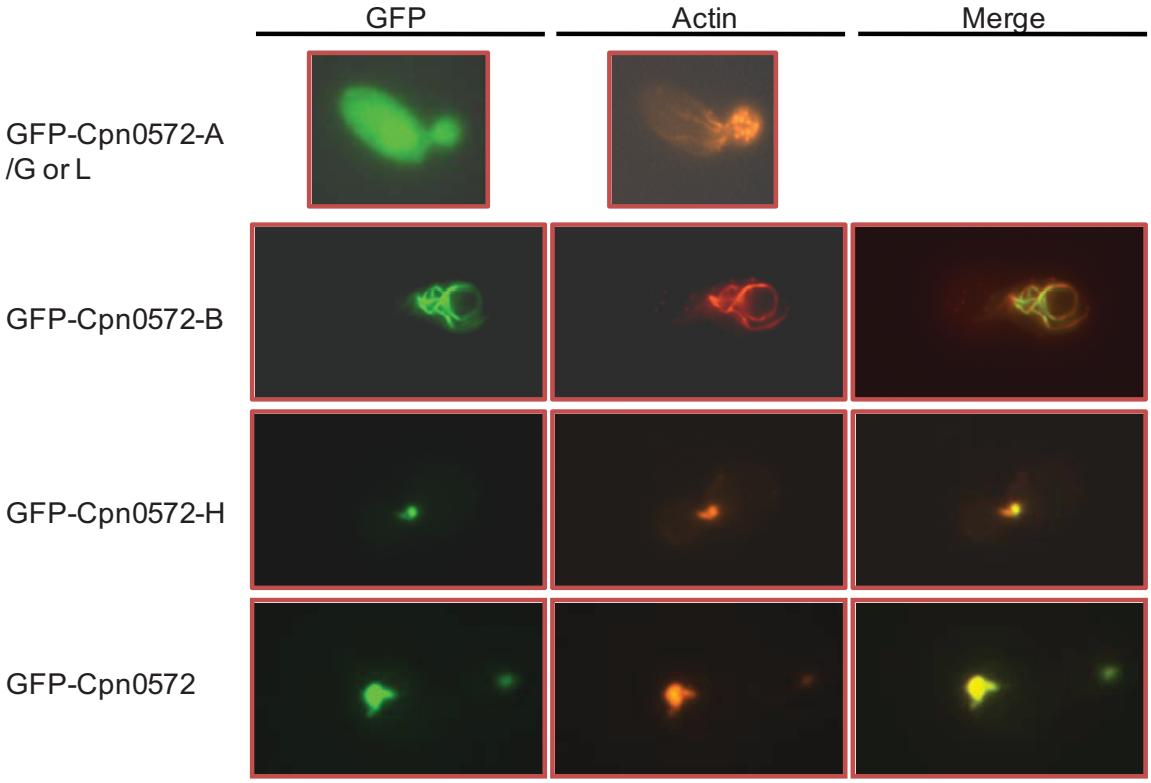

Figure 3-12: DUF is essential for colocalization with and inducing of actin phenotype in yeast.
Actin staining and microscopical analysis of terminal phenotype of actin cytoskeleton in yeast cells expressing GFP-Cpn0572 domains. Cells were grown in inducing selective media until mid-log phase and subsequently fixed with formaldehyde and stained with rhodamine-phalloidin to visualize the actin cytoskeleton.

These results prompted us to further analyze the N-terminal and the C-terminal parts of the Cpn0572 protein. We first dissected the C-terminal part and investigated its role in inducing growth and actin phenotypes in yeast. Therefore, shorter domains within the C-terminus Cpn0572, C (DUF alone), D, E, and K, were analyzed (Figure 3-13-A). Yeast cells expressing Cpn0572-C, -D and -E exhibited a normal viability of yeast cells (Figure 3-13-B).

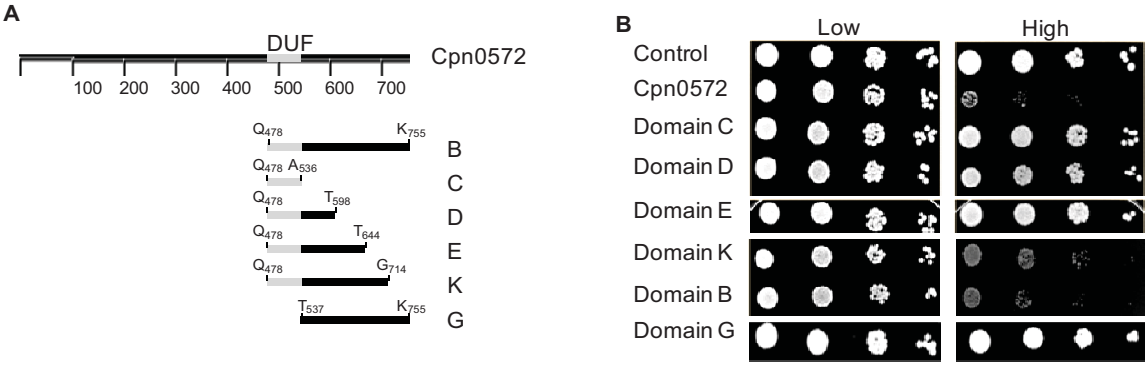

Figure 3-13: DUF is not sufficient to induce a growth defect in yeast cells.
A, schematic representation of the short domains of the C-terminal part of Cpn0572 tested. B, Serial dilution patch test of cells expressing the short domains indicated in (A). Yeast cells expressing the individual domains were subjected to serial dilution patch tests. “Low” and “High” indicate conditions mediating low and high expression, respectively.

The microscopical analysis revealed that the GFP-Cpn0572-C, -D and -E fusion proteins showed colocalization with actin and F-actin bundling activity (Figure 3-14). However, the localization of these domains was not limited to thick actin cables since they were also detectable in the cytosol. This may suggest that shorter domains containing DUF affect the conformation of the protein and subsequently result in weaker interaction with actin. To test that, we expressed longer domain named Cpn0572-K and analyzed it in yeast (Figure 3-13-A). This domain induced a moderate growth phenotype in yeast (Figure 3-13-B). Furthermore, microscopical analysis revealed that yeast cells expressing the fusion protein GFP-Cpn0572-K showed thickened actin cables (Figure 3-14 lower panel). Similar to the fusion protein GFP-Cpn0572-C, -D and –E, GFP-Cpn0572-K colocalized with these thickened actin cables, however less diffused staining of the fusion protein in the cytosol was obtained than when shorter fragments were expressed (Figure 3-14). These results indicate that the interaction of shorter C-terminal domains carrying DUF with actin is probably not as stable as wild type protein and longer domains containing DUF are necessary to stabilize the protein and to properly interact with actin.

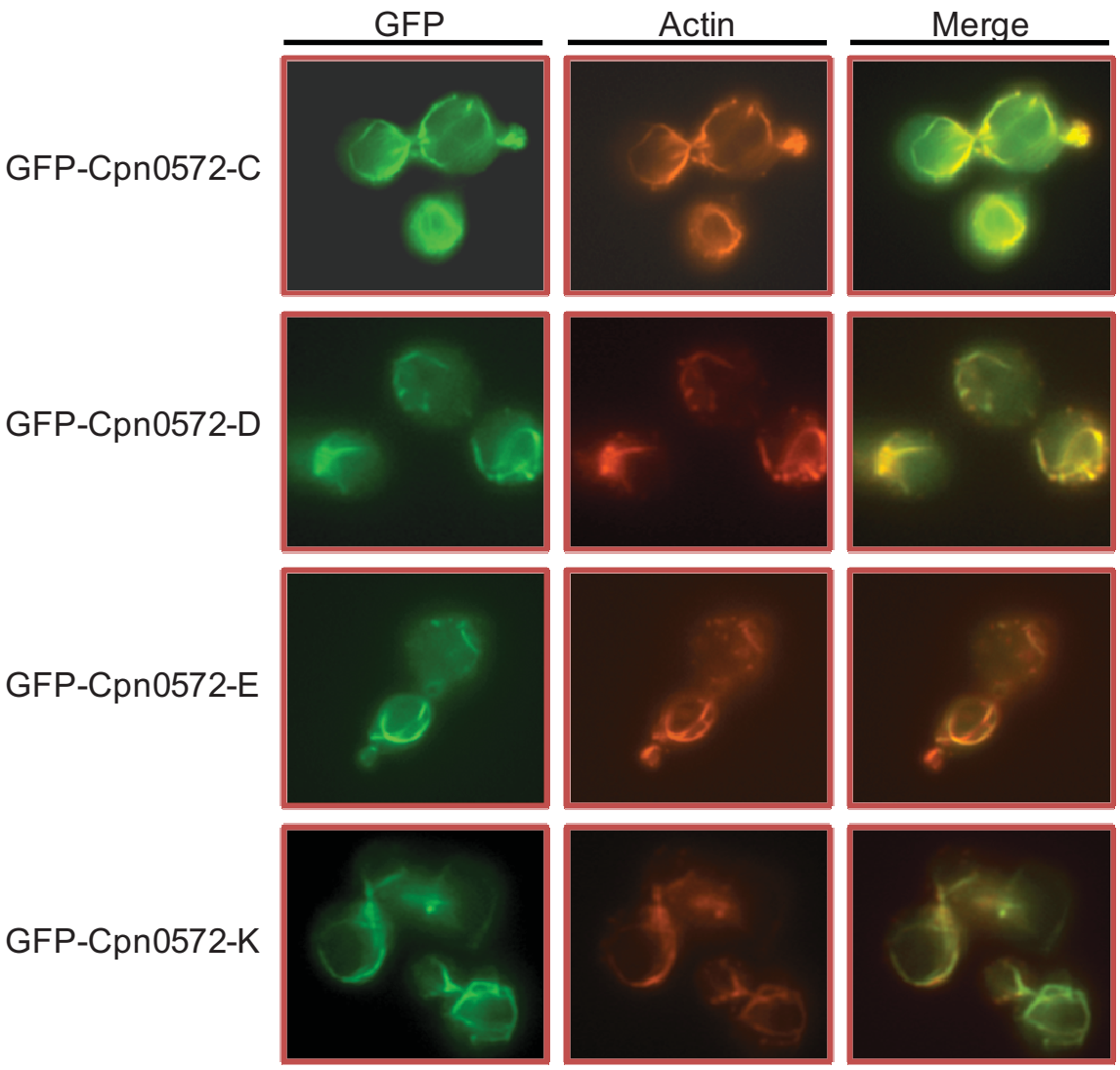

Figure 3-14: DUF is sufficient for colocalization with and inducing of actin phenotype in yeast. Cells were grown in inducing selective media until mid-log phase and subsequently fixed with formaldehyde and stained with rhodamine-phalloidin.

3.3.3. The proline stretch in Cpn0572 is necessary for the formation of actin clumps in yeast

Cpn0572-H, but not Cpn0572-B, transformed the yeast actin cables and patches into small clumps. This suggests that the N-terminal domain is required to induce actin clumping in yeast. To further analyze the N-terminal domain, we performed a manual analysis of the amino acids sequence of the N-terminal domain of Cpn0572 and found a stretch of proline amino acids surrounding a central glutamic acid upstream of DUF (P_{454}PPPGPPP$_{461}$). Many actin-modulating proteins have proline-rich domains that are necessary for modulating actin polymerization and recruitment, for instance formin and N-WASP (Pistor, Chakraborty et al. 1995; Mahoney, Rozwarski et al. 1999). Therefore, we generated mutations in the full length protein and in the Cpn0572-H fragment, in which the proline stretch was substituted by an alanine stretch to yield Cpn0572-ALA and Cpn0572-

H-ALA, respectively (Figure 3-15-A). As shown previously, cells expressing the wild type Cpn0572 or Cpn0572-H showed severe growth phenotypes. Yeast cells expressing either Cpn0572-ALA or Cpn0572-H-ALA showed almost the same severe growth phenotype as the corresponding wild type forms (Figure 16-B). However, both mutants, when they were expressed as a GFP fusion proteins, lost the ability of clumping actin as it was achieved by the wild type proteins and instead cells expressing GFP-Cpn0572-ALA showed thick and tangled actin cables whereas cells expressing Cpn0572-H-ALA showed untangled-thick cables that were in parallel to the mother-bud cell axis (Figure 16-A). Loss of actin clumping was not due to reduced expression of the fusion proteins, as all proteins tested were expressed at similar levels in the cells (Figure 16-B). The results confirm our hypothesis that the proline stretch in Cpn0572 protein has a role in modulating actin.

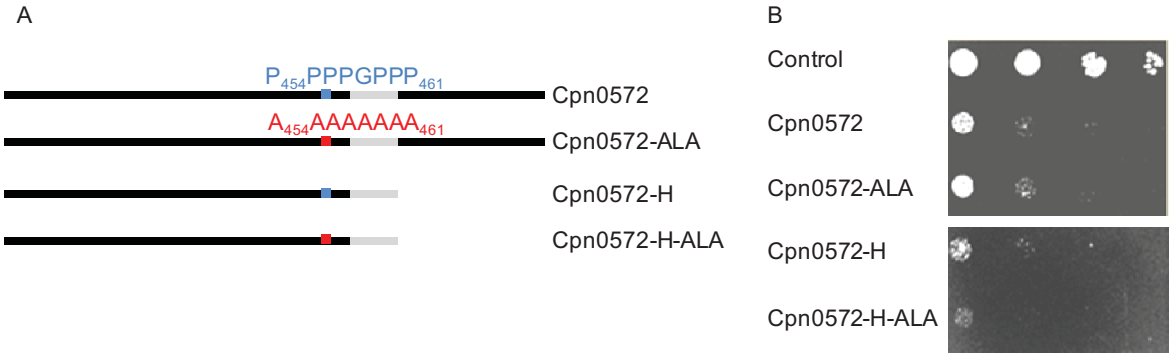

Figure 3-15: Mutating the proline stretch in Cpn0572 does not alleviate the growth phenotype induced by Cpn072 in yeast.
A, schematic representation showing the structure of the Cpn0572 protein and the H domain containing the proline stretch and the mutations generated by replacing the proline stretch (blue box) with alanine stretch (red box).
B, serial dilution patch test of cells expressing wild type Cpn0572 and mutant forms as indicated in (A). Cells were grown in liquid inducing selective media and subsequently dropped onto inducing selective media agar plates.

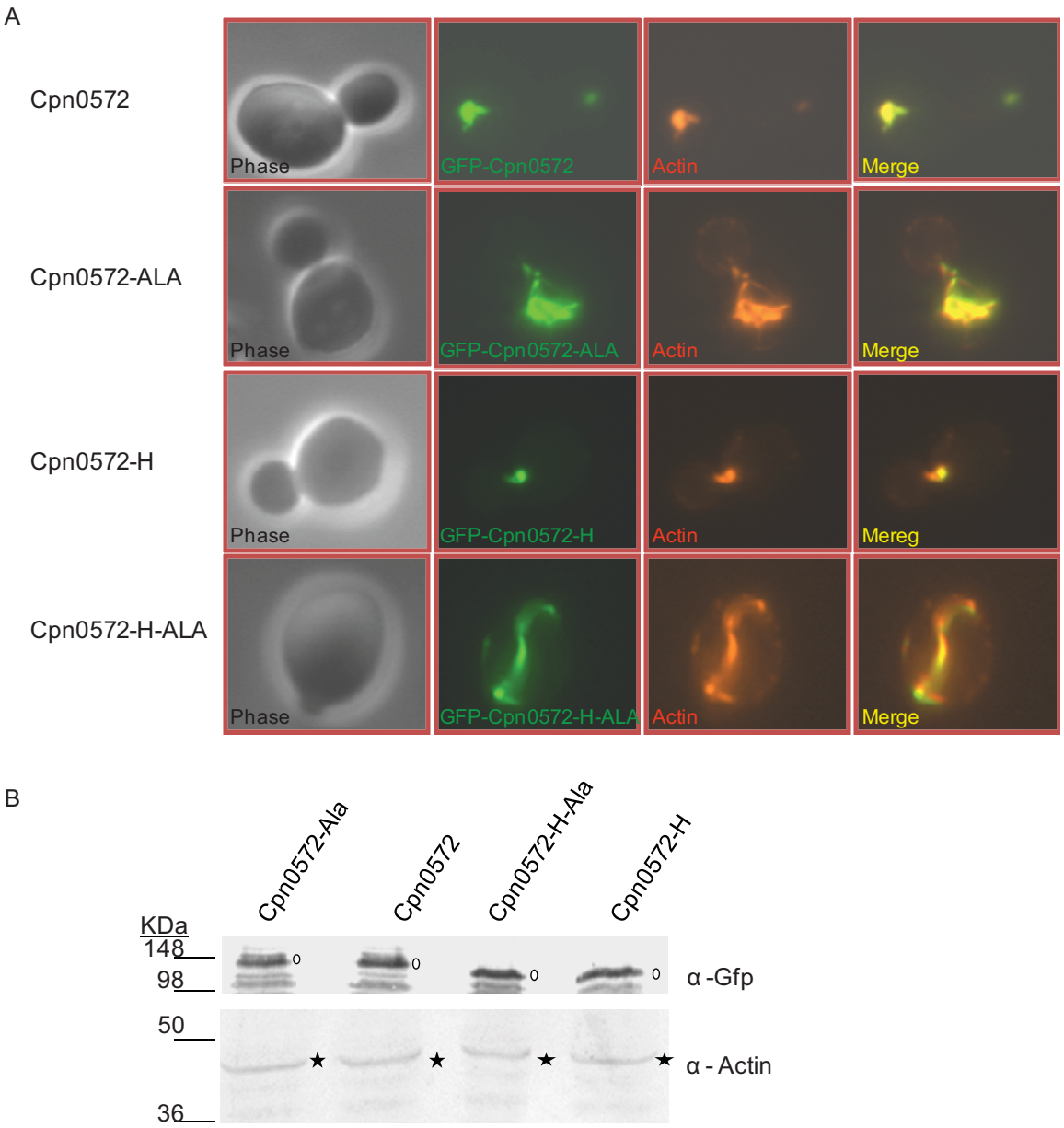

Figure 3-16: Mutating the proline stretch in Cpn0572 disrupts the proper function of Cpn0572 in clumping the actin cytoskeleton of yeast.
A, actin phenotypes induced by Cpn0572, Cpn0572-H and mutant forms. Cells were grown in inducing selective media until mid-log phase and subsequently fixed with formaldehyde and stained with rhodamine-phalloidin.
B, equal cell numbers of the different yeast strains were harvested and whole cell protein extracts were prepared for SDS-PAGE and western blot analysis. The membranes were either incubated with α-GFP antibody followed with α-rabbit antibody to visualize GFP fusion proteins (open circles in the upper membrane) or with α-Actin antibody followed with α-mouse antibody to visualize actin (stars in the upper membrane). Bands were visualized using the alkaline phosphatase method. Proteins sizes are indicated in KDa.

3.3.4. Sequence analysis of DUF identified conserved amino acids

We performed multiple sequence alignments of DUFs from the Cpn0572 homologous proteins in different *Chlamydia* species using the MultAli program (http://bioinfo.genotoul.fr/multalin/multalin.html). This analysis revealed that DUF consists of many conserved amino acids (Shaded in blue in figure 3-17) and in particular, most of

these conserved amino acids are hydrophobic (written in red). Hydrophobic amino acids are known to stabilize the protein core (Abkevich, Gutin et al. 1994; Parthasarathy and Murthy 1997; Berka, Hobza et al. 2009). Therefore, we assumed that the ability of Cpn0572 to interact with actin would be performed by these hydrophobic amino acids.

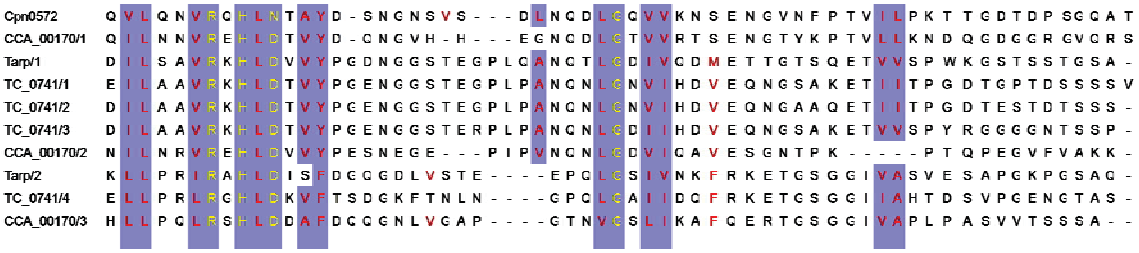

Figure 3-17: Multiple of sequence alignments analysis of DUF from Cpn0572 and the homologous proteins from different *Chlamydia* species. The conserved amino acids are shaded in blue. Hydrophobic amino acids are in red while non-hydrophobic amino acids in yellow.

3.3.5. The conserved hydrophobic amino acids in DUF are essential for the Cpn0572-induced growth and actin phenotype

We further investigated the role of the conserved hydrophobic amino acids within the DUF domain of Cpn0572 by replacing the conserved hydrophobic amino acid residues with hydrophilic or less hydrophobic amino acid residues. Therefore, we generated two mutant forms of Cpn0572 that have mutations in these conserved hydrophobic amino acids. In the first mutant (Cpn0572-M1), the first three conserved hydrophobic amino acid residues in DUF were replaced with hydrophilic amino acid residues (L480N, V483N, L487N). In the second mutant (Cpn0572-M2), three of the hydrophobic amino acid residues in the middle region of DUF were replaced with a less hydrophobic amino acid residue (L505A, V508A, V509A). These mutation forms are schematically represented in (Figure 3-18-A). Yeast cells expressing any of these Cpn0572 mutant forms did not affect yeast growth suggesting that these hydrophobic amino acids are crucial for Cpn0572-dependent growth phenotype (Figure 3-18-B). The inability of these mutant forms to induce growth phenotype was not due to reduced expression of the fusion proteins, as all proteins tested were expressed at similar levels in the cells (Figure 3-18-C). Additionally, cells expressing the fusion proteins GFP-Cpn0572-M1 or GFP-Cpn0572-M2 showed a uniform cytosolic distribution of the fusion protein instead of the clumps shown by the wild type GFP-Cpn0572 fusion protein and the cells showed almost normal actin cytoskeleton (Figure 3-18-D). These results suggest that the conserved hydrophobic amino acids in DUF are essential for interaction with actin.

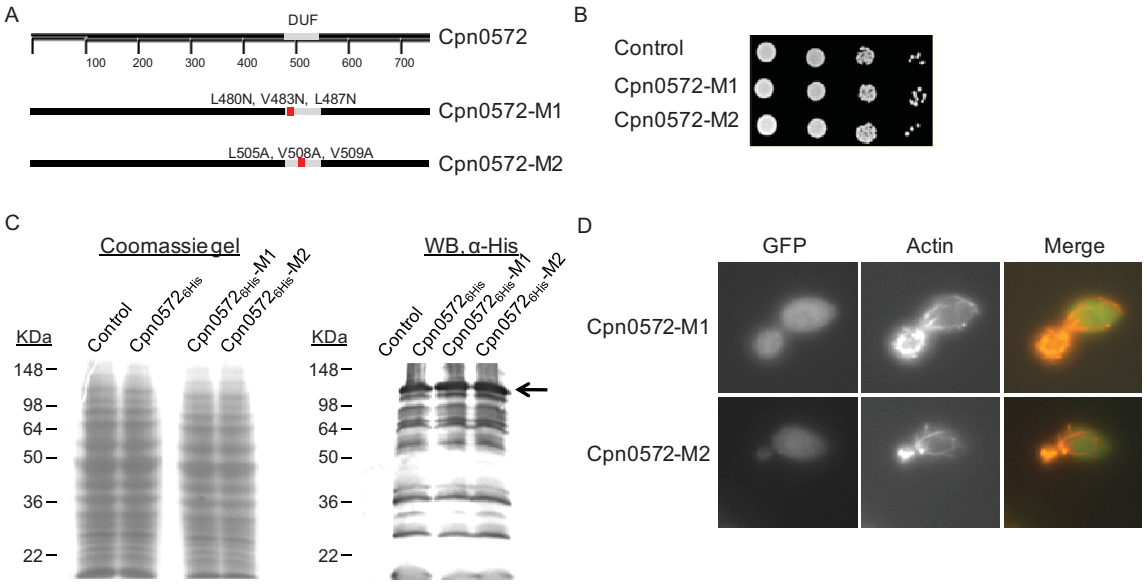

Figure 3-18: Mutations in the conserved hydrophobic amino acids within DUF lead to the loss of Cpn0572 function.

A, schematic representation showing the structure of the Cpn0572 protein and the mutations generated.

B, serial dilution patch test of cells expressing wild type Cpn0572 and mutant forms as indicated in (A). Cells were grown in liquid inducing selective media and subsequently dropped onto inducing selective media agar plates.

C, equal cell numbers of the different yeast strains were harvested and whole cell protein extracts were prepared for SDS-PAGE and western blot analysis. Expression of $Cpn0572_{6His}$ and mutant forms fusion proteins were detected with α-His antibody followed by a secondary antibody and the bands were visualized using the alkaline phosphatase method. Arrows indicated the corresponding bands of $Cpn0572_{6His}$ fusion protein.

D, actin phenotypes induced by Cpn0572 truncated forms. Cells expressing the wild type Cpn0572 or the truncated forms were grown under inducing condition until mid-log phase. Subsequently fixed with formaldehyde and stained with rhodamine-phalloidin.

3.4. Cpn0572 interacts with mammalian actin

Our observations in yeast revealed that Cpn0572 modulates drastically the actin cytoskeleton. Therefore, we next investigated whether the activity of Cpn0572 in interacting with and modulating actin is conserved from yeast to mammals.

3.4.1. Cpn0572 interacts with actin from human epithelial HEp-2 cell lysates

The experiments in yeast had revealed that the C-terminal domains of Cpn0572 (C and B) were sufficient to interact with yeast actin. To test directly the ability of these domains to interact with mammalian actin, we expressed GST alone, GST fused to Cpn0572, Cpn0572-C or Cpn0572-B in *E. coli* (Figure 3-19-A). Recombinant proteins were purified using Glutathione-Sepharose beads and analyzed by western blot analysis. The proteins bands were found at the expected size, however degradation of these fusion proteins were also obtained (Figure 3-19-B, lanes 4 and 6). Subsequently, GST pull-down assays were carried out by incubation of GST or GST fusion proteins-coated glutathione sepharose beads with HEp-2 cell lysates. Bound proteins were eluted and subjected for SDS-PAGE. The coomassie gel showed that GST alone did not precipitate any HEp-2 protein (Figure 3-19-B, lanes 2 and 3). Due to high degradation of GST-Cpn0572, it was hard to identify any band corresponding to HEp-2 cell proteins (compare lanes 4 and 5). Remarkably, GST-Cpn0572-B and GST-Cpn0572-C precipitated a HEp-2 protein of around 43 KDa (Figure 3-19-B, lanes 6-9). Immunoblots using α-actin antibody revealed that the precipitated protein is actin (Figure 3-19-C, lanes 7and 9). Correspondingly, the immunoblots analysis showed also that the full length protein can precipitate actin (Figure 3-19-C, lane 5). These results showed that Cpn0572 and its C-terminal domains interact biochemically with actin.

To test if the conserved hydrophobic amino acids in DUF are necessary for this interaction, we tested the ability of the two mutant forms GST-Cpn0572-BM1 and GST-Cpn0572-BM2 to pull down actin from HEp-2 cell lysates. However, both mutants were not able to precipitate actin from HEp-2 cell lysates (Figure 3-19-B and C, lanes 11 and 13).

Thus, the results indicate that Cpn0572 interacts with mammalian actin via the C-terminal domain and the conserved hydrophobic amino acids in DUF are necessary for this interaction. The results also suggest that probably no other interacting partners can be precipitated by Cpn0572. However, the results do not reveal if Cpn072 binds actin directly.

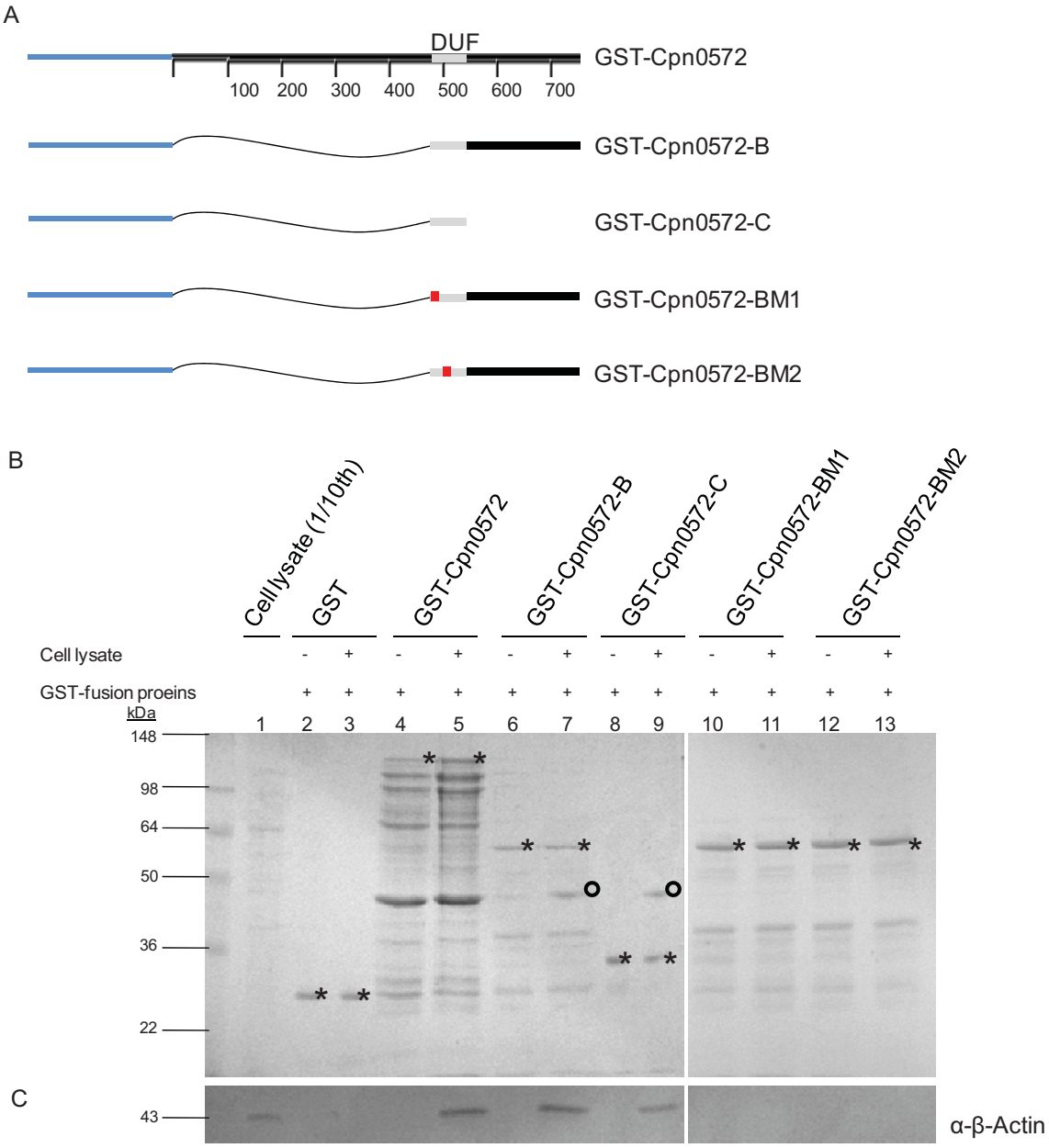

Figure 3-19: The Cpn0572 protein interacts with actin from HEp-2 cells lysate via its C-terminal domain.
A, schematic representation of Cpn0572 domains tested in this experiment.
B, Cpn0572 and its C-terminal domains pull down a HEp-2 cells protein of 43 KDa. GST or GST fusion proteins in (A) bound to beads were incubated with equal amount of lysates from HEp-2 cells. The bound proteins and the corresponding input lysates were resolved by SDS-PAGE. Coomassie gel is shown. Stars mark the bands corresponding to each fusion protein while circles mark the HEp-2 protein pulled down by the GST fusions. Other unmarked bands indicate the degradation of the fusion proteins.
C, the C-terminal domains of Cpn0572 pull down actin from HEp-2 cell lysate. Western blot analysis of the eluted proteins and total cell extracts as described in (C). Actin was detected with an α-β-actin antibody followed by a secondary antibody and the bands were visualized using the alkaline phosphatase method.

3.4.2. Cpn0572 binds mammalian F-actin directly *in vitro*

The pull-down assays had shown that Cpn0572 interacts with mammalian actin. However, it was unclear whether Cpn0572 bound actin directly or indirectly. To address this question, mammalian G-actin protein purified from rabbit muscles were mixed with actin polymerization buffer to yield F-actin. Generated F-actin can be separated from G-actin in a sedimentation assay as schematically described in Figure 3-20-A. Subsequently, F-actin and bound protein were separated from soluble components in a sedimentation assay and analyzed by SDS-PAGE. The majority of actin was found in the pellet while less actin was in the supernatant indicating that F-actin is pelleted under these conditions (Figure 3-20-C, lanes 1 and 2). Furthermore, F-actin was incubated alone with GST-Cpn0572-C or the mutant form GST-Cpn0572-CM2 (Figure 3-20-B). Subsequently, the sedimentation assay showed that in the presence of GST-Cpn0572-C, the majority of actin was also found in the pellet (lanes 4), while GST-Cpn0572-C was found in equal amounts in both the pellet and the supernatant (lanes 3 and 4). In the presence of the mutant form GST-Cpn0572-CM2, the majority of actin was also found in the pellet (lanes 6), however the mutant GST-Cpn0572-CM2 was only found in the supernatant (lanes 5). Thus, these results indicate that GST-Cpn0572-C binds actin directly and at least the hydrophobic amino acids mutated in GST-Cpn0572-CM2 are necessary for this direct interaction.

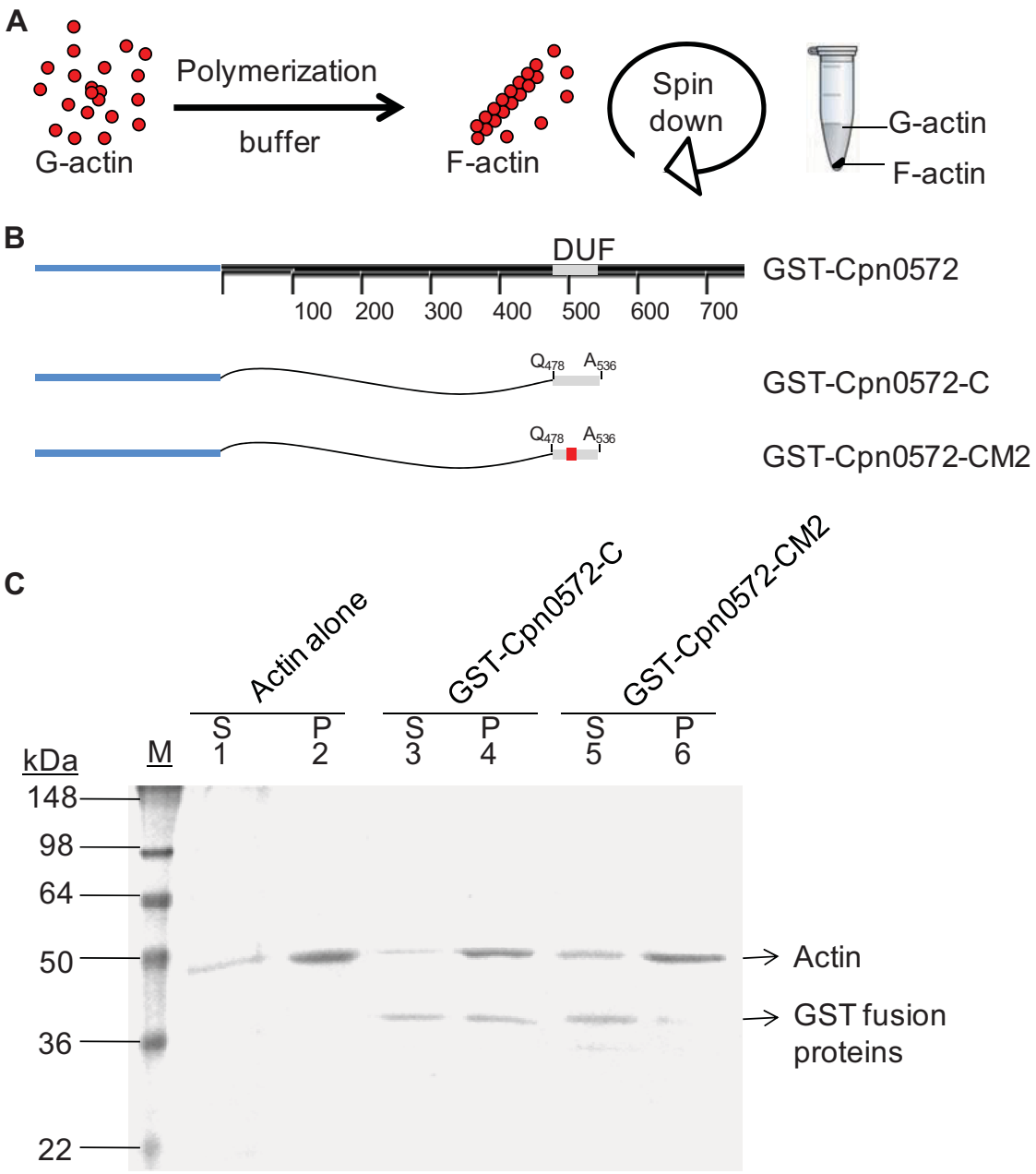

Figure 3-20: DUF binds F-actin directly *in vitro*.
A, schematic representation shows the experimental set-up to generate and separate F-actin out of G-actin *in vitro*.
B, schematic representation of Cpn0572 domains tested in this experiment.
C, a co-sedimentation assay was used to study the ability of GST-Cpn0572-C and the mutant forms GST-Cpn0572-CM2 to bind F-actin. The assay was started by mixing 2 µM pre-polymerized rabbit actin filaments with 2 µM of the GST fusions. The mixtures were incubated for 10 minutes at room temperature before F-actin and bound recombinant proteins were sedimented by centrifugation. Then supernatant and sediment were resolved by SDS–PAGE. Proteins are indicated on the right.

3.4.3. Cpn0572 colocalizes with actin in mammalian cells transfected with a GFP-Cpn0572-expression vector

To investigate whether Cpn0572 colocalizes with mammalian actin, the mammalian GFP-expressing vector pBYE or the GFP-Cpn0572-expressing vector pBYE1 was transfected into the mammalian HEK-293T cells and the localization of the expressed proteins and their effect on the actin cytoskeleton were studied by immunofluorescence. In control cells, expression of GFP alone resulted in a diffuse distribution of GFP throughout the cytoplasm and the actin cytoskeleton appeared normal with some actin fibers (Figure 3-21, upper panel). In contrast, GFP-Cpn0572-expressing cells showed distinct structures of the fusion protein including a bright signal. These cells lost the normal actin cytoskeleton structure and instead showed actin clumps with a reduced number of actin filaments (Figure 3-21, middle panel). Moreover, the fusion protein colocalized with actin fibers and clumps suggesting that the actin clumps were caused by GFP-Cpn0572. Thus, the effect of Cpn0572 on mammalian actin cytoskeleton is similar to that on yeast actin cytoskeleton.

To investigate if the actin phenotypes induced by Cpn0572 mutant forms are conserved in yeast and mammalian cells, we expressed the mutant GFP-Cpn0572-ALA in HEK-293 cells (Figure 3-21).

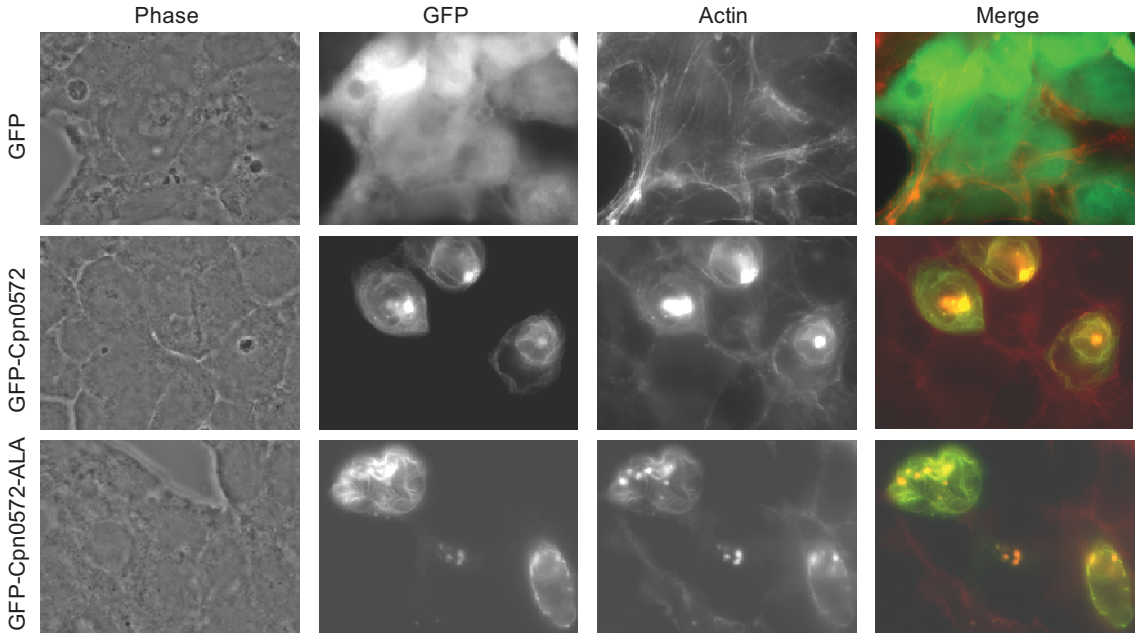

Figure 3-21: Cpn0572 colocalizes with and induces the formation of actin clumps in HEK-293 transfected cells. HEK-293 cells were transfected with the control vector (GFP), the pBYE1 vector (GFP-Cpn0572) or the pBYE1-ALA vector (GFP-Cpn0572-ALA) using the calcium chloride method. After 24 h, transfected cells were fixed, stained with Rhodamine-phalloidin and analyzed using fluorescence microscopy.

The cells showed distinct structures of the fusion protein that colocalized with actin, however the fusion protein had partially lost the ability of clumping actin since more actin

filaments and smaller clumps were found in the cells compared to cells expressing the wild type protein (Figure 3-21, lower panel). Similar to the observation in yeast, these results emphasize that the proline stretch in Cpn0572 is necessary for its actin clumping activity in mammalian cells

To confirm that the conserved hydrophobic amino acids in DUF are necessary for interacting with and modulating of mammalian actin cytoskeleton *in vivo*, the GFP-Cpn0572 mutant forms GFP-Cpn0572-M1 and GFP-Cpn0572-M2 were expressed in HEK-293 cells. Surprisingly, cells expressing any of these mutants showed the fusion proteins into tangled cables. However, these mutant forms of Cpn0572 did not colocalize with actin and the actin cytoskeleton looked similar to that of cells expressing GFP alone (Figure 3-22). These results emphasize that the hydrophobic amino acids in DUF are necessary for colocalization with and modulating of mammalian actin.

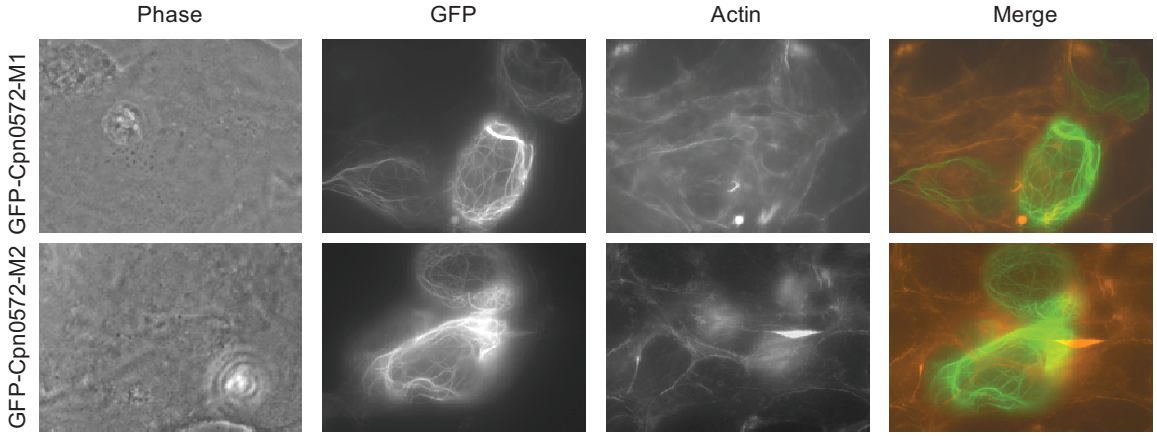

Figure 3-22: Mutations in the conserved hydrophobic amino acids in DUF lead to the loss of Cpn0572 function and its colocalization with the actin cytoskeleton of HEK-293 transfected cells. HEK-293 cells were transfected with the pBYE1-M1 (GFP-Cpn0572-M1) or the pBYE1-M2 vector (GFP-Cpn0572-M2) using the calcium chloride method. After 24, transfected cells were fixed, stained with Rhodamine-phalloidin and analyzed using fluorescence microscopy.

3.5. The role of Cpn0572 in modulating the actin cytoskeleton

Yeast cells expressing Cpn0572 transformed the wild type actin cytoskeleton into clumps, and its C-terminal domains induced the formation of highly polymerized thick actin cables. Interestingly, these actin phenotypes have been previously described in yeast under certain circumstances. For example, the formation of actin clumps has been observed in yeast cells exposed to the actin-stabilizing toxin jasplakinolide, which inhibits actin depolymerization and enhances actin polymerization (Ayscough 2000). It has been also reported in the double mutant strain *aip1Δ cof1-6*, where actin clumps are highly stabilized due to a defect in actin depolymerization (Rodal, Tetreault et al. 1999). Interestingly, similar to yeast cells expressing the C-terminal domains of Cpn0572, the deletion strain *aip1Δ* does not show these actin clumps and instead it shows thickened actin cables that are highly stabilized against the actin destabilizing drug Lat-A (Okada, Ravi et al. 2006). Therefore, we assumed that Cpn0572 has at least two activities in modulating actin, inhibiting actin depolymerization and enhances actin polymerization.

3.5.1. The role of Cpn0572 in actin depolymerization

3.5.1.1. Cpn0572 inhibits actin depolymerization in yeast *in vivo*

Actin clumps and thickened actin cables induced in yeast cells expressing Cpn0572 or its C-terminal domains are similar to those actin phenotypes in yeast strains that have a defect in actin depolymerization and subsequently stabilize actin structures (Ayscough 2000; Okada, Ravi et al. 2006). In yeast, actin depolymerization is regulated by Cof1p in corporation with Aip1p. (Figure 3-23-A and –B, upper panels). In the absence of *AIP1* gene, Cof1p decorates actin filaments and results in stabilized-thickened actin cables (Figure.3-24-A and –B, lower panels).

Alterations in actin depolymerization can be tested experimentally *in vivo* using Lat-A, which binds to actin monomers and blocks assembly of new F-actin. Yeast actin cytoskeleton consists of actin cables and patches (Figure 3-24-A). Actin cables are bundles of actin filaments whereas actin patches are networks of branched actin filaments (Amberg 1998; Young, Cooper et al. 2004). Each filament is composed of two strands of actin monomers that interact with each other (Figure 3-24-B). Actin filament has two ends, the plus end where actin polymerizes and the minus end where Cof1p and Aip1p bind to induce actin depolymerization (Figure 3-24-C). Since the turnover rate of yeast actin cytoskeleton is rapid, Lat-A can disrupt the actin cytoskeleton within a few minutes (5-10

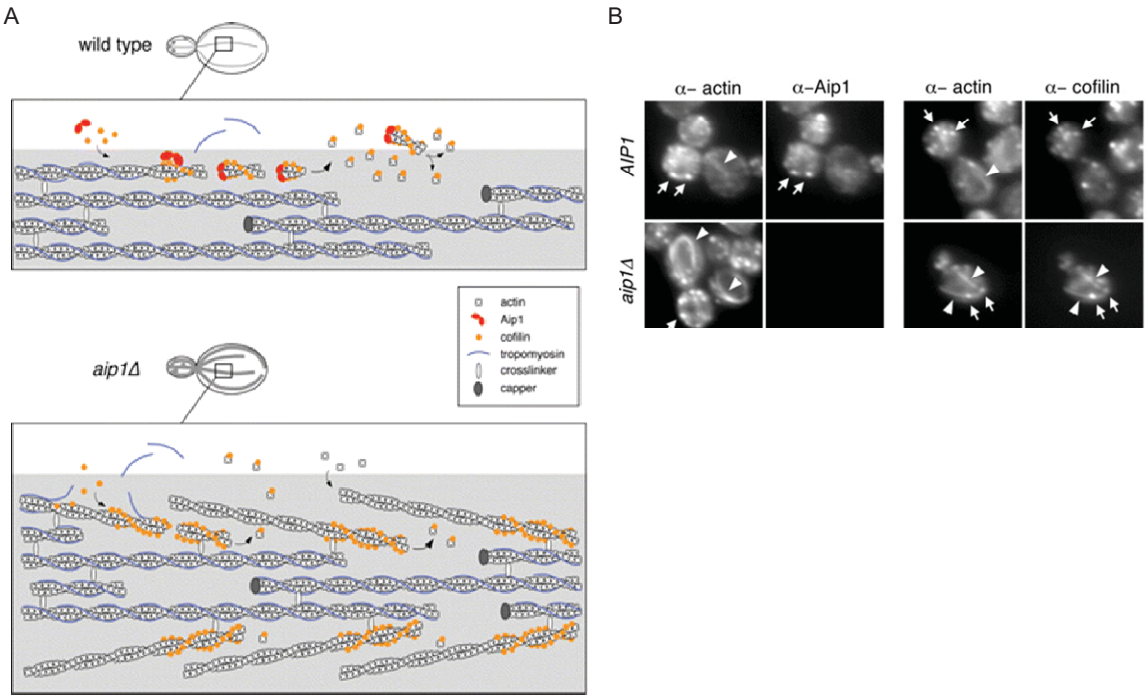

Figure 3-23: The role of Aip1 and Cof1p in actin depolymerization (taken from (Okada, Ravi et al. 2006).
A, a model for Cof1p and Aip1 cellular function: Cof1p binds cooperatively to actin filaments in cables, helping to displace tropomyosin from a subset of filaments. The fate of Cof1p-severed filaments differs greatly depending on whether Aip1 is available. In wild-type cells, Aip1 may assist Cof1p in severing filaments and then rapidly caps the new barbed ends of filaments generated by severing. This leads to rapid net disassembly of those short filaments from their pointed ends. Thus Cof1-decorated filaments in actin cables are extremely short-lived and thus not easily detected in wild-type cells. However, in *aip1Δ* cells, Cof1p severing generates uncapped barbed ends of filaments, which either reanneal or undergo rapid growth, leading to cable thickening. Further, in *aip1Δ* cells, Cof1p -decorated of these cables can be detected by immunostaining because the filaments do not turnover as rapidly as in wild-type cells.
B, actin cytoskeleton organization and Aip1 and Cof1p localization in wild-type and *aip1Δ* cells. Cells with the designated genotypes were double-labeled with anti-actin and anti-Aip1 antibodies (left panels) or anti-actin and anti- Cof1p antibodies (right panels). Arrowheads point to actin cables; arrows point to actin patches.

minutes) depending on the Lat-A concentration and the strain (Okada, Ravi et al. 2006). However, Lat-A does not alter the disassociation of actin from filaments (Ayscough, Stryker et al. 1997; Belmont and Drubin 1998). Thus, Lat-A can be used to measure the rate of actin depolymerization *in vivo* as described in Figure 3-24-C (Coue, Brenner et al. 1987; Okada, Ravi et al. 2006).

To test if the actin clumps induced by Cpn0572 are more stable against actin depolymerization than those observed in control cells, yeast cells expressing GFP alone or GFP-Cpn0572 were exposed to Lat-A and the fate of the actin cytoskeleton was examined at different time points by immunofluorescence microscopy using phalloidin-rhodamine staining. Without Lat-A, about 88 % of GFP-expressing cells showed regular actin cables and patches (Figure 3-25-A and -B, see at time zero). In contrast GFP-Cpn0572 expressing cells transformed the wild type actin into clumps (Figure 3-25-A and -B, see at time zero). In the presence of Lat-A, all cells expressing GFP alone showed no

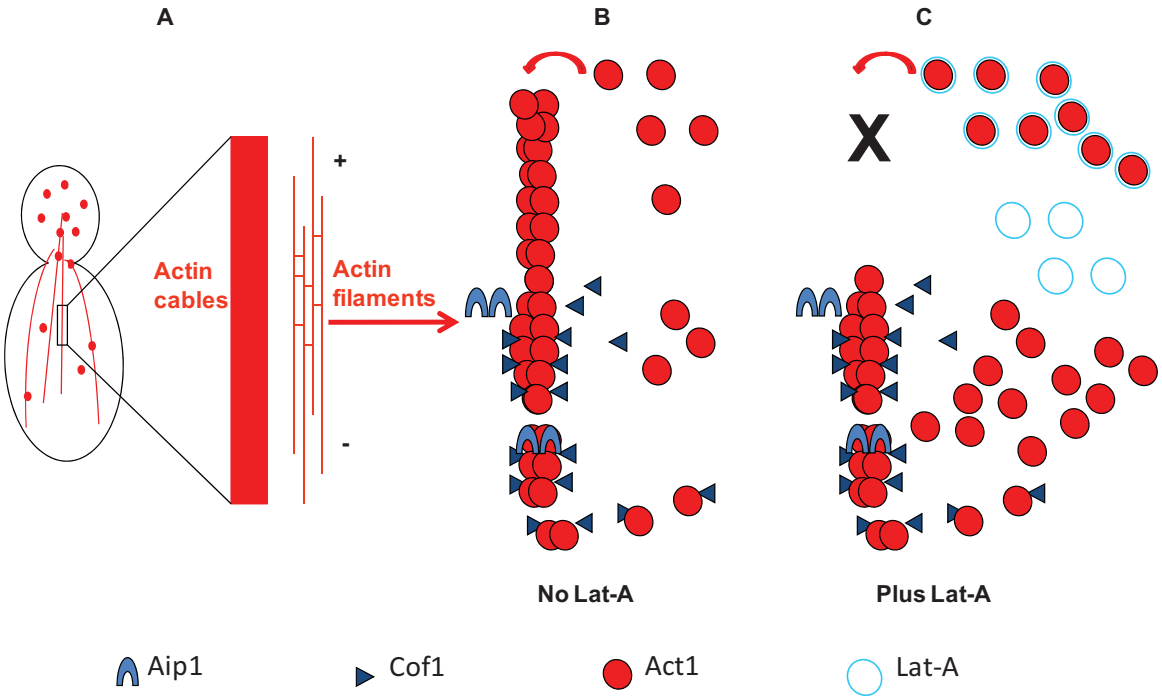

Figure 3-24: The scheme shows the effect of Lat-A on actin assembly in yeast.
The yeast actin cytoskeleton consists of actin cables and patches (A). Actin cables are bundles of F-actin. F-actin is a double-helical filament. G-actin association into F-actin leads to actin polymerization at the barbed end (+ end) while actin disassociation from F-actin at the pointed end (- end) leads to actin depolymerization due to the binding and severing activity of Cof1p in a process enhanced by Aip1p (B). In the presence of Lat-A, Lat-A binds G-actin and prevents its association into F-actin which results in repression of actin polymerization and thus no actin cables can be detected in Lat-A treated cells(C).

visible actin cables after 5 minutes exposition to Lat-A. However, actin patches were still visible even after 1 h exposition to Lat-A (Figure 3-25-A and B). In contrast, GFP-Cpn0572-expressing cells showed actin clumps even after 1 h exposition to Lat-A (Figure 3-25-A and -C). Thus, these results suggest that Cpn0572 inhibits actin depolymerization and yielding stabilized actin clumps.

We next asked if the thickened actin cables induced by the expression of the C-terminal domains GFP-Cpn0572-B and GFP-Cpn0572-C are also resistant to lat-A treatment and stabilized. As shown previously, these proteins colocalized with actin and transformed actin cables into thickened actin cables (Figure 3-26-B, left side in middle and lower panels). In this experiment, we prolonged exposition time of Lat-A to test how long the thickened actin cables induced by these domains of Cpn0572 were stabilized and can resist the effect of Lat-A. After 1 h exposition of Lat-A, GFP-expressing cells showed no visible actin cables (Figure 3-26-A and -B, right side in upper panel). In contrast, yeast cells expressing the Cpn0572 domains showed stabilized actin cables albeit to different degrees. Remarkably, actin was stable against Lat-A in almost 100% of yeast cells expressing GFP-Cpn0572-B in a similar matter as when full length Cpn0572 was expressed. This was also the case even after 4 h of Lat-A treatment. In contrast, yeast

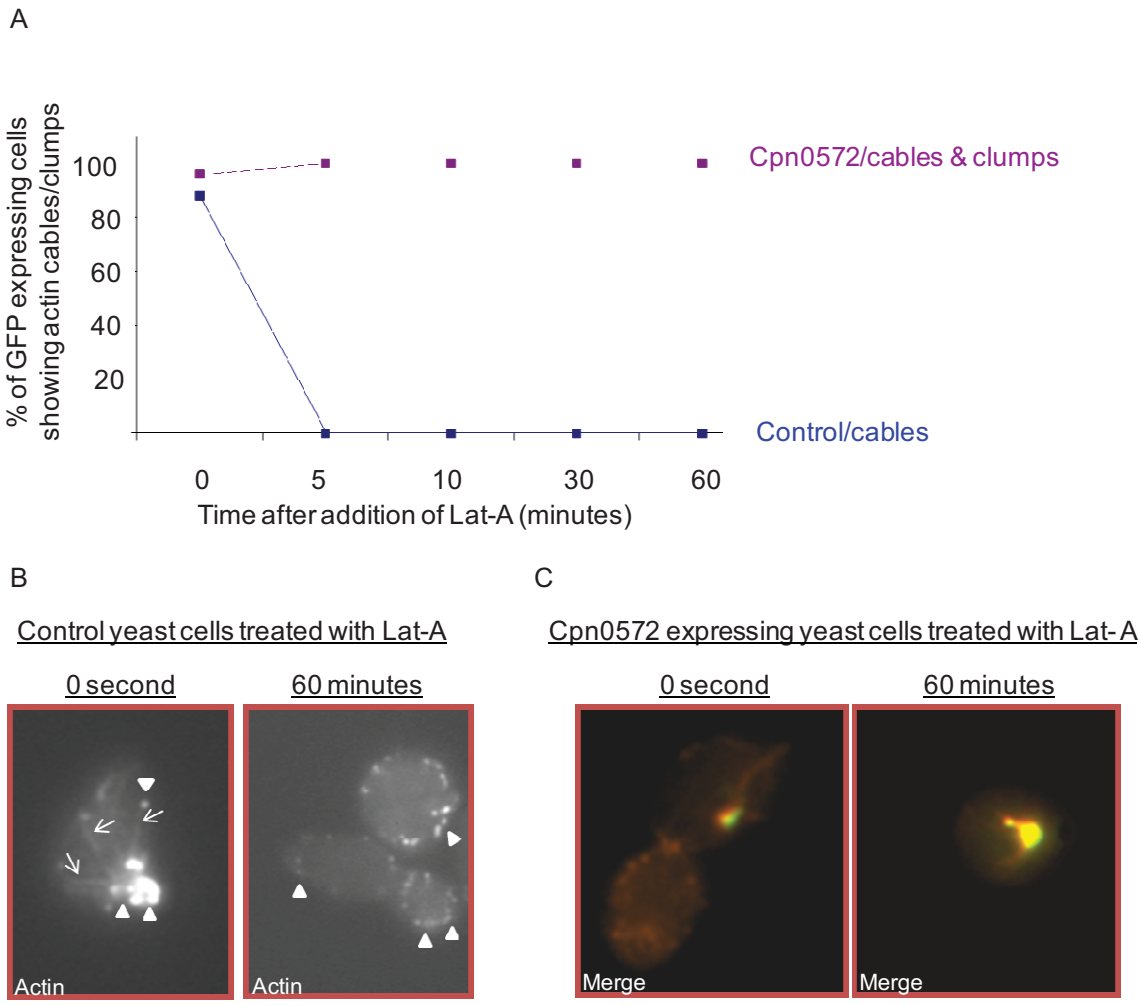

Figure 3-25: Cpn0572 induced actin structures are resistant to Lat-A.
A, yeast cells carrying pRZ1 vector (GFP-Cpn0572) or the GFP expressing vector (Control) were grown in inducing selective media until mid-log phase. Portion of cells were collected and fixed with formaldehyde either before (non Lat-A treated control cells) or at different time points after exposition to Lat-A (final concentration 2.5 µM). Subsequently fixed cells were stained with Rhodamine-phalloidin. Cells showing actin cables or clumps were quantified.
B, microscopical pictures showing examples obtained in (A).

cells expressing GFP-Cpn0572-C showed in about 50% of the cells visible actin cables. Thus, the C-terminal part of Cpn0572 stabilized actin cables against actin depolymerization more than 800 fold compared to the 25% of control cells that showed visible actin cables after 1 minute exposing to Lat-A. Collectively, these results suggest that Cpn0572 somehow stabilizes actin by inhibiting actin depolymerization in yeast *in vivo*.

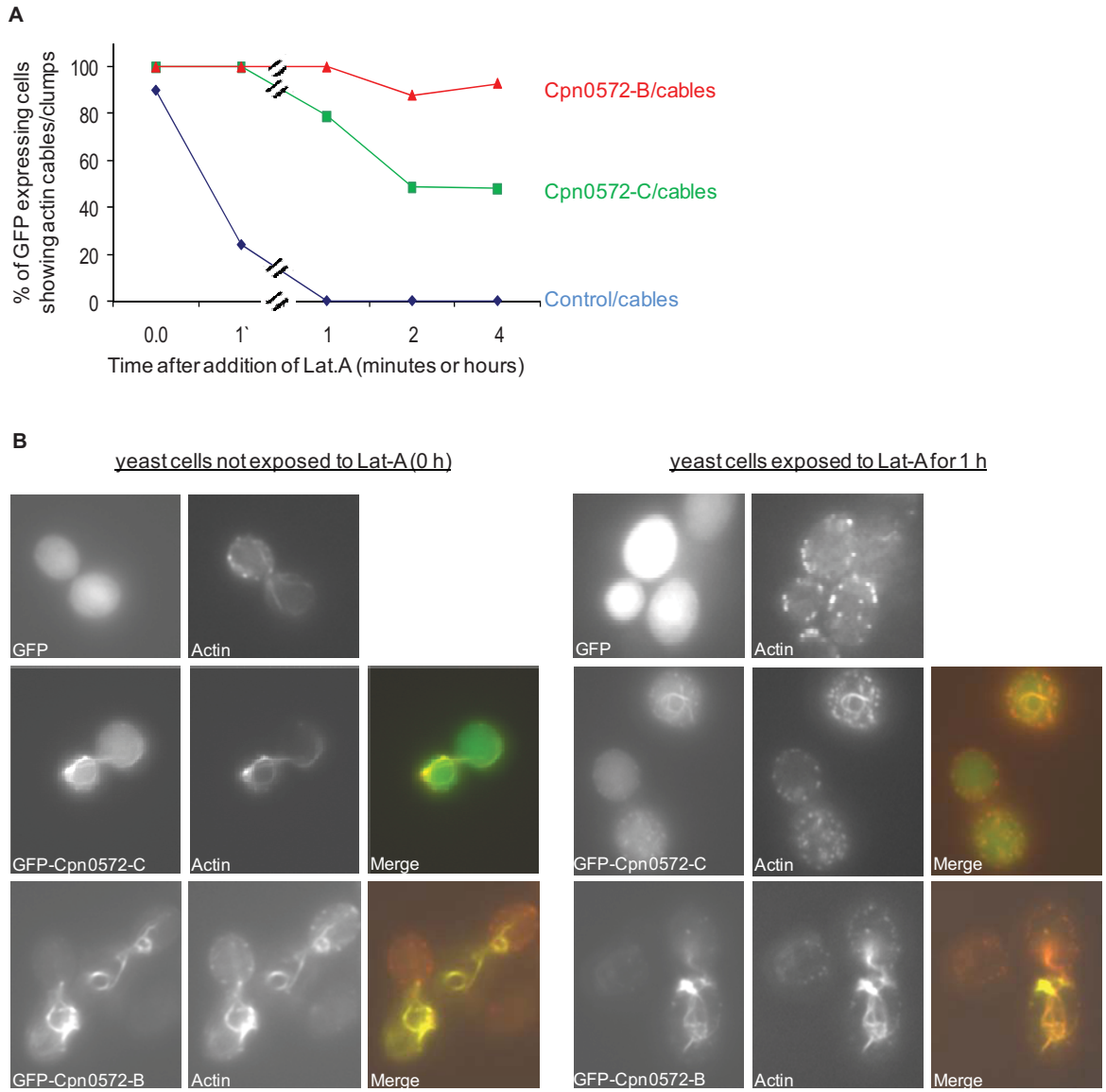

Figure 3-26: The C-terminus of Cpn0572 stabilizes actin against Lat-A.
A, yeast cells expressing pRZ1-C, pRZ1-C -B (GFP-Cpn0572-B or GFP-Cpn0572-C) or the GFP expressing vector (Control) were grown in inducing selective media until mid-log phase. Cells were treated with Lat-A, fixed and stained as described in Figure 3-25. Exposition time to Lat-A is indicated.
B, microscopical pictures showing examples obtained in (A).

3.5.1.2. Cpn0572 competes with and displaces cofilin from yeast actin filaments *in vivo*

Cpn0572 stabilizes actin cables and clumps by inhibiting actin depolymerization. Actin depolymerization can be inhibited either by displacing Aip1p from the barbed end of severed-short actin filaments or by displacing cofilin (Cof1p) from the pointed end of actin filaments. In wild type yeast cells, cofilin colocalizes with actin patches. However, Cof1p has been proposed to bind F-actin at the minus end within actin cables, but it is not possible to be visualized colocalizing with actin cables (Okada, Ravi et al. 2006). Interestingly, a *aip1Δ* strain showed cofilin colocalizing with all actin structures. Therefore,

we used these strains to analyze the localization of cofilin in yeast cells expressing Cpn0572.

To do so, we localized cofilin in wild type yeast cells expressing the empty vector or $Cpn0572_{6His}$ expressing vector. Control cells expressing the empty vector exhibited distinct structures of cofilin mostly staining actin patches as described previously (Figure 3-27-A and Figure 23-3-B upper panel). In yeast cells strongly expressing $Cpn0572_{6His}$, most of cofilin structures were gone and only a diffuse staining of cofilin was visible. However, neighbor cells expressing little or no $Cpn0572_{6His}$ showed distinct cofilin structures. Merge picture revealed that Cpn0572 clumps, which have been shown to completely colocalize with actin clumps, do not colocalize with cofilin (Figure 3-27-A, lower panel). However, it is unwise to assume that Cpn0572 displaces cofilin from actin clumps since the composition of actin clumps is illusive and it cannot be excluded that the clumps composed of or mimic actin cables structure in wild type cells, on which cofilin is not visible.

To accomplish this problem we used a *aip1Δ* strain, in which actin cables are enriched with cofilin and therefore cofilin can be visualized colocalizing with all actin structures. *aip1Δ* cells expressing the empty vector showed distinct structures of cofilin, presumably staining actin cables and patches as described previously (Figure 3-27- B and Figure 3-23-B, lower panel). Remarkably, $Cpn0572_{6His}$-expressing yeast cells showed clumps of the fusion protein. In contrast to cells expressing the empty vector, these cells exhibited a cytosolic cofilin staining. Merge picture revealed that Cpn0572 clumps, which have been previously shown to completely colocalize with actin clumps, do not colocalize with cofilin (Figure 3-27-A, lower panel). These results suggest that Cpn0572 inhibits and/or blocks actin depolymerization in yeast by displacing cofilin from actin cytoskeleton.

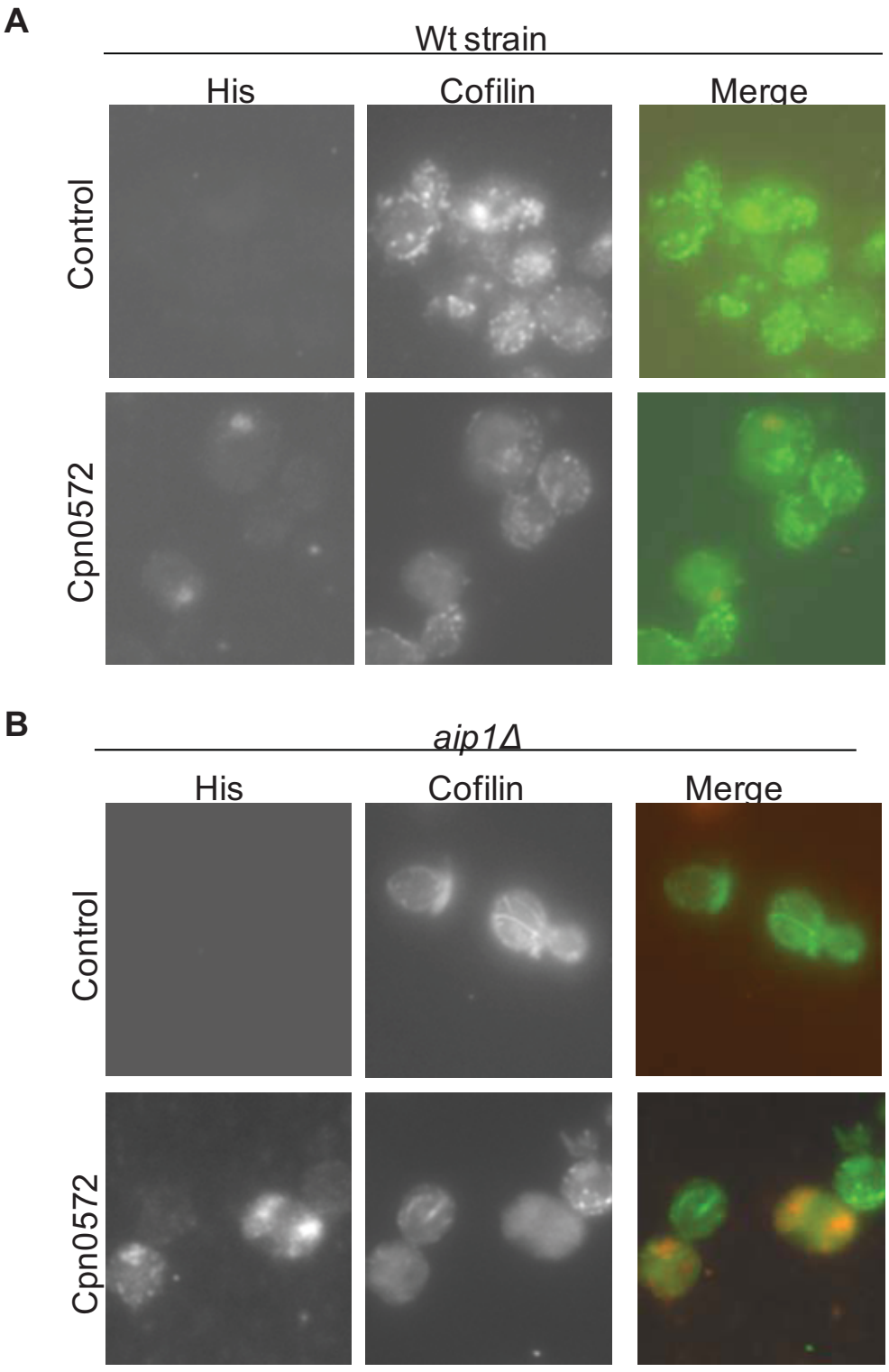

Figure 3-27: Cofilin localization in wild-type and *aip1Δ* cells expressing Cpn0572.
Wild type yeast cells (Left side) or *aip1Δ* cells expressing p423GAL1 (Control) vector or pRZ9 (Cpn0572) vector were grown in inducing selective media until mid-log phase and fixed with methanol. Fixed cells were stained with α-cofilin antibody (counterstained with α-chicken-FITC labeled) and α-His antibody (counterstained with α-Maus-Cy3 labeled) to visualize cofilin and $Cpn0572_{6His}$.

3.5.1.3. Cpn0572 competes with and displaces mammalian cofilin from mammalian F-actin *in vitro*

In vivo colocalization of Cpn0572 with actin resulted in the loss of cofilin from actin cytoskeleton of Cpn0572 expressing yeast cells. Cofilin and actin are highly conserved proteins among eukaryotes. Therefore, we next examined the ability of Cpn0572 to compete with mammalian cofilin in binding mammalian actin *in vitro* using purified proteins. Cofilin binds both G- and F-actin at a 1:1 molar ratio in a pH dependent manner. Below pH 7.0 cofilin binds to F-actin while above pH 7.0 cofilin binds G-actin (Ono 2007). Therefore, we performed cosedimentation assays using mammalian pre-assembled F-actin and human recombinant cofilin. F-actin was stable at the different pH values tested since the majority of actin was found in the pellet (Figure 3-28, lanes 1-4). When F-actin was mixed with cofilin at pH 7.8, cofilin was found in the supernatant indicating that cofilin does not bind F-actin but binds G-actin (Figure 3-28, lanes 5-6). In contrast, when both proteins were mixed at pH 6.8, cofilin was found in the pellet indicating that cofilin binds F-actin (Figure 3-28, lanes 7-8). To investigate the effect of F- actin-binding activity of cofilin in the presence of Cpn0572, recombinant cofilin and GST- Cpn0572 were mixed with F-

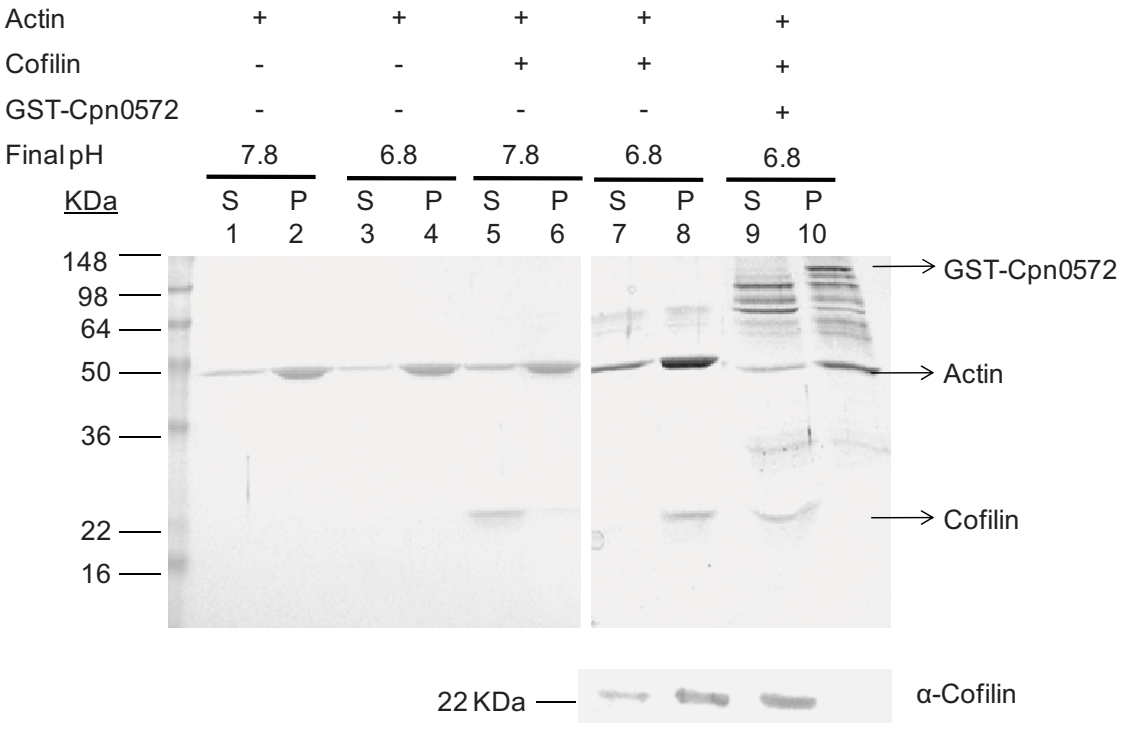

Figure 3-28: Cpn0572 competes with and displaces cofilin from F-actin. Co-sedimentation assay was used to study competition between cofilin and Cpn0572 to bind F-actin. The assay was performed by mixing 2 µM pre-polymerized rabbit actin filaments in the presence or absence of 2 µM of cofilin and 2 µM of GST-Cpn0572 at different pH values as indicated. The mixtures were incubated for 30 minutes at room temperature and F-actin was sedimented by centrifugation. Supernatant and sediment were resolved by SDS–PAGE. Protein bands are marked on the right.

actin at pH 6.8. Remarkably, the band representing the full length protein GST-Cpn0572 was found in the pellet with F-actin while bands representing degraded fusion protein were found in both the supernatant and the pellet. Interestingly, the presence of GST-Cpn0572 with F-actin in the pellet completely shifted cofilin to the supernatant fraction (Figure 3-28, lanes 9-10). Thus, these results show that Cpn0572 competes with and/or displaces mammalian cofilin from mammalian F-actin.

To test if the C-terminal domains of Cpn0572 are sufficient for this activity, we repeated the experiment using the GST-Cpn0572-C and GST-Cpn0572-B fusion proteins and tested their ability to compete with cofilin in binding F-actin. Approximately, 50% of GST-Cpn0572-C was found in the pellet with F-actin, while the other 50% was in the supernatant. In the presence of cofilin, more actin and GST-Cpn0572-C was observed in the supernatant compared to the control (compare lanes 3 and 5 in Figure 3-29). In addition, cofilin was found mostly in the pellet suggesting that it binds F-actin (lane 6). However, one fold increase in GST-Cpn0572-C concentration mixed with F-actin resulted

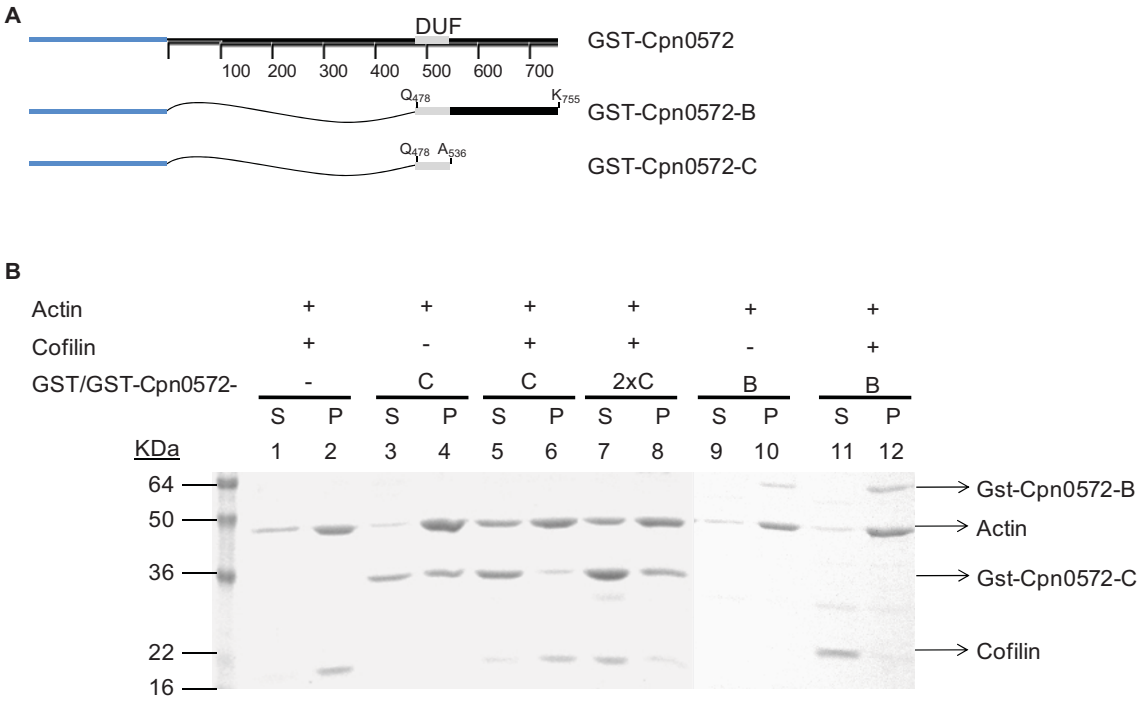

Figure 3-29: The C-terminal domains of Cpn0572 compete with and displace cofilin from F-actin.
A, schematic representation of Cpn0572 domains tested in this experiment.
B, co-sedimentation assay was performed at pH 6.8 as described in Figure 3-29. The assay was performed by mixing 2 µM pre-polymerized rabbit actin filaments in the presence or absence of 2 µM of cofilin and 2 µM of GST-Cpn0572-C or GST-Cpn0572-B as indicated. Protein bands are marked on the right.

in higher association of the fusion protein with F-actin and subsequently cofilin was mostly shifted to the supernatant indicating that Cpn0572-C compete with cofilin in binding F-actin in a concentration dependent manner (lanes 7-8). Interestingly, GST-Cpn0572-B completely bound F-actin in the pellet (compare lanes 9 and 10). In the presence of cofilin,

GST-Cpn0572-B bound almost totally to F-actin, while cofilin was completely shifted to the supernatant (lanes 11-12). The activity of GST-Cpn0572-B in displacement of cofilin from F-actin is almost similar to the activity induced by the full length protein. Thus, Cpn0572 and its C-terminus compete with and displace mammalian cofilin from mammalian F-actin *in vitro*. Collectively, the ability of Cpn0572 and its domains to displace cofilin from F-actin is consistent with their ability to stabilize F-actin against Lat-A in yeast cells.

3.5.2. The role of Cpn0572 in actin polymerization

3.5.2.1. Cpn0572 nucleates and induces actin polymerization *in vitro*

Cpn0572 induces the formation of actin clumps. The C-terminal part of Cpn0572 is sufficient to inhibit actin depolymerization and subsequently stabilizes F-actin in yeast. However, inhibition of actin depolymerization is not sufficient to induce the formation of actin clumps and Cpn0572 needs the N-terminal domain for this activity. Recently, the *C. trachomatis* Tarp has been found to nucleate actin assembly *in vitro* (Jewett, Fischer et al. 2006). Interestingly, the region within Tarp that induces actin nucleation is highly conserved among the homologous proteins from different *Chlamydia* species. Correspondingly, Cpn0572 binds actin directly assuming that it may affect actin polymerization and independently from other ABPs. Therefore, we tested the ability of Cpn0572 to nucleate and induce actin polymerization *in vitro.*

F-actin can be assembled spontaneously *in vitro* under physiological conditions. So far, the most versatile, sensitive and easiest *in vitro* assay used to study the effects of ABPs on actin polymerization is the pyrene actin assembly assay. Fluorescence of polymerized pyrene actin is 7–10 times higher than pyrene actin monomers and can be measured in a fluorimeter to follow polymerization over time (Cooper and Pollard 1982). *In vitro*, actin polymerization follows three phases as depicted in Figure 1-5 in the introduction chapter. The lag phase represents the time required for actin nucleation (formation of G-actin trimers or tetramers) followed by a rapid polymerization phase representing the time during which short filaments are formed and elongate. Steady state represents the equilibrium between growth and shortening of the filaments due to addition of monomers to and loss of monomers from F-actin, respectively. Thus, we used this assay to study the effect of GST-Cpn0572 on actin polymerization. After the addition of the actin polymerization buffer, actin alone exhibited the typical assembly kinetics. Co-incubation of G-actin with GST did not affect actin assembly kinetics. Interestingly, GST-Cpn0572 accelerated the kinetics of actin polymerization and the initial lag phase was eliminated (Compare the lag phases Figure 3-30). Thus, these observations are identical to the finding obtained for actin nucleator proteins such as the Arp2/3 complex with N-WASP (D'Agostino and Goode 2005), the *Salmonella* actin nucleator protein SipC (Hayward and Koronakis 1999) and the recently published *C. trachomatis* homologous of Cpn0572, Tarp (Jewett, Fischer et al. 2006), proofing that Cpn0572 nucleates and induces actin polymerization.

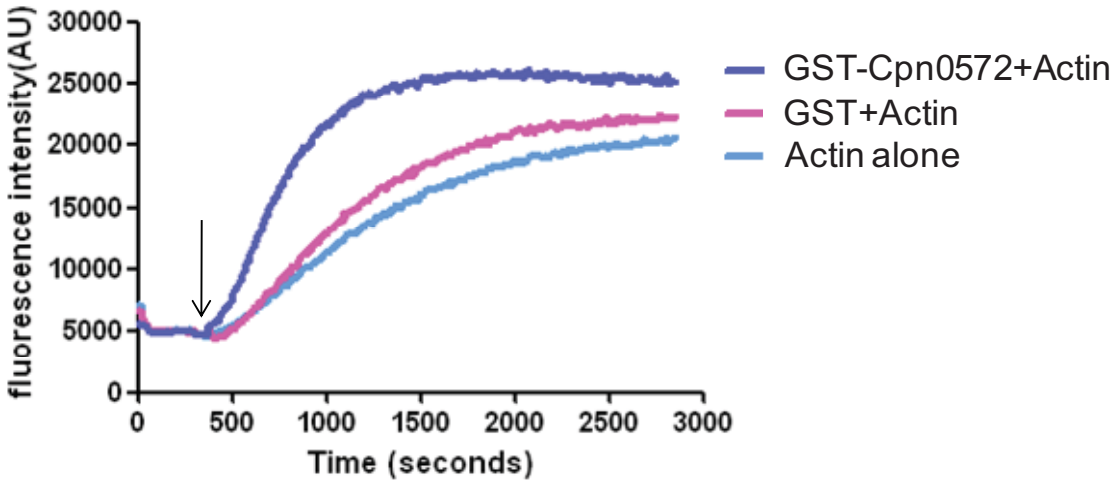

Figure 3-30: Cpn0572 promotes actin nucleation and polymerization.
Actin polymerization kinetics was determined by the pyrene−actin assembly assay. Actin polymerization buffer was added to induce actin polymerization as indicated by arrow. Actin (2.5 µM) was polymerized alone, in the presence of GST (0.25 µM) or GST-Cpn0572 (0.25 µM) for 50 minutes at room temperature and the increase in fluorescence intensity at the excitation wavelength of 355 nm and emission 405 nm was measured in arbitrary units (AU) during incubation time.

3.5.2.2. The C-terminal domain of Cpn0572 does not nucleate/induce actin polymerization *in vitro*

To test if the F-actin stabilizing C-terminal domain of Cpn0572 also has a role in actin polymerization, we tested the GST-Cpn0572-C and GST-Cpn0572-B fusion proteins in a pyrene actin assembly assay. Both fusion proteins did not nucleate or induce actin polymerization, but in contrast surprisingly showed a strikingly distinct actin-polymerization-inhibiting activity (Figure 3-31). To investigate if this inhibiting activity due to binding actin, we included the mutant GST-Cpn0572-C-M2 in this assay, a mutant that lost its ability to bind actin. In the presence of this mutant, actin assembly exhibited typical assembly kinetics similar to actin alone suggesting that this mutant did not affect actin assembly *(*Figure 3-31*)*. These results suggest that binding actin via the C-terminal domain of Cpn0572 is not only insufficient to induce actin polymerization but it also blocks *de novo* actin polymerization. These results indirectly imply that the actin binding and nucleation activities require multiple regions of the protein.

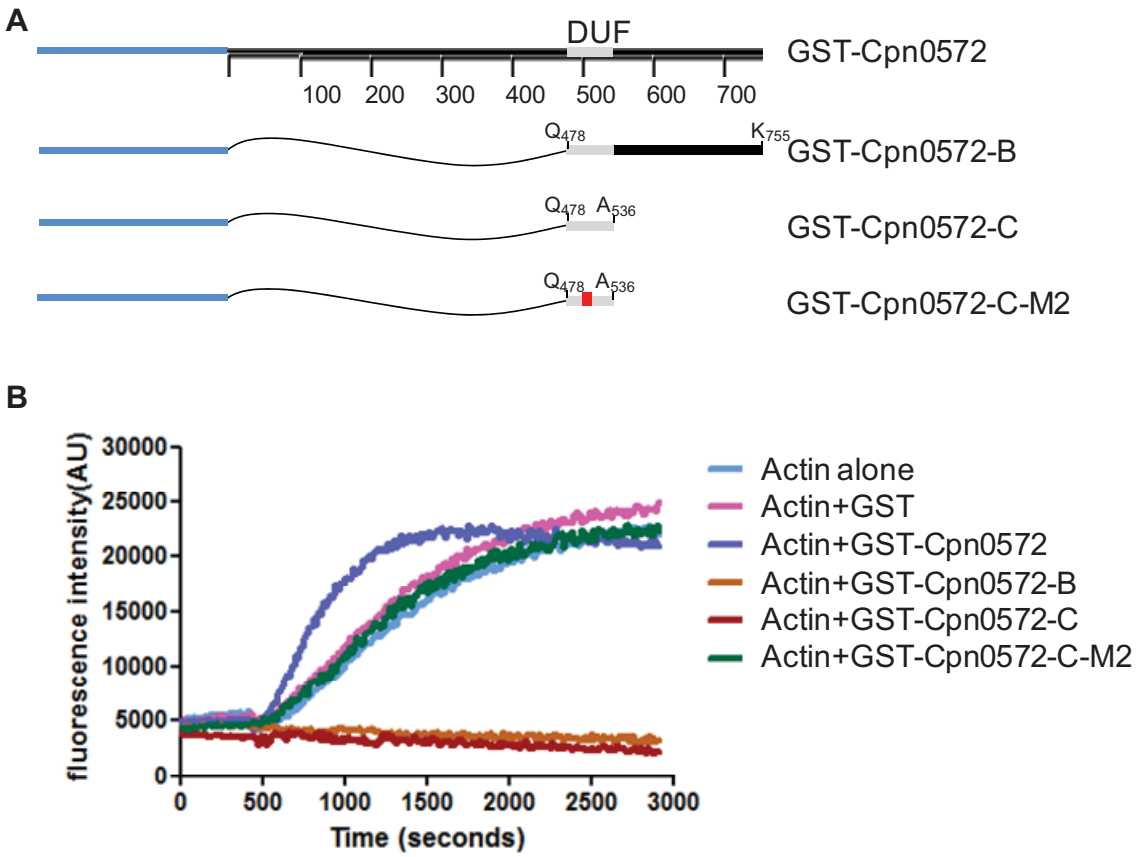

Figure 3-31*:* The C-terminal domains of Cpn0572 inhibit actin polymerization.
A, schematic representation of Cpn0572 domains tested in this experiment. The red box indicates the mutation generated as described previously: L505A, V508A, V509A (section 3.3.5.).
B, actin polymerization kinetics was determined by the pyrene−actin assembly assay. Actin (2.5 µM) was polymerized alone, in the presence of GST, GST-Cpn0572-B, GST-Cpn0572-C, or GST-Cpn0572-C-M2 at final concentration of 0.25 µM for 50 minutes at room temperature.

3.5.2.3. The central domain of Cpn0572 is sufficient to nucleate and induce actin polymerization *in vitro*

For Tarp, the shortest fragment that induces actin polymerization *in vitro* is fragment 8d (Jewett, Fischer et al. 2006 and Figure 3-32-A). Therefore we tested the ability of the homologous fragment of Tarp-8d in Cpn0572 (Cpn0572-N1) in actin polymerization (Figure 3-32-B). Our investigation revealed that GST-Cpn0572-N1 is sufficient to induce actin polymerization *in vitro* in a concentration dependent manner (Figure 3-32-C). It has been suggested that the proline repeats (PR) upstream of the first DUF in Tarp are necessary for actin polymerization activity and the oligomerization of Tarp, since a shorter fragment lacking the PR containing region (8e in Figure 3-32-A) does not induce actin polymerization (Jewett, Fischer et al. 2006). Cpn0572-N1 also has the PR. Additionally, Cpn0572-N1 contains a second proline rich

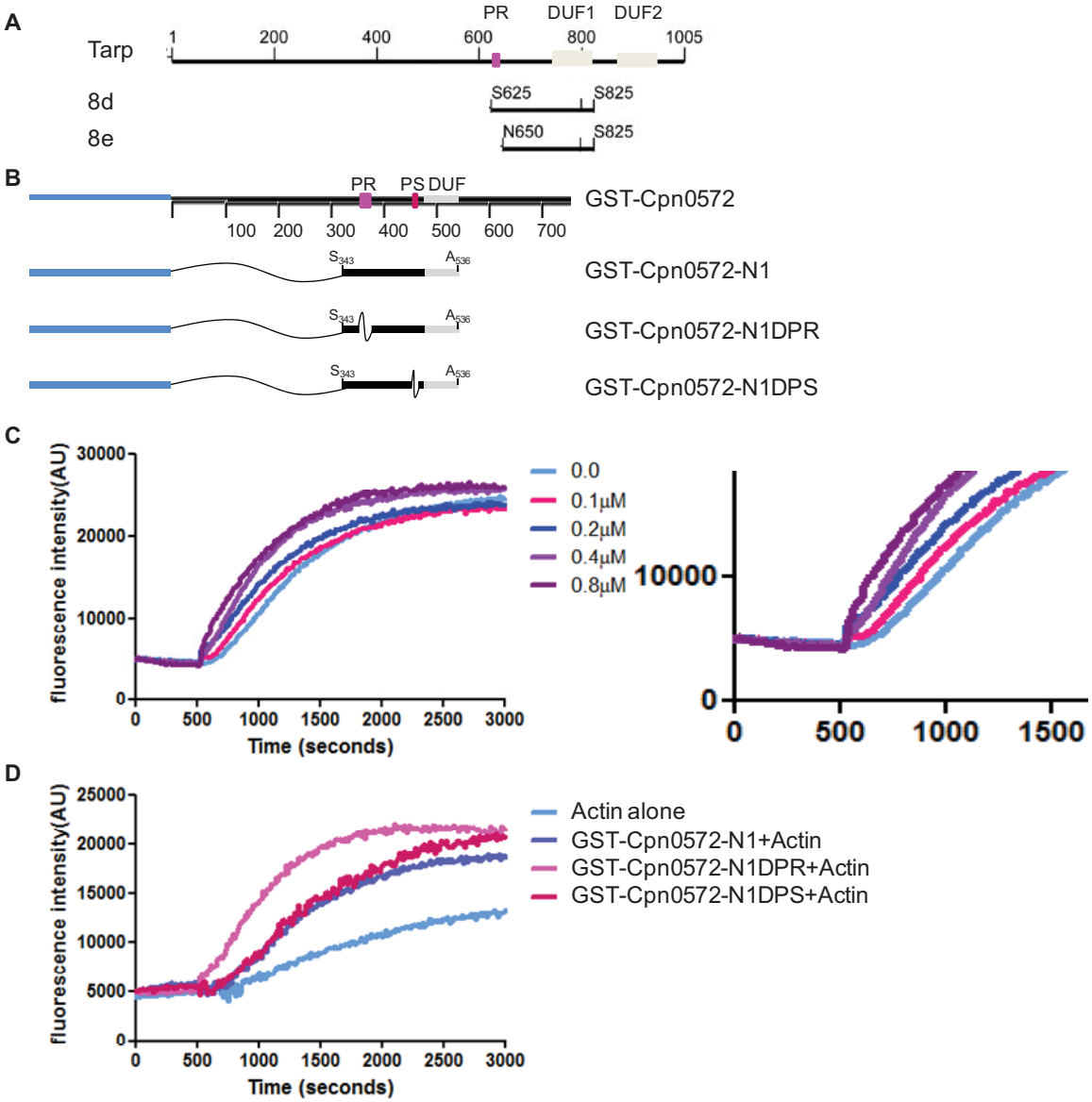

Figure 3-32*:* Part of the N-terminal domain of Cpn0572 is sufficient to nucleate and induce actin polymerization.
A, schematic representation of Tarp and the shortest fragment in Tarp (8d) which nucleates and induces actin polymerization (modified after (Jewett, Fischer et al. 2006).
B, schematic representation of Cpn0572 constructs tested here. The PR and the PS are indicated as PR and PS, respectively. Curved lines indicate deletions. Starting and ending amino acids for each fragment are indicated.
C, Cpn0572-N1 nucleates and induces actin polymerization in a concentration dependent manner. Actin (2.5 μM) was polymerized in the absence or presence of Cpn0572-N1 (0.1 μM, 0.2 μM, 0.4 μM, or 0.8 μM) as indicated in the graph. Kinetics of the first 1500 sec are enlarged on the right side.
D, the deletion of proline repeats or proline stretch does not repress the actin polymerization activity of Cpn0572-N1. Actin (2.5 μM) was polymerized alone, in the presence of GST-Cpn0572-N1, GST-Cpn0572-N1DPR or GST-Cpn0572-N1DPS at final concentration of 0.25 μM for 50 minutes.

region termed proline stretch (PS), which is 16 residues upstream of DUF (Figure 3-32-B). As we had identified in yeast experiments, the PS is necessary for the proper modulation of actin (see section 3.3.3. in this chapter). To investigate the possible role of the PR and the PS of Cpn0572-N1 in actin polymerization activity *in vitro*, we individually deleted

these proline motifs to generate GST-Cpn0572-N1DPR or GST-Cpn0572-N1DPS, respectively (Figure 3-32-B). Surprisingly, both GST-Cpn0572-N1DPR and GST-Cpn0572-N1DPS induced actin polymerization either better than or similar to the wild type fragment, respectively (Figure 3-32-D). Similar results also were obtained when these deletion are generated in the full length proteins (Data not shown). These results suggest that the two proline regions are not prerequisites for the actin polymerization activity of the protein *in vitro*.

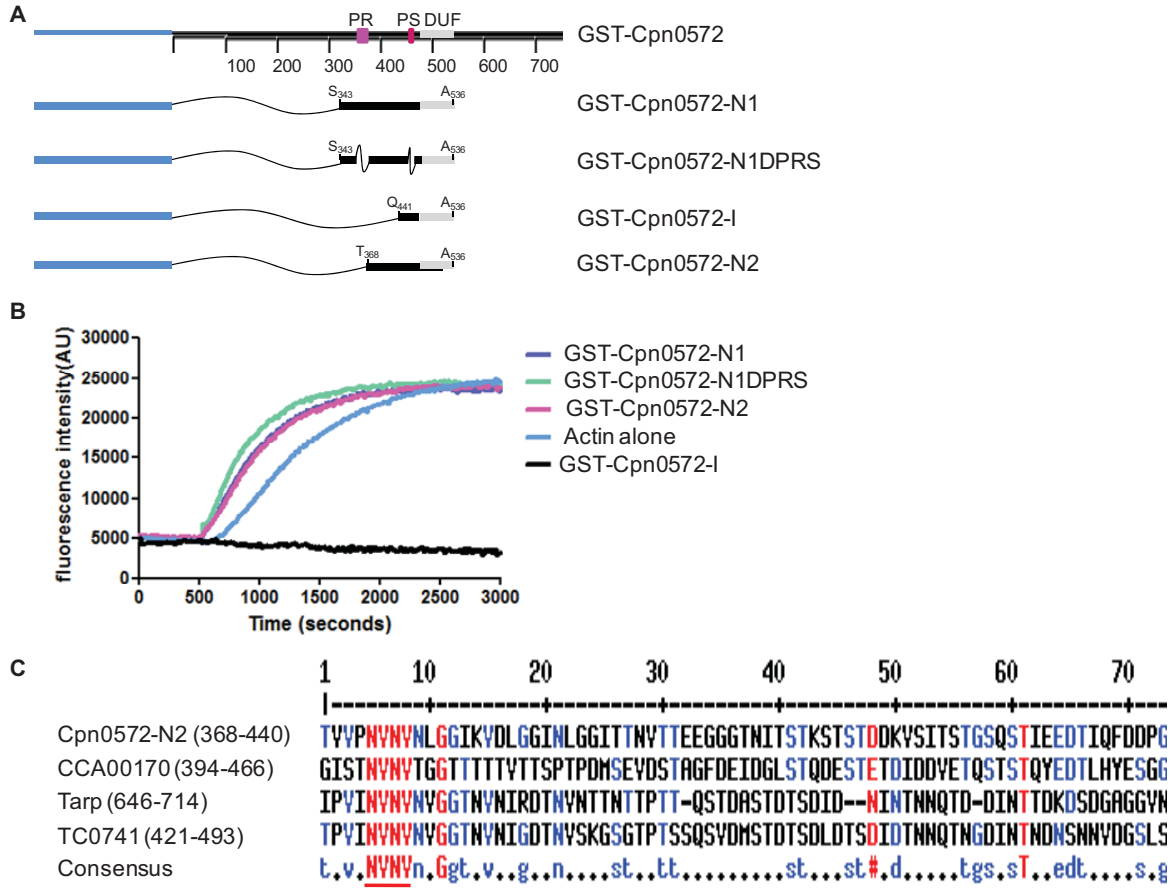

Figure 3-33: The shortest fragment of Cpn0572 nucleating and inducing actin polymerization *in vitro* is Cpn072-N2 contains a putative motif presents also in the Cpn0572 homologous proteins from different *Chlamydia* species.
A, schematic representation of Cpn0572 domains including deletion tested in this experiment.
B, Cpn0572-N2 is the shortest fragment nucleates and induces actin polymerization *in vitro*. Actin (2.5 µM) was polymerized in the presence of GST, GST-Cpn0572-N1, GST-Cpn0572-N1DPRS, GST-Cpn0572-I or GST-Cpn0572-N2 at final concentration of 0.25 µM for 50 minutes.
C, a multiple alignment of amino acids sequences from the Cpn0572-N2 fragment and the corresponding regions in homologous proteins from different *Chlamydia* species. The starting and ending amino acid number of each fragment is indicated in brackets. Highly or less conserved amino acids are in red or blue, respectively. The highly predicted necessary residues are underlined in red.

To further confirm that, we generated a mutant where both the PR and the PS are deleted from the N1 domain generating GST-Cpn0572-N1DPRS and tested its ability to induce actin polymerization (Figure 3-33-A). Our results showed that the double deletion fragment also nucleates and induces actin polymerization *in vitro* and this activity is even

better than the wild type fragment (Figure 3-33-B). Again, the results confirm that the PR and the PS are not necessary for the actin polymerization activity of the protein *in vitro*.
After that, we extended the characterization and tested the ability of shorter fragments of Cpn0572-N1 to nucleate and induce actin polymerization *in vitro* and generated GST-Cpn0572-N2 and GST-Cpn0572-I (Figure 3-33-A). GST-Cpn0572-N2 was also able to nucleate and induce actin polymerization (Figure 3-33-B). In contrast, GST-Cpn0572-I was not able to nucleate and induce actin polymerization and instead it provoked actin polymerization completely. Thus, the region that is necessary for this activity localizes between the amino acids T_{368} and G_{440} in the Cpn0572 protein. Interestingly, this region contains a motif (NVNV) which is also found in the Cpn072 homologous proteins from different *Chlamydia* species (Figure 3-33-C). Therefore, our results suggest that this motif is necessary for the actin polymerization activity of the Cpn0572 protein *in vitro*.

3.6. Expression, localization and secretion of Cpn0572 during *C. pneumoniae* infection

3.6.1. *C. pneumoniae* expresses Cpn0572

Cpn0572 was annotated as a *C. pneumoniae* hypothetical protein. To test if this protein is expressed by *C. pneumoniae*, we used polyclonal antibody raised against the recombinant full length protein $Cpn0572_{6His}$ ($rCpn0572_{6His}$). The predicted molecular weight for Cpn0572 is 78 KDa. The $rCpn0572_{6His}$ was visualized by western blot analysis using α-His antibody and showed a major band with a molecular weight of 110-115 KDa (Figure 3-34-A). This unusual migration behaviour can probably be explained by the fact, that Cpn0572 is predicted to have a low isoelectric point (pI: 5.7), which makes it migrating aberrantly on SDS/PAGE. A band of similar molecular weight was also detected, when we used our α-Cpn0572 antibody indicating that the antibody indeed can detect the recombinant Cpn0572 protein (Figure 3-34-B). Therefore, we used α-Cpn0572 to test for the presence of Cpn0572 in purified EBs. In cellular extracts from purified EBs separated on SDS gel and analyzed by western blot, our α-Cpn0572 antibody, but not the corresponding preimmune sera, could recognize a band of similar molecular weight (Figure 3-34-B and -C). Thus, Cpn0572 is expressed by *C. pneumoniae* and found in the infectious EBs.

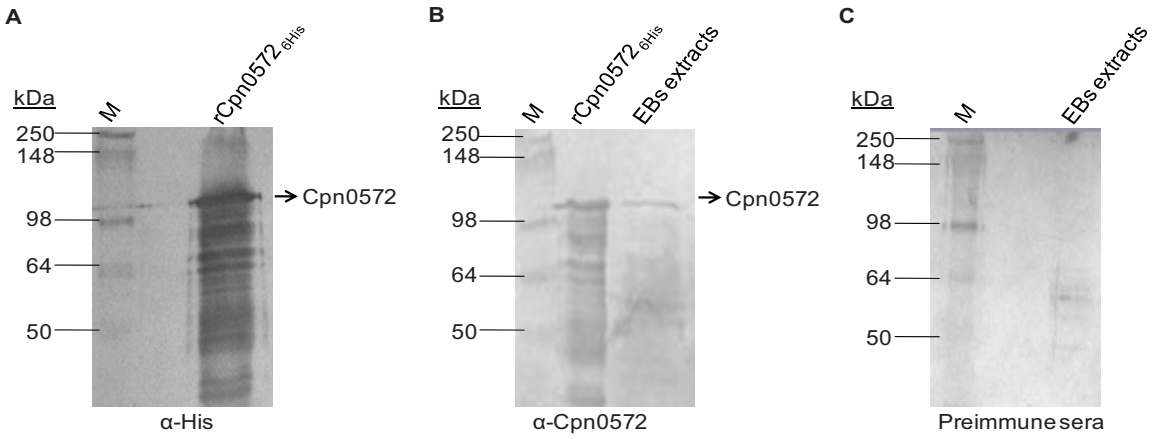

Figure 3-34: Expression of Cpn0572 in *E. coli* and in *C. pneumoniae*.
A, the coding sequence of a 6xHis tagged Cpn0572 protein was amplified and integrated into the *E. coli* expression vector pAC2 to yield pRZ3. $rCpn0572_{6His}$ was purified under denaturing conditions and detected by western blot using α-His antibody.
B, purified rCpn0572 protein and *C. pneumoniae* EBs total lysates were probed with α-Cpn0572 antibody.
C, an immunoblot of *C. pneumoniae* EBs total lysates was probed with preimmune sera.

Next, the expression of Cpn0572 by *C. pneumoniae* during the *Chlamydia* developmental cycle was determined. Immunoblots were performed using α-Cpn0572 antibody on *C. pneumoniae*-infected HEp-2 cell lysates produced over the course of the infection. During the first 36 h post of infection, we did not find a Cpn0572 specific signal. After 48 h, a

weak signal corresponding to Cpn0572 was observed and this signal increased in intensity late in the cycle, after 60 and 72 h (Figure 3-35, A). However, the *C. pneumoniae* protein Momp, which was used as a positive control that is known to be in equal levels in EBs and RBs, was only detected 48 h post of infection suggesting that the amount of *C. pneumoniae* particles before 48 h is less than the level to detect *C. pneumoniae* proteins (Figure 3-35, B). Therefore, we cannot exclude the presence of Cpn0572 during early time of infection. Nevertheless, Cpn0572 is found late in the cycle where the majority of *C. pneumoniae* particles have been redifferentiated back to EBs.

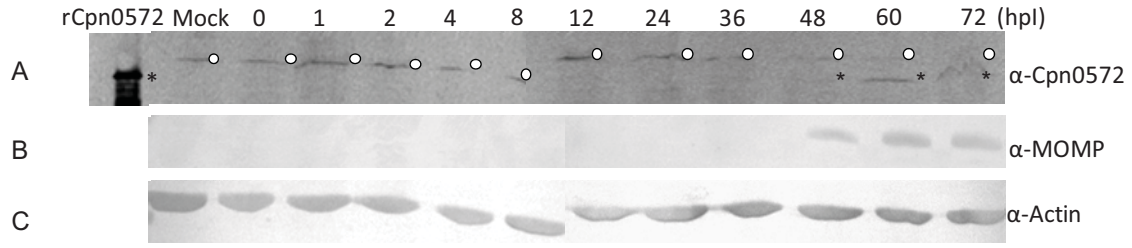

Figure 3-35: Expression of Cpn0572 protein during the *C. pneumoniae* developmental cycle.
A, mock-infected and *C. pneumoniae*-infected HEp-2 cells (multiplicity of infection, MOI 10) were incubated at 37°C for the time points indicated in the figure. Total cell lysates and rCpn0572 were separated by SDS/PAGE and probed with α-Cpn0572 antibody. The asterisk indicates Cpn0572 protein, while open circles indicate background that also appears in the sample obtained from mock-infected cells.
(B) in separate blot both the protein lysates were probed with α-actin antibody to visualize actin as a loading control for HEp-2 cells or with α-MOMP antibody to visualize MOMP as a loading control for *C. pneumoniae* (C).

3.6.2. Cpn0572 is not exposed on the surface of EBs

Effector proteins, which are found in EBs, are very likely relevant for early events in the infection and they are either adhesins or needed for the entry of these EBs. Adhesins are exposed on the surface of pathogens while other effector proteins that are needed for internalization are either exposed on the surface or internal proteins that secreted into the host cell via one of the different secretion pathways, for instance TTSS. Surface proteins, but not internal proteins, can be stained on the surface of living EBs using the corresponding antibodies by microimmunofluorescence (MIF). For example, MOMP is a surface protein that can be detected on the surface of living EBs stained with α-MOMP while the intrachlamydial protein DnaK cannot be stained with α-DnaK under this condition (Figure 3-36-A and B) and served as a control to test that bacterial lysis is negligible. Using α-Cpn0572 antibody in the MIF experiment, no staining on living EBs could be detected showing a similar pattern as obtained for DnaK, thus (Figure 3-36, C). These results suggest that Cpn0572 is not exposed on the surface of EBs.

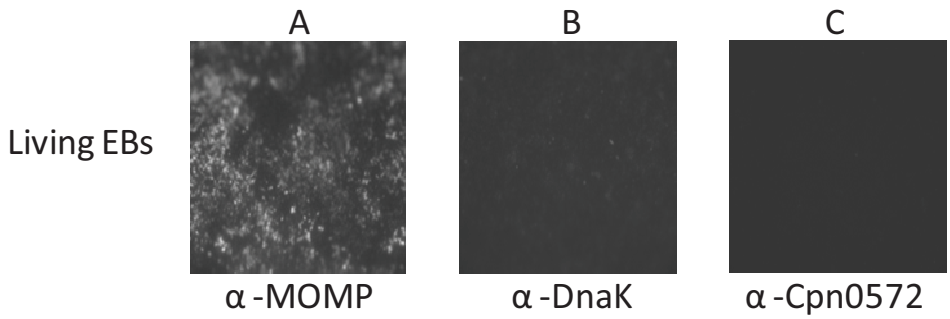

Figure 3-36: Cpn0572 is not localized on the surface of *C. pneumoniae* EBs.
Exposure of antigen on living *C. pneumoniae* EBs was assayed by microimmunofluorescence (MIF) analysis. Equal amounts of purified living *C. pneumoniae* EBs (not fixed) were individually stained by indirect immunofluorescence with α-MOMP(A), α-DnaK (B) or α-Cpn0572 antibodies (C).

3.6.3. Cpn0572 is translocated into HEp-2 cells early during infection

We have shown that Cpn0572 is found in the EBs, however it is not exposed on the surface of purified EBs. Our findings *in vitro* as well as in yeast and human cultured cells ectopically expressing Cpn0572 indicated that Cpn0572 protein interacts directly with and modulates the eukaryotic actin cytoskeleton. Indeed, many pathogens secrete their actin modulating effector proteins early during infection to facilitate their entry into host cells. Consistent with these facts, we hypothesized that Cpn0572 is secreted into the host cells early during infection.

To test this hypothesis, we investigated the secretion of Cpn0572 by *C. pneumoniae* at an early time of infection using immunofluorescence microscopy. Therefore, human epithelial HEp-2 cells were infected with purified *C. pneumoniae* EBs at 4°C to allow EBs adhesion but not entry. The infected cells were fixed with formaldehyde plus Triton X-100 to visualize intra-HEp-2 cell and extrachlamydial, but not intrachlamydial, antigens. Staining with α-MOMP and α-Cpn0572 antibodies were used to visualize the surface of *C. pneumoniae* EBs and Cpn0572 protein, respectively. Surface-associated EBs showed a strong immunoreactivity with α-MOMP but not with α-Cpn0572 antibodies (S1 in Figure 3-37-A and -B). The results indicate that Cpn0572 is not exposed on the EBs surface nor secreted at 4 °C. The results also show that the EBs are not lysed.

The experiment was repeated but this time after addition of EBs at 4 °C, the cells were shifted to 37 °C for 10 min to initiate the TIIISS. MOMP Antibody staining again identified the EBs and this time the α-Cpn0572 antibody detected the protein (S2 in Figure 3-37-A and –B). Both the MOMP and the Cpn0572 ligands colocalized indicating that Cpn0572 was secreted from the EBs. To specifically show that under these experimental conditions Cpn0572 was secreted into the HEp-2 cells, the experiment was repeated but cells were formaldehyde fixed in the absence of Triton X-100, which leaves the human membrane intact and therefore intra-HEp-2 cell antigens are not accessible to the corresponding

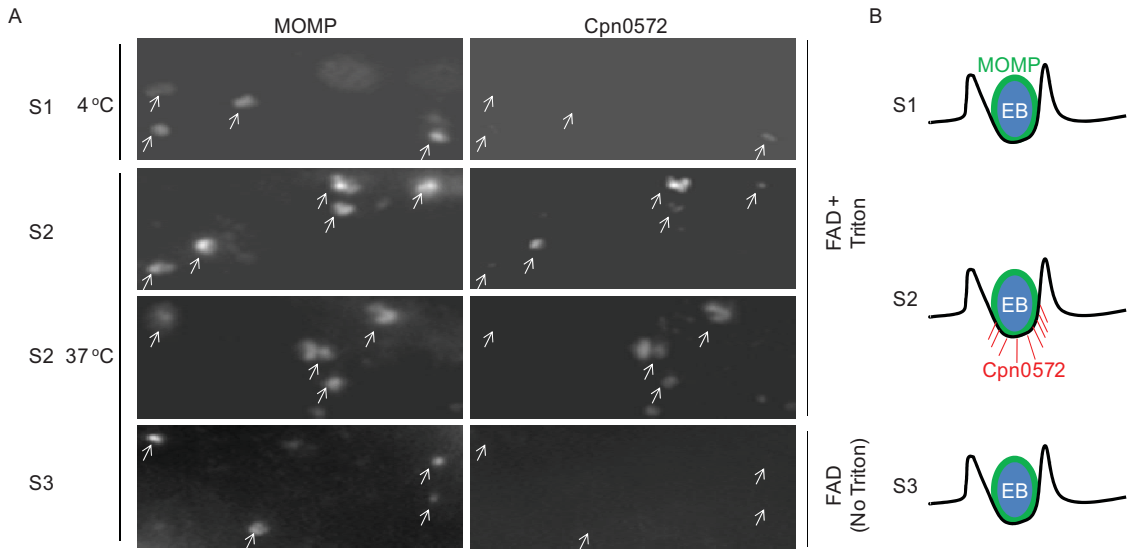

Figure 3-37: Cpn0572 is an intrachlamydial protein secreted into HEp-2 cells early during infection.
A, HEp-2 cells were infected with purified *C. pneumoniae* EBs at 4°C, the medium was replaced, and the cultures were then held at 4°C (situation 1, or S1) or shifted to 37°C (situation 2, or S2) for 10 minutes before fixation with formaldehyde plus Triton X-100. In the third situation (S3) infected cells that were shifted to 37°C for 10 minutes, were fixed with formaldehyde minus Triton X-100. Fixed cells were then stained by indirect immunofluorescence with anti-MOMP and α-Cpn0572 antibodies. Note that 2 different examples for S2 are shown. Arrows indicate locations of EBs on HEp-2 surface.
B, schematic representation to simplify the results obtained in A. In S1, only the surface localized protein (MOMP) could be stained and visualized but not Cpn0572. In S2, both surface localized (MOMP) and secreted protein (Cpn0572 within the HEp-2 cells) could be visualized. In S3, only surface localized protein (MOMP) could be visualized.

antibodies (S3 in Figure 3-37-B). MOMP could still be detected indicating that they were still outside of HEp-2 cells. In contrast, Cpn0572 was not detected (S3 in Figure 3-37-A) indicating that Cpn0572 localized into the HEp-2 cell. Collectively, these results suggest that EBs secrete Cpn0572 early during infection, presumably via TIIISS, into the host cell. After that, we wanted to extend our investigation to determine whether Cpn0572 is secreted into the host cell late in *C. pneumoniae* developmental cycle. Therefore, 72 h post infected cells were first methanol fixed to stain all *Chlamydia* and HEp-2 cells antigens with the corresponding antibodies. *C. pneumoniae* inclusions were visible within HEp-2 cells (Phase picture in Figure 3-38-A). Staining with α-Cpn0572 resulted in bright signals within HEp-2 cells, which is always identical to the inclusions pattern (Figure 3-38-A). These results show that Cpn0572 is bacteria-associated or secreted into the lumen of the inclusion. However, the results do not show if Cpn0572 is secreted within the *C. pneumoniae* inclusions. Therefore, we repeated the experiment but this time the infected cells were fixed and permeabilized with formaldehyde and triton X-100 to stain extrachlamydial antigens. Phase contrast pictures showed that HEp-2 cells contain *C. pneumoniae* inclusions. However no Cpn0572 staining could be observed (Figure 3-38, B). Similar results were obtained for cells tested 48 h or 96 h post of infection (Data not shown). Thus, the results suggest that, although the bacteria contain contain the Cpn0572

protein at least in the second half of *C. pneumoniae* developmental cycle, the bacteria do not secrete Cpn0572 into the host cell or into the *C. pneumoniae* inclusion lumen nor is the protein bacteria cell surface-located.

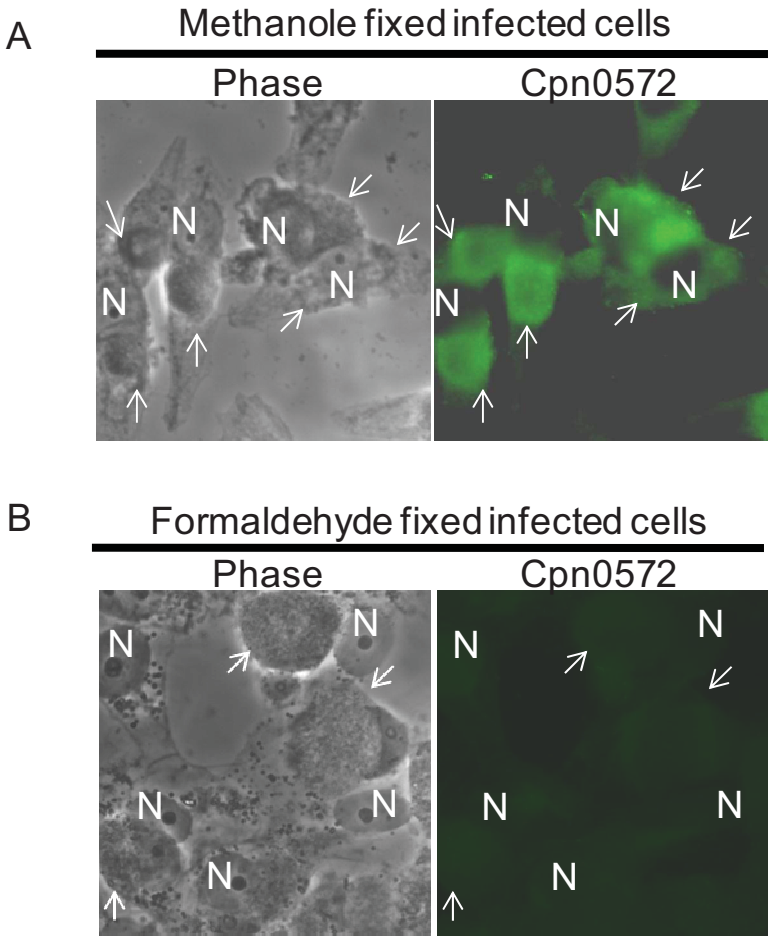

Figure 3-38: Localization of Cpn0572 late in the *C. pneumoniae* developmental cycle.
A, HEp-2 cells were infected with purified *C. pneumoniae* EBs at MOI 5 in the presence of 1.2 µg/ml cycloheximide for 72 h. Cells were then fixed with methanol and stained by indirect immunofluorescence with anti-MOMP and α-Cpn0572 antibodies.
B, infected cells as described in (A) were fixed with formaldehyde permeabilized with 0.1% Triton X-100 and stained by indirect immunofluorescence with anti-MOMP and α-Cpn0572. Arrows indicate locations of *C. pneumoniae* inclusions while N mark the HEp-2 nucleus.

4. DISCUSSION

In the beginning of this study, the only *Chlamydia* protein known to interact with the host actin cytoskeleton was the *C. trachomatis* Tarp. Here we analyzed the *C. pneumoniae* homologous protein Cpn0572. Thus, we studied the expression, secretion, localization and the function of this protein using different genetic and biochemical strategies and approaches. Due to the inability of genetically manipulating *Chlamydia*, these strategies included analyzing the protein in the well established eukaryotic model system *S. cerevisiae*, in cultured mammalian cells and in *in vitro* biochemical assays.

4.1. The yeast *S. cerevisiae* system leads to the identification of the role of Cpn0572 in stabilizing actin structures

Although unicellular eukaryotes such as yeast cannot serve as models for the bacterial infection of host cells, the utility of the genetic tractability of yeast to determine cellular targets of bacterial effector proteins is well established (Lesser and Miller 2001). However, only in few examples *S. cerevisiae* has been used to investigate the molecular function of bacterial effector proteins in detail.

In this study, we were able to express the full length Cpn0572 protein in yeast suggesting that *S. cerevisiae* represents an ideal organism to express chlamydial genes. A bioinformatical analysis of codon usage in *Chlamydia* revealed that the yeast *S. cerevisiae* might be more suitable for the expression of chlamydial genes than other organisms such as *E. coli*, adenovirus or *Homo sapiens* (Lu, Zhao et al. 2005). Sisko and co-workers (2006) showed that many of the potential *C. trachomatis* effector proteins could be successfully expressed in yeast.

Yeast cell-expressing Cpn0572 showed a severe growth phenotype suggesting that Cpn0572 targets and leads to a defect in at least one of the essential cellular processes in yeast. This cellular defect is irreversible as indicated by the lethality assay. Expression of many of *C. trachomatis* effector proteins in yeast result in reduced growth of yeast cells. Interestingly, among these effector proteins, Expression of Tarp in yeast results in a severe growth phenotype (Sisko, Spaeth et al. 2006). Recently, it has been shown that expression of the *C. pneumoniae* TIIISS component protein CopN, which is detected on the *C. pneumoniae* inclusion membrane during infection, in yeast cells results in a severe growth phenotype (Huang, Lesser et al. 2008). Other studies showed that most of the bacterial effector proteins involved in mammalian infection retain their biological function in yeast and subsequently impair yeast growth (Lesser and Miller 2001; Kramer, Slagowski et al. 2007)

To identify the cellular processes affected, we used the advantages of the yeast system.

Clifton and co-workers (2004) reported that the *C. trachomatis* homologous protein Tarp modulates the host actin cytoskeleton. Therefore, we tested the possibility of Cpn0572 to interact with and modulate the yeast actin cytoskeleton. Expression of the Cpn0572 protein in the actin mutant strains and testing the sensitivity of Cpn0572-expressing yeast cells to the actin destabilizing drug Lat-A clearly suggests that Cpn0572 targets the actin cytoskeleton. This observation were further clarified when we immunoprecipitated c-myc-Cpn0572 fusion protein from the extracts of yeast cells expressing the fusion protein and found actin and other actin interacting proteins in the precipitate revealing that Cpn0572 interacts with the yeast actin cytoskeleton. Impaired growth of yeast cells expressing bacterial effector proteins is due alterations in the essential cellular functions. Actin is essential for viability and thus the Cpn0572-induced lethality of yeast cells is due to alterations in the actin cytoskeleton. Other bacterial effector proteins inhibit the yeast growth by altering the actin cytoskeleton. For example, The *Yersinia pestis* YopE effector protein inhibit yeast growth by disrupting actin polymerization (Lesser and Miller 2001). The *E. coli* (EPEC) EspD, EspG and Map effector proteins also inhibit yeast growth by depolarizing the actin cortical cytoskeleton (Rodriguez-Escudero, Hardwidge et al. 2005).

Microscopical analysis showed that Cpn0572 transforms the yeast actin structures into clumps. Interestingly, Cpn0572-transfected human HEK-293 also form actin clumps, thus the formation of Cpn0572-induced actin clumps is conserved in yeast and human cells. It has been shown recently that exposition of the mammalian cells to the actin stabilizing drug jasplakinolide results in actin-clumps formation (Lazaro-Dieguez, Aguado et al. 2008). However, our results imply that the mechanism and the requirements for actin clumping are conserved in yeast and mammals.

The yeast system was also used to define functional domains in Cpn0572 by expressing truncated and variants versions; it was concluded that DUF alone is sufficient for interaction with actin and the conserved hydrophobic amino acids within DUF are necessary for this interaction, DUF or the C-terminal region of the protein is necessary for actin stabilization, the proline stretch 5`of DUF is required for clumping actin.

The fact that Cpn0572 or Cpn0572 deletion versions induce actin structures which are highly resistant against the actin depolymerizing drug Lat-A suggest that Cpn0572 might stabilize yeast actin structures by inhibiting actin depolymerization. The actin cytoskeleton in yeast has been extensively studied and several actin phenotypes have been described in yeast mutant or deletion strains. Additionally, different actin phenotypes have been described in response to certain chemical or physical conditions or after expression of certain pathogen effectors. Actin phenotypes induced by Cpn0572 or Cpn0572 domains are comparable to some of those actin phenotypes described previously. For example, the transformation of wild-type actin into actin clumps has been described in yeast cells

exposed to the actin-stabilizing toxin jasplakinolide (Figure 4-1-A), (Ayscough 2000). Recently, it has been shown that mammalian cells exposed to Jasplakinolide forms also actin clumps (Figure 4-1-B) suggesting that the mechanism of actin clumps formation due to Jasplakinolide is conserved in yeast and mammalian cells (Lazaro-Dieguez, Aguado et al. 2008). Jasplakinolide stabilizes actin filaments and inhibits actin depolymerization *in vitro* and *in vivo* (Bubb, Senderowicz et al. 1994; Vallotton, Gupton et al. 2004).

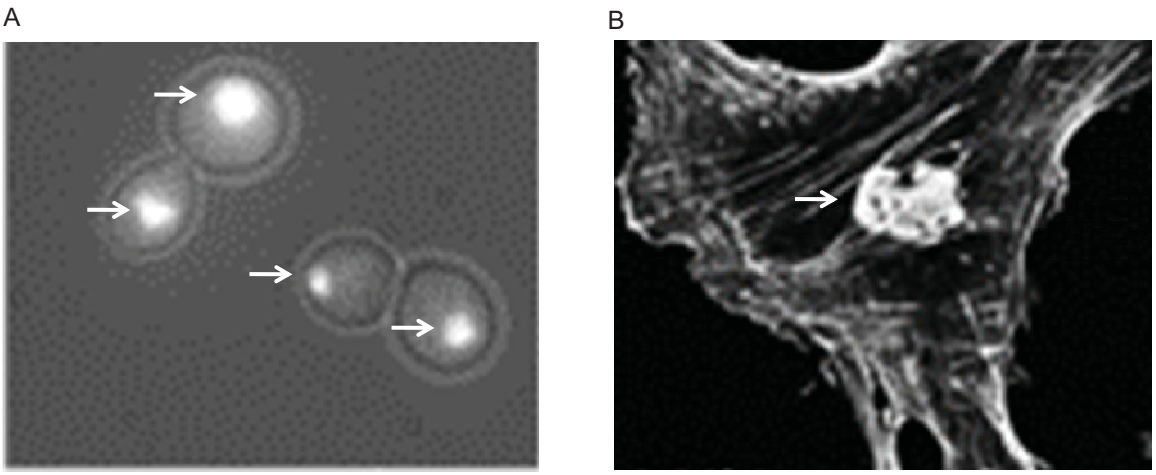

Figure 4-1: Effect of jasplakinolide on the yeast and mammalian actin cytoskeleton.
A, actin staining of yeast cells in the presence of jasplakinolide (taken from (Ayscough 2000).
B, actin staining of mammalian cells in the presence of jasplakinolide (taken from Lazaro-Dieguez, Aguado et al. 2008)

Furthermore, the formation of actin clumps instead of wild-type actin structures was also reported for the yeast double mutant strain *aip1Δ cof1-6* and these actin clumps are stable against the actin depolymerizing drug Lat-A (Rodal, Tetreault et al. 1999). Although the *aip1Δ* strain does not show actin clumps, this strain induces the formation of thick actin cables that are resistant to Lat-A activity (Okada, Ravi et al. 2006). Interestingly, this phenotype is similar to those obtained in yeast cells expressing Cpn0572-B and Cpn0572-C, which are also resistant against Lat-A-induced actin depolymerization. Similarly, expression of SipA, a *Salmonella* effector protein which inhibits actin depolymerization, induces the formation of thick actin cables in yeast which are resistant to Lat-A (Figure 4-2 and (Lesser and Miller 2001). Collectively, this suggests that the possible function of Cpn0572 is to stabilize F-actin by inhibiting actin depolymerization.

Correspondingly, it has been found that Tarp stabilizes *in vitro* polymerized F-actin against the HEp-2 cell extract, however the molecular mechanism by which Tarp achieves this was not characterized (Jewett, Fischer et al. 2006). Recently, it has been shown that the *C. pneumoniae* secreted protein Cpn0712 colocalizes with actin bodies that are partially similar to those actin structures induced in Cpn0572-expressing HEK-293 cells. However, the mechanism how Cpn0712 interacts with and modulates the host actin cytoskeleton was not analyzed (Müller, Sattelmacher et al. 2008). Our experiments showed that

Cpn0572 and Cpn0572 domains stabilize F-actin in a mechanism involving cofilin displacement. This mechanism was also confirmed biochemically using purified mammalian actin and cofilin proteins *in vitro*. Cofilin is known as a key regulator that promotes actin depolymerization (Bamburg, McGough et al. 1999; Brieher, Kueh et al. 2006). Stabilizing F-actin has also been reported for other effectors from other pathogens. The *Salmonella* effector protein SipA, which is secreted by TIIISS early during infection, stabilizes F-actin *in vitro* by displacing actin severing and depolymerizing factors from F-actin (Zhou, Mooseker et al. 1999; McGhie, Hayward et al. 2004). Thus, it is likely that stabilization of the host actin filaments is a general property of pathogens which depend on the host actin cytoskeleton for their internalization.

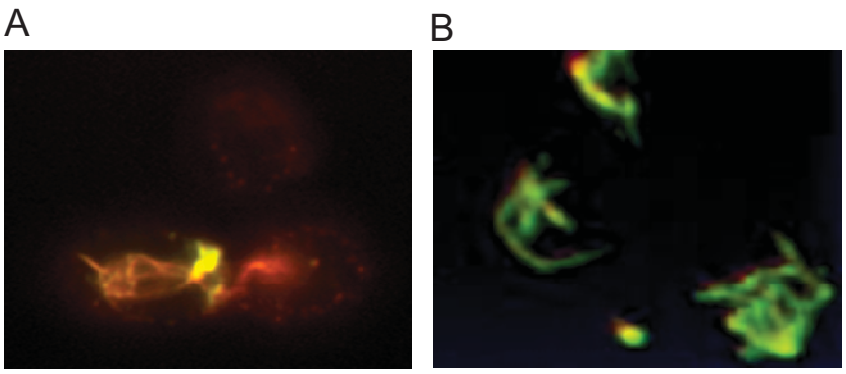

Figure 4-2: Cpn0572 and the *Salmonella* SipA stabilize F-actin against Lat-A induced actin depolymerization.
A, a merge picture of yeast cells expressing GFP-Cpn0572-B (green) after exposition to Lat-A. Actin is in red.
B, a merge picture of yeast cells expressing GFP-SipA (green) after exposition to Lat-A. Actin in red (taken from (Lesser and Miller 2001).

4.2. Cpn0572 is an actin nucleator

Cpn0572 nucleates actin *in vitro* and therefore enhances actin assembly independently from other cellular actin nucleators. The central region containing DUF is necessary for actin nucleation. However DUF alone is not sufficient to nucleate actin polymerization and instead it inhibits *de novo* actin polymerization. DUF requires at least the region 5`of DUF to be capable actin nucleation. So far, three classes of proteins have been identified that initiate new filament polymerization: the actin-related protein-2/3 (Arp2/3) complex, the formins and spire (reviewed in(Baum and Kunda 2005; Goley and Welch 2006; Kovar 2006). The mechanisms of how these actin nucleators initiate actin assembly are summarized in Figure 4-3.

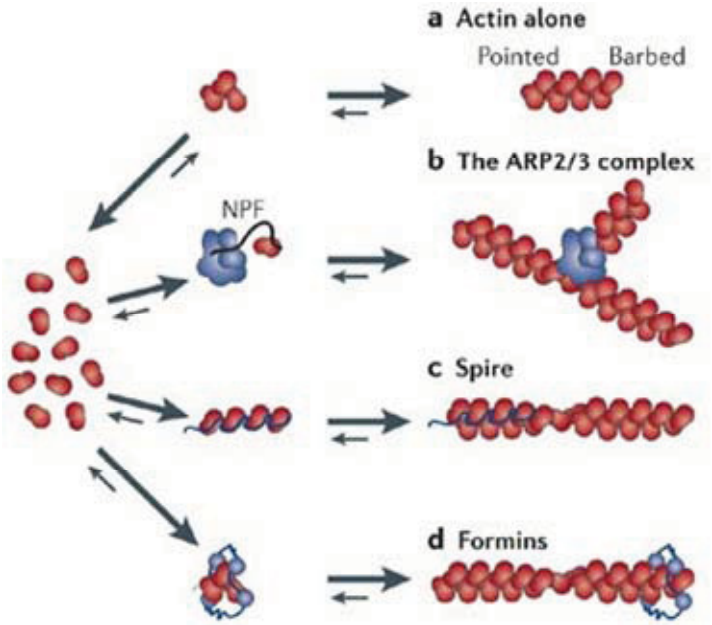

Figure 4-3: Paths to nucleation (taken from Goley and Welch 2006).
(a) The spontaneous initiation of actin-filament assembly requires the formation of a trimeric nucleus in a process that is called nucleation. Spontaneous nucleation is kinetically unfavorable because the actin dimers/trimers intermediate is very unstable. (b) Three main classes of protein have been identified to nucleate actin. The Arp2/3 complex is thought to mimic an actin dimer or trimer and to function as a template for the initiation of a new actin filament that branches off of an existing filament, generating y-branched actin networks. Nucleation activity of the Arp2/3 complex required nucleation-promoting factor (NPF) such as WASP, N-WASP, SCAR/WAVE. (c) The spire proteins, which are conserved among metazoan species, were recently discovered to nucleate actin assembly. The spire proteins nucleate actin via its four tandem G-actin-binding Wiskott–Aldrich syndrome protein (WASP)-homology-2 (WH2) domains which mediate longitudinal association of four actin subunits and function as a scaffold for polymerization into an unbranched filament. (d) The formins, which are conserved in most eukaryotes, also promote the nucleation of unbranched filaments. Formin dimerization via the formin-homology-2 (FH2) domains stabilizes an actin dimer or trimer to facilitate the nucleation event.

Most of the bacterial effector proteins induce actin polymerization by activating the Arp2/3 complex, directly or indirectly (Smith and Portnoy 1997; Geese, Schluter et al. 2000; Rottner, Stradal et al. 2005). Cpn0572 nucleates actin *in vitro* independent from these actin nucleators and there is no evidence that Cpn0572 interacts with any of these

nucleators *in vivo*. For example, Cpn0572 does not bear domains that are known for interaction with and activation of the Arp2/3 complex or of formin. Additionally, it is unlikely that Cpn0572 nucleation activity mimics any of the mechanisms described for these actin nucleators. Arp2/3 complex nucleation activity requires nucleation-promoting factor (NPF) proteins, while Cpn0572 nucleates actin independent from these factors. Cpn0572 harbors one WH2 domain, therefore it cannot be suggested that it nucleates actin in the same mechanism described for Spire. Moreover, it is unlikely that Cpn0572 nucleate actin by stabilizing the actin dimers or trimers as formin does, since shorter domains of Cpn0572 containing DUF were able to stabilize F-actin but suppress any actin polymerization.

To date, besides Tarp, two effectors from other pathogens have been shown to nucleate actin directly *in vitro* and independent of eukaryotic factors. The first protein, the *Salmonella* SipC protein binds and nucleates actin by forming dimers and multimers which in turn brings actin monomers together to form actin nuclei (Hayward and Koronakis 1999). The second protein is the *Vibrio parahaemolyticus* VopL which harbors multiple WH2 domains, therefore it has been suggested to nucleate actin in a similar manner described for the Spire protein (Liverman, Cheng et al. 2007). Although the Cpn0572 homologous from different *Chlamydia* species harbor more than one DUF, it is unlikely that Cpn0572 (which harbors one DUF) nucleates actin in a similar manner like Spire.

For Tarp, It has been shown that the shortest fragment of Tarp (Tarp-8d, see figure 3-32 in the results part) that capable actin nucleation forms oligomers *in vitro* while a shorter fragment losing a region containing the proline repeats (Tarp-8e, see figure 3-32 in the results part) is not oligomerized and cannot nucleate actin (Jewett, Fischer et al. 2006). Therefore, it has been suggested that the proline repeats are responsible for the oligomerization and actin nucleation activity of Tarp (Jewett, Fischer et al. 2006). However, our results showed that deletion of a region containing the proline repeats to yield Cpn0572-N2 fragment, which starts 3 amino acids before the homologous region of Tarp-8e, does not suppress the actin nucleation activity achieved by Cpn057-N1 suggesting that this 3 amino acids are necessary for the actin nucleation activity of Cpn0572-N2. It is possible that Cpn0572-N2 is able to form trimers and the proline rich repeats increase the self association of these trimers to yield bigger oligomers. This hypothesis is consistent with our results that the specific deletion of the proline repeats (Cpn0572-N1-DPR) showed more enhanced actin polymerization profile than the wild type fragment Cpn0572-N1(see figure 3-32 in the results part). It could be explained that highly oligomerized wild type Cpn0572 has a certain number of WH2 domains exposed to the media containing G-actin. In contrast, Cpn0572-N1-DPR which might not be able to form big oligomers, but possibly trimers that are sufficient to enhance actin nuclei, exposes

more WH2 domain to the media containing G-actin and thereby more G-actin could bind which result in the formation of more actin nuclei and subsequently more enhanced actin polymerization. Thus, further analysis should be carried out to test if Cpn0572-N1 and the other deletion variant form trimers and/or oligomers and if this is correlated to its actin nucleation activity or not.

Additionally, the Cpn0572 protein contains a proline stretch 5`of DUF which is absent in the homologous region of Tarp. Our data showed that this proline stretch is necessary for actin clumping in yeast and HEK93 cells expressing Cpn0572. It is unlikely that this mutation affect the actin depolymerization inhibiting activity of the protein since the DUF and Cpn0572-B domains are capable of inhibiting actin depolymerization. Additionally, deletion of the proline stretch does not affect the actin nucleation activity of the protein *in vitro*.

Remarkably, many of the proteins involved in enhancing actin nucleation and polymerization *in vitro* require other proteins to perform their function *in vivo* (Kovar 2006; Stradal and Scita 2006). This may indicate that the region containing the proline stretch in Cpn0572 is necessary for interaction with other actin regulating proteins that enhances actin polymerization *in vivo*. In this context, proteins implicated in Arp2/3 complex activation (WASP, N-WASP, WAVE2, WIP and VASP) bear proline rich sequences that precede the WH2 domain and comprise consensus profilin-binding sites (Figure 4-4). Profilin is the major ATP-actin monomer carrier in the cell. By delivering actin monomers to growing actin filaments, profilin stimulates actin filament elongation by WASP, WAVE2 and VASP (Kang, Laine et al. 1997; Suetsugu, Miki et al. 1998; Yang, Huang et al. 2000; Yarar, D'Alessio et al. 2002).

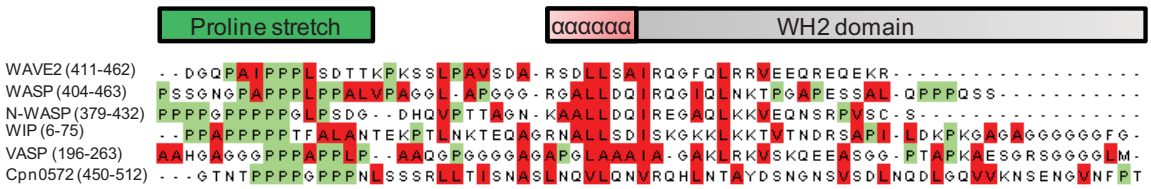

Figure 4-4: comparison and multiple alignments of the sequences of WH2 domains and the N-terminal proline stretch from different proteins involved in actin polymerization. The N-terminal α-helix is indicated within the WH2 domain. WH2 hydrophobic amino acids are marked in red and the proline in green. The alignment was performed using Clustal W2 program (http://www.ebi.ac.uk/Tools/clustalw2/index.html).

The role of profilin in elongation appears to be common among cytoskeletal proteins. Formins, for instance, function in a similar way, promoting elongation in a profilin dependent manner by combining an actin binding FH2 domain C-terminal to a proline rich FH1 domain that mediates profilin binding (Higgs 2005). Thus, Cpn0572 and profilin are potentially cooperating to enhance actin polymerization. Therefore, it might be important to test if profilin interacts and enhances the actin polymerization activity of Cpn0572.

4.3. How do small Cpn0572-induced-actin aggregates form one or two big clump(s)?

When Cpn0572 is expressed in yeast, it first forms small aggregates which shortly after start to colocalize and induce the formation of small actin clumps. By the time, Cpn0572-expressing yeast cells carry one or two big clumps of the fusion protein colocalizing with actin. The actin clumps are mainly F-actin and not G-actin since they can be stained with rhodamine-phalloidin.

There are at least two possible mechanisms to bring multiple small actin aggregates together into 1-2 big actin clumps: either actin monomers are released from existing small clumps and then polymerize again into an increasingly large actin clump, or that existing small actin clumps can coalesce and fuse to form a large actin clump. Indeed, we do not support the first possibility because it might be hard to disassociate actin monomers from Cpn0572-stabilized small clumps where actin depolymerization is inhibited by Cpn0572. Therefore, it is more likely that a large actin clump results from the fusion of the small actin clumps. Although the early formed small actin clumps are not dynamic (in term of actin treadmilling) due to the alteration in actin depolymerization, actin dynamics seems not to be necessary for actin clump movement (Lappalainen and Drubin 1997; Belmont and Drubin 1998).

It could be suggested that the small actin clumps, at early time of expression, migrate along actin cables that are not associated with Cpn0572 yet (dynamic F-actin). The fusion of small actin clumps into big actin clumps is probably achieved by the actin cross-linking proteins. In this context, the yeast F-actin cross-linking protein coronin (Crn1) is precipitated with Cpn0572 in the coimmunoprecipitation assay using the cell extracts of Cpn0572-expressing yeast cells. Expression of Cpn0572 in a deletion strain (crn1*Δ*) does not alleviate the Cpn0572-induced growth defect in these cells. However, growth inhibition of yeast cells expressing Cpn0572 is not “only” due to actin clumping since fragments losing clumping activity (Cpn0572-ALA and Cpn0572-B) achieved by the wild type protein are also lethal for yeast. Therefore, it should be investigated whether Cpn0572 induce the formation of proper actin clumps in this deletion strain. Another possibility, in case Cpn0572 is able to form oligomers, is that actin clumps associated with Cpn0572 interact because Cpn0572 has a tendency to form oligomers.

Nevertheless, these actin clumps are formed when the protein is highly expressed and has not been reported in *C. pneumoniae* infected mammalian cells. During *C. pneumoniae* infection, EBs secrete much less of Cpn0572 and thus Cpn0572 localization (activity) is very limited to a subcellular region within the cytosol underneath a bound EB.

4.4. Cpn0572 is secreted into the host cell

Known pathogen effector proteins target host pathways, mainly the actin cytoskeleton, to ensure bacterium uptake and replication. To do so, pathogens either expose their effector proteins on the pathogen surface or translocate them into the host cell via different secretion systems (Zhou and Galan 2001; Cossart, Pizarro-Cerda et al. 2003; Ghosh 2004).

Cpn0572 is found late in the cycle where the majority of *C. pneumoniae* particles have been redifferentiated back to EBs. For chlamydiologist, It is believed that proteins which are found in EBs, are very likely relevant for early events in the infection and they are either adhesins or secreted proteins that are required for the entry of the EBs. Adhesins are exposed on the surface of pathogens. Although the *C. pneumoniae* EBs contain Cpn0572 protein, Cpn0572 is neither exposed on the EBs nor later in infection on the inclusion membrane. Instead, Cpn0572 localizes within the chlamydia and it is found within the host cell shortly after adhesion, but prior to EB entry, suggesting that it is translocated into the host cell.

Chlamydia have protein homologs to the bacterial type II, III, and IV secretion systems and therefore it is predicted that they can secrete proteins into the host cell cytoplasm and within the inclusion (Vandahl, Pedersen et al. 2002; Birkelund S. and G. 2005). Type II and IV secreted proteins do have a leader sequence and type IV secreted proteins have characteristic structural motifs. Type III secreted proteins have no known motifs. Due to the inability of growing *Chlamydia* out of the host cell, it cannot be tested if such a protein is secreted by TIIISS. Additionally, some *Chlamydia* proteins use TVSS, also called the autotransporter system, which forms a beta-barrel with their C-terminus that is inserted into the outer membrane (Henderson and Lam 2001). Our bioinformatical search did not show any prediction for Cpn0572 to contain the leader sequence for TIISS, TIVSS or to form beta-barrel. Thus, it seems that Cpn0572 use the other option, TIIISS.

In agreement with this view, the *C. trachomatis* homologous protein Tarp is secreted by a heterologous TIIISS machinery indicating that Tarp could indeed be a substrate for TIIISS (Clifton, Fields et al. 2004). Moreover, Cpn0572 and Tarp contain all of the predicted properties of TIIISS effectors, including delivering into the host cell, mimicking or capturing the activity of eukaryotic proteins and the interacting partners are found only in eukaryotes (Liverman, Cheng et al. 2007). Thus, it is likely that Cpn0572 and Tarp are secreted by TIIISS.

4.5. Cpn0572 interacts directly with actin *in vitro*

In vitro experiments showed that Cpn0572 binds actin directly by the DUF domain (Cpn0572-C), a 60 amino acids domain. Our results are consistent with the results obtained for Tarp, where the shortest fragment containing the first DUF (Tarp-D, 100 amino acids: 725-825) binds actin but not a shorter fragment which lacks the N-terminal part of DUF (Tarp-L, 50 amino acids: 776-825) (Jewett, Fischer et al. 2006).

DUF is highly conserved among Cpn0572 homologous proteins from different *Chlamydia* species and harbors many of the conserved hydrophobic amino acids. Mutations introduced in the conserved amino acids within DUF (Cpn0572-M1: L480N, V483N, L487N and Cpn0572-M2: L505A, V508A, V509A) result in loss of Cpn0572 activities including the interaction with the actin cytoskeleton.

A structure-based prediction, using the NPS program (http://npsa-pbil.ibcp.fr/cgi-bin/npsa_automat.pl?page=/NPSA/npsa seccons.html) revealed that DUF is rich in potential amphipathic α-helices (Figure 4-5-A). Remarkably, DUF contains several hydrophobic amino acids that appear regularly every third and seventh amino acid residue (Figure 4-5-B). When the sequence is arranged in α-helical heptad repeats, hydrophobic amino acid residues at positions a and d form a hydrophobic surface (Figure 4-5-C). Interestingly, these hydrophobic amino acid residues are conserved in all DUFs of the Cpn0572 homologous proteins from different *Chlamydia* species (Figure 3-5-D). Thus, the mutations introduced within DUF lead to the disruption of the predicted α-helices and subsequently the interaction with actin.

Bacterial effector proteins secreted into the host cell have evolved different strategies to interact with and modulate the host actin cytoskeleton, either directly or indirectly (Tran Van Nhieu, Bourdet-Sicard et al. 2000; Liverman, Cheng et al. 2007). Those proteins binding actin directly bear actin binding motifs. The most common actin binding motifs are the Formin homology domain 2 (FH2), Calponin homology domain (CH), and the WASP homology domain 2 (WH2), (Castresana and Saraste 1995; Lappalainen, Kessels et al. 1998; Van Troys, Vandekerckhove et al. 1999). Interestingly, the N-terminal part of DUF in Tarp shows high similarity and identity to the sequence of the WH2 domain from WAVE2 (Jewett, Fischer et al. 2006). The primary sequences of the WH2 domain varies among different proteins but the most important part is the N-terminal α-helix. In some proteins, the C-terminal part can vary in length and therefore two types of WH2 domain have been described, short as in WASP and WAVE2 and long as in WASP interacting protein (WIP), missing in metastasis (Yoshida, Katayama et al.) and in the WH2-like thymosinβ4 (Tβ4)(Chereau, Kerff et al. 2005). Protein structure studies suggest that the N-terminal α-helix which binds the actin cleft between subdomain 1 and 3, allosterically potentiates the binding of the C-terminal portion of the long WH2 domain which interacts with other sub-

domains of actin. Moreover, the absence of the C-terminal structured part of the long WH2 domain highly affect the actin-interacting capability of these proteins (Chereau, Kerff et al. 2005). From this point of view, we propose that both the N-terminal and C-terminal α-helices in DUF cooperate to result in stable interaction with actin sub-domain(s).

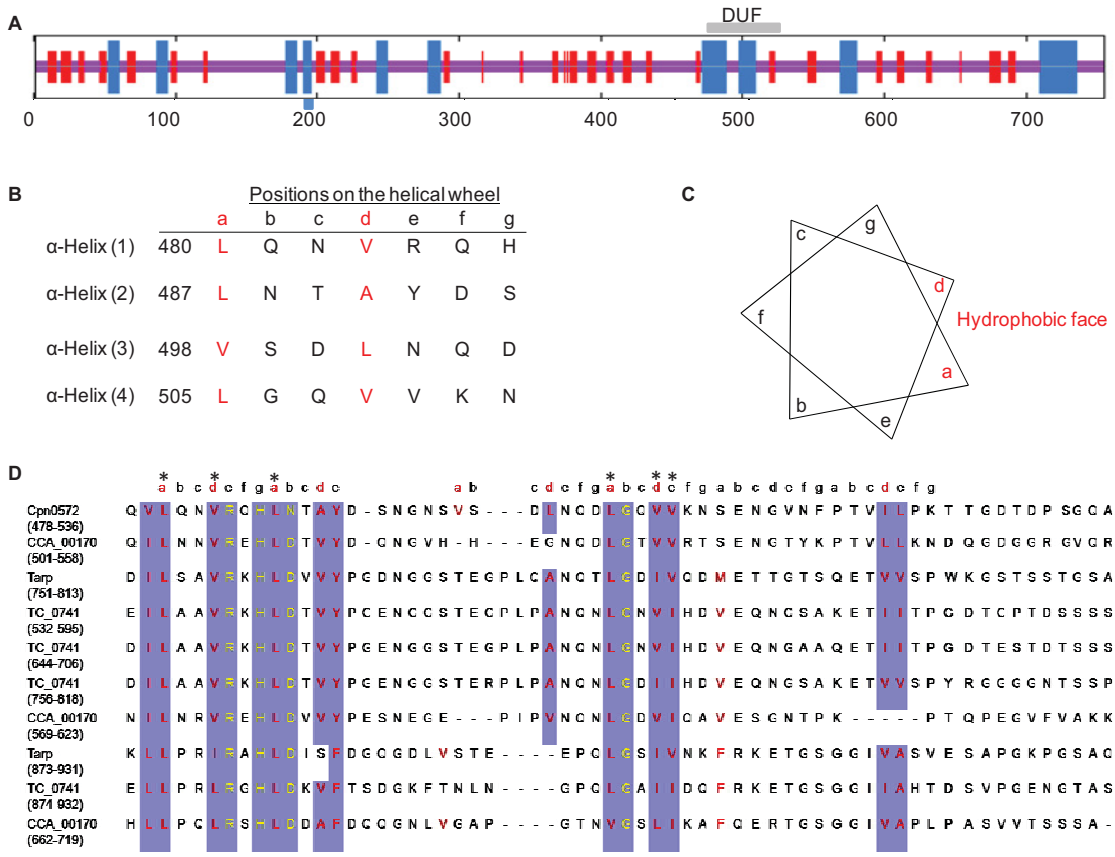

Figure 4-5: Bioinformatic analysis of DUF from Cpn0572 and from the homologous proteins from different *Chlamydia* species.
A, schematic representation of the secondary structure prediction of Cpn0572. The predicted α-helical structures are shown in blue and extended strands shown in red. DUF is predicted to contain α-helices as indicated.
B, the sequences of seven amino acids repeats in Cpn0572 DUF. Amino acids positions on the α-helix wheel are indicated (Moraczewska, Wawro et al.).
C, the position of amino acids (represented as a,b,c...g) were organized on the α-helix. Note that positions a and d in red represent the hydrophobic face of the wheel.
D, Multiple alignments of structure-based sequences of the complete DUF from different *Chlamydia* species. The conserved amino acids are shaded in blue. Amino acids that are located on position a or d on the wheel are in red. Stars indicate the site of mutations introduced in this study.

4.6. The role of Cpn0572 in *C. pneumoniae* infection

Pathogens manipulate the host cytoskeleton for diverse reasons, to induce their uptake or facilitating their motility into, out of, and within the host cells (Aktories and Barbieri 2005). Most of the pathogen effectors manipulating actin for pathogen motility are exposed on the surface of the pathogen, for instance the *Shigella* LcsA, the *Listeria* ActA and the *Rickettsia* RickA (reviewed in (Gouin, Welch et al. 2005). The majority of bacterial pathogens secrete their effectors into the host prior to entry to recruit actin at this site and subsequently facilitating pathogen entry, for instance the *Salmonella* SipC and SipA and the *Shigella* IpaC effector (reviewed in (Rottner, Stradal et al. 2005).

One of the hallmarks of *Chlamydia* infection is the recruitment of actin and formation of actin pedestals at the site of entry directly after EBs attachment to the host cell surface (Majeed and Kihlstrom 1991; Carabeo, Grieshaber et al. 2002; Coombes and Mahony 2002; Subtil, Wyplosz et al. 2004). Formation of actin pedestals is due to alterations in actin polymerization, depolymerization or bundling (Hayward and Koronakis 1999; Shaner, Sanger et al. 2005). Cpn0572, which is secreted and recruited at the site of but prior to EB entry, is at least involved in two of these processes: it enhances actin polymerization and inhibits actin depolymerization. Actin recruitment and microvillar reorganization induced by the attachment of *C. trachomatis* and *C. pneumoniae* on cultured mammalian cells is a transient process and disappears 2 h after infection (Carabeo, Grieshaber et al. 2002; Coombes and Mahony 2002). So far Cpn0572 and Tarp are the only chlamydial proteins known to be secreted early during infection and interacting with actin. Cpn0572 has not been found to be secreted later in the chlamydial developmental cycle, however, it has not been analyzed for how long after infection Cpn0572 or Tarp are present in the HEp-2 cell cytosol. Therefore, we propose that Cpn0572 and Tarp are required for actin pedestals formation underneath the attached EB.

Recently, it has been shown that actin and intermediate filaments stabilize the *C. trachomatis* inclusion by forming dynamic structural scaffolds during the inclusion progression, however the chlamydial proteins required for this activity are still unknown (Kumar, Cocchiaro et al. 2008). Stabilization of the inclusion of other *Chlamydia* species has not been tested so far. However, if the *C. pneumoniae* inclusion is stabilized by actin, it cannot be due to Cpn0572 because Cpn0572 is not detected in the host cytosol mid or late during *C. pneumoniae* developmental cycle. Recently, Cpn0712 which has been shown to be secreted 60h after infection surrounding the inclusions has been found to colocalize with actin (Müller, Sattelmacher et al. 2008).Therefore, it might be that Cpn0712 is involved in actin recruitment around the inclusion.

The dual function of Cpn0572 is incompatible, since actin assembly requires a G-actin flux which is presumably normally gained from an active actin depolymerization process. The

secreted Cpn0572 localizes close to the attached EBs. It is possible that inhibiting the depolymerization of Cpn0572-associated F-actin by competing with cofilin leads to an increase in the availability of cofilin in other regions of the cell and in turn increases actin depolymerization in that region in order to enhance the G-actin flux required for Cpn0572-directed actin assembly. Thus inhibition of the depolymerization of Cpn0572-associated F-actin and the actin polymerization activity of Cpn0572 together eventually will lead to highly polymerized actin.

Incompatible activities have been also reported for the cooperated functions of the two *Salmonella* effector proteins SipC and SipA. SipC, which is secreted prior to *Salmonella* entry, can nucleate actin filament assembly. At the same time the activity of SipA, which inhibits actin depolymerization by binding F-actin and competing with cofilin and gelsolin activities, appears to augment the cellular activity of SipC (McGhie, Hayward et al. 2004). SipC is essential for *Salmonella* entry while SipA enhances the efficiency of, but is not necessary for *Salmonella* entry (Zhou, Mooseker et al. 1999; Higashide, Dai et al. 2002). Thus, Cpn0572 resembles the cooperated functions of these two *Salmonella* effector proteins. From this point of view, we propose that Cpn0572 is possibly necessary for *C. pneumoniae* entry.

The inability to genetically modify *Chlamydia* limits our possibilities to prove this hypothesis. To bypass this limitation, our future plan is to inhibit Cpn0572 activity by either delivering an α-Cpn0572 antibody into mammalian cells before *C. pneumoniae* infection or to express a dominant negative variant of Cpn0572 in the human cell perior to infection.

An alternative strategy could be to use the yeast system to screen for Cpn0572 antagonist. Infection of mammalian cells overexpressing this antagonist with *C. pneumoniae* may give us an idea about the necessity of Cpn0572 for *Chlamydia* infection. A Cpn0572 antagonist could be a host protein activated after infection or a chlamydial protein that is secreted downstream of Cpn0572 to turn off Cpn0572 activity. The availability of *C. pneumoniae* genome library and human cDNA libraries in yeast vectors will advance the identification of potential Cpn0572 antagonist to turn off Cpn0572 activity. How Cpn0572 activity is turned off after *C. pneumoniae* entry is not clear right now. It could be modified and actively turned off by antagonists, degraded by the host proteasomes.

In summary, Cpn0572 is present in EBs. Attached EBs secrete Cpn0572 into the host cell, probably by TIIISS, underneath the attached EBs. Cpn0572 either occupies the pre-assembled F-actin and/or nucleates new F-actin at the site of EBs entry. Cpn0572 inhibits actin depolymerization of Cpn0572-associated F-actin by displacing and blocking of cofilin from F-actin. As a result, the association to and the depolymerizing activity of cofilin probably increase in Cpn0572-non-associated F-actin structures which in turn enhances

G-actin flux required for Cpn0572-directed actin assembly. Eventually, this dual function of Cpn0572 leads to highly polymerized and stable actin that overpassing other F-actin directed by other host regulators to direct the membrane protrusions of host cells and thus facilitate EBs entry (Figure 4-6-A). The dual function of Cpn0572 mimics the function of the *Salmonella* proteins SipA and SipC (Figure 4-6-B).

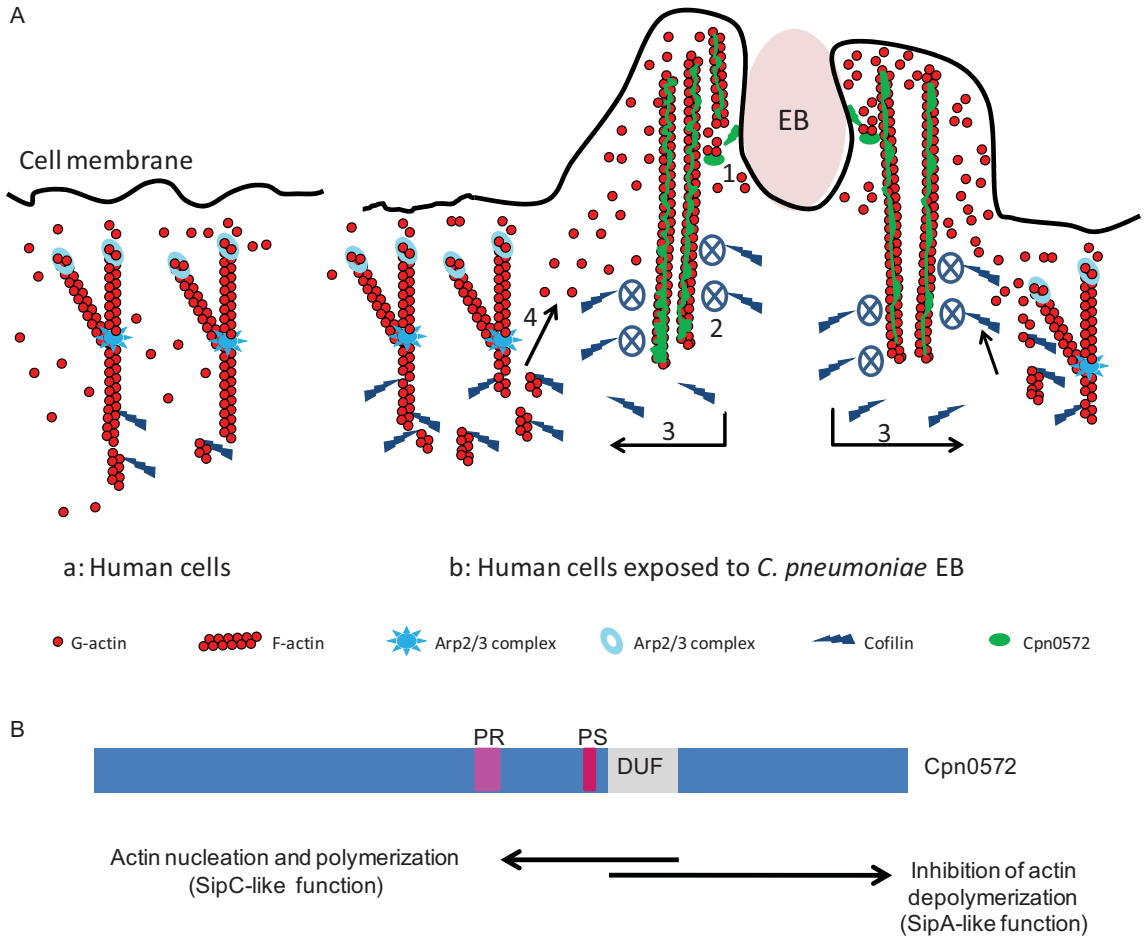

Figure 4-6: The dual function of the *C. pneumoniae* Cpn0572 protein in modulating the host actin cytoskeleton.
A, model: the role of Cpn0572 in modulating the host actin cytoskeleton at the site of entry. Actin dynamics are basically regulated by the host regulators Arp2/3 complex and forming (a). During *C. pneumoniae* infection (b), Cpn0572 is secreted underneath the attached EB. The secreted Cpn0572 nucleate and enhances actin assembly (1). Cpn0572 stabilizes F-actin by blocking the binding of the actin cofilin (2). Thus, cofilin probably increase in Cpn0572-non-associated F-actin structures and enhances their depolymerization (3) which in turn increase G-actin flux (4) required for Cpn0572 actin polymerization activity. As a results, actin is highly polymerized and stabilized underneath the attach EB to enhance membrane invagination and EB entry. .
B, Schematic representation shows the regions within Cpn0572 that mimics SipA and SipC functions. PR and PS indicate the proline rich and the proline stretch regions, respectively.

REFERENCES

Abkevich, V. I., A. M. Gutin, et al. (1994). "Specific nucleus as the transition state for protein folding: evidence from the lattice model." Biochemistry **33**(33): 10026-36.

Aktories, K. and J. T. Barbieri (2005). "Bacterial cytotoxins: targeting eukaryotic switches." Nat Rev Microbiol **3**(5): 397-410.

Alto, N. M., F. Shao, et al. (2006). "Identification of a bacterial type III effector family with G protein mimicry functions." Cell **124**(1): 133-45.

Amberg, D. C. (1998). "Three-dimensional imaging of the yeast actin cytoskeleton through the budding cell cycle." Mol Biol Cell **9**(12): 3259-62.

Asakura, T., T. Sasaki, et al. (1998). "Isolation and characterization of a novel actin filament-binding protein from Saccharomyces cerevisiae." Oncogene **16**(1): 121-30.

Ayscough, K. R. (2000). "Endocytosis and the development of cell polarity in yeast require a dynamic F-actin cytoskeleton." Curr Biol **10**(24): 1587-90.

Ayscough, K. R., J. Stryker, et al. (1997). "High rates of actin filament turnover in budding yeast and roles for actin in establishment and maintenance of cell polarity revealed using the actin inhibitor latrunculin-A." J Cell Biol **137**(2): 399-416.

Balin, B. J., H. C. Gerard, et al. (1998). "Identification and localization of Chlamydia pneumoniae in the Alzheimer's brain." Med Microbiol Immunol (Berl) **187**(1): 23-42.

Bamburg, J. R., A. McGough, et al. (1999). "Putting a new twist on actin: ADF/cofilins modulate actin dynamics." Trends Cell Biol **9**(9): 364-70.

Baum, B. and P. Kunda (2005). "Actin nucleation: spire - actin nucleator in a class of its own." Curr Biol **15**(8): R305-8.

Belland, R. J., S. P. Ouellette, et al. (2004). "Chlamydia pneumoniae and atherosclerosis." Cell Microbiol **6**(2): 117-27.

Belmont, L. D. and D. G. Drubin (1998). "The yeast V159N actin mutant reveals roles for actin dynamics in vivo." J Cell Biol **142**(5): 1289-99.

Berka, K., P. Hobza, et al. (2009). "Analysis of energy stabilization inside the hydrophobic core of rubredoxin." Chemphyschem **10**(3): 543-8.

Birkelund, S., A. G. Lundemose, et al. (1990). "The 75-kilodalton cytoplasmic Chlamydia trachomatis L2 polypeptide is a DnaK-like protein." Infect Immun **58**(7): 2098-104.

Birkelund S. and C. G. (2005). Chlamydia proteomes. 15th European Congress of Clinical Microbiology and Infectious Diseases Copenhagen / Denmark, European Society of Clinical Microbiology and Infectious Diseases.

Bishop, A. L. and A. Hall (2000). "Rho GTPases and their effector proteins." Biochem J **348 Pt 2**: 241-55.

Boleti, H., A. Benmerah, et al. (1999). "Chlamydia infection of epithelial cells expressing dynamin and Eps15 mutants: clathrin-independent entry into cells and dynamin-dependent productive growth." J Cell Sci **112**(Pt 10): 1487-96.

Bretscher, A. (2003). "Polarized growth and organelle segregation in yeast: the tracks, motors, and receptors." J Cell Biol **160**(6): 811-6.

Brieher, W. M., H. Y. Kueh, et al. (2006). "Rapid actin monomer-insensitive depolymerization of Listeria actin comet tails by cofilin, coronin, and Aip1." J Cell Biol **175**(2): 315-24.

Bubb, M. R., A. M. Senderowicz, et al. (1994). "Jasplakinolide, a cytotoxic natural product, induces actin polymerization and competitively inhibits the binding of phalloidin to F-actin." J Biol Chem **269**(21): 14869-71.

Buttner, D. and U. Bonas (2002). "Getting across--bacterial type III effector proteins on their way to the plant cell." Embo J **21**(20): 5313-22.

Byrne, G. I. (1978). "Kinetics of phagocytosis of Chlamydia psittaci by mouse fibroblasts (L cells): separation of the attachment and ingestion stages." Infect Immun **19**(2): 607-12.

Cain, R. J., R. D. Hayward, et al. (2008). "Deciphering interplay between Salmonella invasion effectors." PLoS Pathog **4**(4): e1000037.

Carabeo, R. A., S. S. Grieshaber, et al. (2002). "Chlamydia trachomatis induces remodeling of the actin cytoskeleton during attachment and entry into HeLa cells." Infect Immun **70**(7): 3793-803.

Carabeo, R. A., S. S. Grieshaber, et al. (2004). "Requirement for the Rac GTPase in Chlamydia trachomatis invasion of non-phagocytic cells." Traffic **5**(6): 418-25.

Carabeo, R. A., D. J. Mead, et al. (2003). "Golgi-dependent transport of cholesterol to the Chlamydia trachomatis inclusion." Proc Natl Acad Sci U S A **100**(11): 6771-6.

Carlier, M. F., F. Ressad, et al. (1999). "Control of actin dynamics in cell motility. Role of ADF/cofilin." J Biol Chem **274**(48): 33827-30.

Castresana, J. and M. Saraste (1995). "Does Vav bind to F-actin through a CH domain?" FEBS Lett **374**(2): 149-51.

CDC, C. f. D. C. a. P. (1993). "Recommendations for the prevention and management of Chlamydia trachomatis infections, 1993." MMWR **42**(RR-12): 1-39.

Chen, H., B. W. Bernstein, et al. (2000). "Regulating actin-filament dynamics in vivo." Trends Biochem Sci **25**(1): 19-23.

Chereau, D., F. Kerff, et al. (2005). "Actin-bound structures of Wiskott-Aldrich syndrome protein (WASP)-homology domain 2 and the implications for filament assembly." Proc Natl Acad Sci U S A **102**(46): 16644-9.

Chhabra, E. S. and H. N. Higgs (2007). "The many faces of actin: matching assembly factors with cellular structures." Nat Cell Biol **9**(10): 1110-21.

Clifton, D. R., C. A. Dooley, et al. (2005). "Tyrosine phosphorylation of the chlamydial effector protein Tarp is species specific and not required for recruitment of actin." Infect Immun **73**(7): 3860-8.

Clifton, D. R., K. A. Fields, et al. (2004). "A chlamydial type III translocated protein is tyrosine-phosphorylated at the site of entry and associated with recruitment of actin." Proc Natl Acad Sci U S A **101**(27): 10166-71.

Cocchiaro, J. L., Y. Kumar, et al. (2008). "Cytoplasmic lipid droplets are translocated into the lumen of the Chlamydia trachomatis parasitophorous vacuole." Proc Natl Acad Sci U S A **105**(27): 9379-84.

Coombes, B. K., D. L. Johnson, et al. (2002). "Strategic targeting of essential host-pathogen interactions in chlamydial disease." Curr Drug Targets Infect Disord **2**(3): 201-16.

Coombes, B. K. and J. B. Mahony (2002). "Identification of MEK- and phosphoinositide 3-kinase-dependent signalling as essential events during Chlamydia pneumoniae invasion of HEp2 cells." Cell Microbiol **4**(7): 447-60.

Cooper, J. A. and T. D. Pollard (1982). "Methods to measure actin polymerization." Methods Enzymol **85 Pt B**: 182-210.

Cortes, C., K. A. Rzomp, et al. (2007). "Chlamydia pneumoniae inclusion membrane protein Cpn0585 interacts with multiple Rab GTPases." Infect Immun **75**(12): 5586-96.

Cossart, P., J. Pizarro-Cerda, et al. (2003). "Invasion of mammalian cells by Listeria monocytogenes: functional mimicry to subvert cellular functions." Trends Cell Biol **13**(1): 23-31.

Coue, M., S. L. Brenner, et al. (1987). "Inhibition of actin polymerization by latrunculin A." FEBS Lett **213**(2): 316-8.

D'Agostino, J. L. and B. L. Goode (2005). "Dissection of Arp2/3 complex actin nucleation mechanism and distinct roles for its nucleation-promoting factors in Saccharomyces cerevisiae." Genetics **171**(1): 35-47.

Davis, C. H. and P. B. Wyrick (1997). "Differences in the association of Chlamydia trachomatis serovar E and serovar L2 with epithelial cells in vitro may reflect biological differences in vivo." Infect Immun **65**(7): 2914-24.

Delevoye, C., M. Nilges, et al. (2008). "SNARE protein mimicry by an intracellular bacterium." PLoS Pathog **4**(3): e1000022.

Dominguez, R. (2004). "Actin-binding proteins--a unifying hypothesis." Trends Biochem Sci **29**(11): 572-8.

Elwell, C. A., A. Ceesay, et al. (2008). "RNA interference screen identifies Abl kinase and

PDGFR signaling in Chlamydia trachomatis entry." PLoS Pathog **4**(3): e1000021.
Entian, K. D. and P. Kötter (1998). Yeast mutant and plasmid collections. In: Yeast Gene Analysis, vol. 26, , ed. A.J.P. Brown and M.F. Tuite, London: Academic Press, United Kingdom, 431-449.
Escalante-Ochoa, C., R. Ducatelle, et al. (2000). "Optimal development of Chlamydophila psittaci in L929 fibroblast and BGM epithelial cells requires the participation of microfilaments and microtubule-motor proteins." Microb Pathog **28**(6): 321-33.
Everett, K. D., R. M. Bush, et al. (1999). "Emended description of the order Chlamydiales, proposal of Parachlamydiaceae fam. nov. and Simkaniaceae fam. nov., each containing one monotypic genus, revised taxonomy of the family Chlamydiaceae, including a new genus and five new species, and standards for the identification of organisms." Int J Syst Bacteriol **49 Pt 2**: 415-40.
Fiedler, T. A., T. S. Karpova, et al. (2002). "The vesicular transport protein Cgp1p/Vps54p/Tcs3p/Luv1p is required for the integrity of the actin cytoskeleton." Mol Genet Genomics **268**(2): 190-205.
Ford, P. J., E. Gemmell, et al. (2005). "Cross-reactivity of GroEL antibodies with human heat shock protein 60 and quantification of pathogens in atherosclerosis." Oral Microbiol Immunol **20**(5): 296-302.
Gabel, B. R., C. Elwell, et al. (2004). "Lipid raft-mediated entry is not required for Chlamydia trachomatis infection of cultured epithelial cells." Infect Immun **72**(12): 7367-73.
Geese, M., K. Schluter, et al. (2000). "Accumulation of profilin II at the surface of Listeria is concomitant with the onset of motility and correlates with bacterial speed." J Cell Sci **113 (Pt 8)**: 1415-26.
Ghosh, P. (2004). "Process of protein transport by the type III secretion system." Microbiol Mol Biol Rev **68**(4): 771-95.
Goffeau, A. (1996). "1996: a vintage year for yeast and Yeast." Yeast **12**(16): 1603-5.
Goley, E. D. and M. D. Welch (2006). "The ARP2/3 complex: an actin nucleator comes of age." Nat Rev Mol Cell Biol **7**(10): 713-26.
Goode, B. L., J. J. Wong, et al. (1999). "Coronin promotes the rapid assembly and cross-linking of actin filaments and may link the actin and microtubule cytoskeletons in yeast." J Cell Biol **144**(1): 83-98.
Gouin, E., M. D. Welch, et al. (2005). "Actin-based motility of intracellular pathogens." Curr Opin Microbiol **8**(1): 35-45.
Grieshaber, S. S., N. A. Grieshaber, et al. (2003). "Chlamydia trachomatis uses host cell dynein to traffic to the microtubule-organizing center in a p50 dynamitin-independent process." J Cell Sci **116**(Pt 18): 3793-802.
Guldener, U., G. J. Koehler, et al. (2004). "Characterization of the Saccharomyces cerevisiae Fol1 protein: starvation for C1 carrier induces pseudohyphal growth." Mol Biol Cell **15**(8): 3811-28.
Gunst, S. J. and W. Zhang (2008). "Actin cytoskeletal dynamics in smooth muscle: a new paradigm for the regulation of smooth muscle contraction." Am J Physiol Cell Physiol **295**(3): C576-87.
Hayward, R. D. and V. Koronakis (1999). "Direct nucleation and bundling of actin by the SipC protein of invasive Salmonella." Embo J **18**(18): 4926-34.
Heise, T. and P. Dersch (2006). "Identification of a domain in Yersinia virulence factor YadA that is crucial for extracellular matrix-specific cell adhesion and uptake." Proc Natl Acad Sci U S A **103**(9): 3375-80.
Henderson, I. R. and A. C. Lam (2001). "Polymorphic proteins of Chlamydia spp.--autotransporters beyond the Proteobacteria." Trends Microbiol **9**(12): 573-8.
Higashide, W., S. Dai, et al. (2002). "Involvement of SipA in modulating actin dynamics during Salmonella invasion into cultured epithelial cells." Cell Microbiol **4**(6): 357-65.
Higgs, H. N. (2005). "Formin proteins: a domain-based approach." Trends Biochem Sci **30**(6): 342-53.
Hodinka, R. L., C. H. Davis, et al. (1988). "Ultrastructural study of endocytosis of

Chlamydia trachomatis by McCoy cells." Infect Immun **56**(6): 1456-63.
Hodinka, R. L. and P. B. Wyrick (1986). "Ultrastructural study of mode of entry of Chlamydia psittaci into L-929 cells." Infect Immun **54**(3): 855-63.
Holmes, K. C., D. Popp, et al. (1990). "Atomic model of the actin filament." Nature **347**(6288): 44-9.
Hsia, R. C., Y. Pannekoek, et al. (1997). "Type III secretion genes identify a putative virulence locus of Chlamydia." Mol Microbiol **25**(2): 351-9.
Huang, J., C. F. Lesser, et al. (2008). "The essential role of the CopN protein in Chlamydia pneumoniae intracellular growth." Nature **456**(7218): 112-5.
Hueck, C. J. (1998). "Type III protein secretion systems in bacterial pathogens of animals and plants." Microbiol Mol Biol Rev **62**(2): 379-433.
Humphries, C. L., H. I. Balcer, et al. (2002). "Direct regulation of Arp2/3 complex activity and function by the actin binding protein coronin." J Cell Biol **159**(6): 993-1004.
Hybiske, K. and R. S. Stephens (2007). "Mechanisms of host cell exit by the intracellular bacterium Chlamydia." Proc Natl Acad Sci U S A **104**(27): 11430-5.
Jewett, T. J., C. A. Dooley, et al. (2008). "Chlamydia trachomatis tarp is phosphorylated by src family tyrosine kinases." Biochem Biophys Res Commun **371**(2): 339-44.
Jewett, T. J., E. R. Fischer, et al. (2006). "Chlamydial TARP is a bacterial nucleator of actin." Proc Natl Acad Sci U S A **103**(42): 15599-604.
Jutras, I., L. Abrami, et al. (2003). "Entry of the lymphogranuloma venereum strain of Chlamydia trachomatis into host cells involves cholesterol-rich membrane domains." Infect Immun **71**(1): 260-6.
Kabsch, W. and K. C. Holmes (1995). "The actin fold." Faseb J **9**(2): 167-74.
Kabsch, W., H. G. Mannherz, et al. (1990). "Atomic structure of the actin:DNase I complex." Nature **347**(6288): 37-44.
Kang, F., R. O. Laine, et al. (1997). "Profilin interacts with the Gly-Pro-Pro-Pro-Pro-Pro sequences of vasodilator-stimulated phosphoprotein (VASP): implications for actin-based Listeria motility." Biochemistry **36**(27): 8384-92.
Kovar, D. R. (2006). "Molecular details of formin-mediated actin assembly." Curr Opin Cell Biol **18**(1): 11-7.
Kramer, R. W., N. L. Slagowski, et al. (2007). "Yeast functional genomic screens lead to identification of a role for a bacterial effector in innate immunity regulation." PLoS Pathog **3**(2): e21.
Kumar, Y., J. Cocchiaro, et al. (2006). "The obligate intracellular pathogen Chlamydia trachomatis targets host lipid droplets." Curr Biol **16**(16): 1646-51.
Kuo, C. C., J. T. Grayston, et al. (1995). "Chlamydia pneumoniae (TWAR) in coronary arteries of young adults (15-34 years old)." Proc Natl Acad Sci U S A **92**(15): 6911-4.
Lad, S. P., J. Li, et al. (2007). "Cleavage of p65/RelA of the NF-kappaB pathway by Chlamydia." Proc Natl Acad Sci U S A **104**(8): 2933-8.
Laemmli, U. K. (1970). "Cleavage of structural proteins during the assembly of the head of bacteriophage T4." Nature **227**(5259): 680-5.
Land, J. A., A. P. Gijsen, et al. (2002). "Chlamydia trachomatis in subfertile women undergoing uterine instrumentation. Screen or treat?" Hum Reprod **17**(3): 525-7.
Lane, B. J., C. Mutchler, et al. (2008). "Chlamydial entry involves TARP binding of guanine nucleotide exchange factors." PLoS Pathog **4**(3): e1000014.
Lappalainen, P. and D. G. Drubin (1997). "Cofilin promotes rapid actin filament turnover in vivo." Nature **388**(6637): 78-82.
Lappalainen, P., M. M. Kessels, et al. (1998). "The ADF homology (ADF-H) domain: a highly exploited actin-binding module." Mol Biol Cell **9**(8): 1951-9.
Lazaro-Dieguez, F., C. Aguado, et al. (2008). "Dynamics of an F-actin aggresome generated by the actin-stabilizing toxin jasplakinolide." J Cell Sci **121**(Pt 9): 1415-25.
Lee, C. A. (1997). "Type III secretion systems: machines to deliver bacterial proteins into eukaryotic cells?" Trends Microbiol **5**(4): 148-56.
Leinonen, M. and P. Saikku (2000). "Infections and atherosclerosis." Scand Cardiovasc J

34(1): 12-20.
Lesser, C. F. and S. I. Miller (2001). "Expression of microbial virulence proteins in Saccharomyces cerevisiae models mammalian infection." Embo J **20**(8): 1840-9.
Liepina, I., C. Czaplewski, et al. (2003). "Molecular dynamics study of a gelsolin-derived peptide binding to a lipid bilayer containing phosphatidylinositol 4,5-bisphosphate." Biopolymers **71**(1): 49-70.
Littlefield, R. and V. M. Fowler (2002). "A minor actin catastrophe." Nat Cell Biol **4**(9): E209-11.
Liu, H. P. and A. Bretscher (1989). "Disruption of the single tropomyosin gene in yeast results in the disappearance of actin cables from the cytoskeleton." Cell **57**(2): 233-42.
Liverman, A. D., H. C. Cheng, et al. (2007). "Arp2/3-independent assembly of actin by Vibrio type III effector VopL." Proc Natl Acad Sci U S A **104**(43): 17117-22.
Lu, H., W. M. Zhao, et al. (2005). "Analysis of synonymous codon usage bias in Chlamydia." Acta Biochim Biophys Sin (Shanghai) **37**(1): 1-10.
Mahoney, N. M., D. A. Rozwarski, et al. (1999). "Profilin binds proline-rich ligands in two distinct amide backbone orientations." Nat Struct Biol **6**(7): 666-71.
Majeed, M. and E. Kihlstrom (1991). "Mobilization of F-actin and clathrin during redistribution of Chlamydia trachomatis to an intracellular site in eucaryotic cells." Infect Immun **59**(12): 4465-72.
McGhie, E. J., R. D. Hayward, et al. (2004). "Control of actin turnover by a salmonella invasion protein." Mol Cell **13**(4): 497-510.
Mehlitz, A., S. Banhart, et al. (2008). "Complex kinase requirements for Chlamydia trachomatis Tarp phosphorylation." FEMS Microbiol Lett **289**(2): 233-40.
Michael, B. (2006). LGV in the UK: almost 350 cases reported and still predominantly affecting HIV-positive gay men. Aidsmap: 17 May 2006
Miller, W. C., C. A. Ford, et al. (2004). "Prevalence of chlamydial and gonococcal infections among young adults in the United States." Jama **291**(18): 2229-36.
Moelleken, K. and J. H. Hegemann (2008). "The Chlamydia outer membrane protein OmcB is required for adhesion and exhibits biovar-specific differences in glycosaminoglycan binding." Mol Microbiol **67**(2): 403-19.
Moraczewska, J., B. Wawro, et al. (1999). "Divalent cation-, nucleotide-, and polymerization-dependent changes in the conformation of subdomain 2 of actin." Biophys J **77**(1): 373-85.
Morton, W. M., K. R. Ayscough, et al. (2000). "Latrunculin alters the actin-monomer subunit interface to prevent polymerization." Nat Cell Biol **2**(6): 376-8.
Moseley, J. B. and B. L. Goode (2006). "The yeast actin cytoskeleton: from cellular function to biochemical mechanism." Microbiol Mol Biol Rev **70**(3): 605-45.
Müller, N., F. Sattelmacher, et al. (2008). "Characterization and intracellular localization of putative Chlamydia pneumoniae effector proteins." Med Microbiol Immunol **197**(4): 387-96.
Munshi, R., K. A. Kandl, et al. (2001). "Overexpression of translation elongation factor 1A affects the organization and function of the actin cytoskeleton in yeast." Genetics **157**(4): 1425-36.
Nicholson-Dykstra, S., H. N. Higgs, et al. (2005). "Actin dynamics: growth from dendritic branches." Curr Biol **15**(9): R346-57.
Niggli, V. (2005). "Regulation of protein activities by phosphoinositide phosphates." Annu Rev Cell Dev Biol **21**: 57-79.
Oba, Y. and G. Salzman. (2007). "Chlamydial pneumonias. Overview of infection with the three main chlamydial species that cause respiratory disease in humans. eMedicine, February 2007." from http://www.emedicine.com/med/TOPIC341.HTM.
Ohkubo, S. and N. Nakahata (2007). "[Role of lipid rafts in trimeric G protein-mediated signal transduction]." Yakugaku Zasshi **127**(1): 27-40.
Ojala, P. J., V. Paavilainen, et al. (2001). "Identification of yeast cofilin residues specific for actin monomer and PIP2 binding." Biochemistry **40**(51): 15562-9.
Okada, K., H. Ravi, et al. (2006). "Aip1 and cofilin promote rapid turnover of yeast actin

patches and cables: a coordinated mechanism for severing and capping filaments." Mol Biol Cell **17**(7): 2855-68.
Ono, S. (2007). "Mechanism of depolymerization and severing of actin filaments and its significance in cytoskeletal dynamics." Int Rev Cytol **258**: 1-82.
Owen, C. H., D. J. DeRosier, et al. (1992). "Actin crosslinking protein EF-1a of Dictyostelium discoideum has a unique bonding rule that allows square-packed bundles." J Struct Biol **109**(3): 248-54.
Parthasarathy, S. and M. R. Murthy (1997). "Analysis of temperature factor distribution in high-resolution protein structures." Protein Sci **6**(12): 2561-7.
Peters, J., D. P. Wilson, et al. (2007). "Type III secretion a la Chlamydia." Trends Microbiol **15**(6): 241-51.
Pistor, S., T. Chakraborty, et al. (1995). "The bacterial actin nucleator protein ActA of Listeria monocytogenes contains multiple binding sites for host microfilament proteins." Curr Biol **5**(5): 517-25.
Pollard, T. D. (2003). "The cytoskeleton, cellular motility and the reductionist agenda." Nature **422**(6933): 741-5.
Prain, C. J. and J. H. Pearce (1989). "Ultrastructural studies on the intracellular fate of Chlamydia psittaci (strain guinea pig inclusion conjunctivitis) and Chlamydia trachomatis (strain lymphogranuloma venereum 434): modulation of intracellular events and relationship with endocytic mechanism." J Gen Microbiol **135 (Pt 7)**: 2107-23.
Prebeck, S., C. Kirschning, et al. (2001). "Predominant role of toll-like receptor 2 versus 4 in Chlamydia pneumoniae-induced activation of dendritic cells." J Immunol **167**(6): 3316-23.
Rafelski, S. M. and J. A. Theriot (2004). "Crawling toward a unified model of cell mobility: spatial and temporal regulation of actin dynamics." Annu Rev Biochem **73**: 209-39.
Read, T. D., R. C. Brunham, et al. (2000). "Genome sequences of Chlamydia trachomatis MoPn and Chlamydia pneumoniae AR39." Nucleic Acids Res **28**(6): 1397-406.
Roca, B. (2007). "[Chlamydial infections]." An Med Interna **24**(6): 292-9.
Rockey, D. D., M. A. Scidmore, et al. (2002). "Proteins in the chlamydial inclusion membrane." Microbes Infect **4**(3): 333-40.
Rodal, A. A., J. W. Tetreault, et al. (1999). "Aip1p interacts with cofilin to disassemble actin filaments." J Cell Biol **145**(6): 1251-64.
Rodriguez-Escudero, I., P. R. Hardwidge, et al. (2005). "Enteropathogenic Escherichia coli type III effectors alter cytoskeletal function and signalling in Saccharomyces cerevisiae." Microbiology **151**(Pt 9): 2933-45.
Rosqvist, R., A. Forsberg, et al. (1991). "Intracellular targeting of the Yersinia YopE cytotoxin in mammalian cells induces actin microfilament disruption." Infect Immun **59**(12): 4562-9.
Rottner, K., T. E. Stradal, et al. (2005). "Bacteria-host-cell interactions at the plasma membrane: stories on actin cytoskeleton subversion." Dev Cell **9**(1): 3-17.
Rupp, J., J. Gieffers, et al. (2007). "Chlamydia pneumoniae directly interferes with HIF-1alpha stabilization in human host cells." Cell Microbiol **9**(9): 2181-91.
Rzomp, K. A., A. R. Moorhead, et al. (2006). "The GTPase Rab4 interacts with Chlamydia trachomatis inclusion membrane protein CT229." Infect Immun **74**(9): 5362-73.
Rzomp, K. A., L. D. Scholtes, et al. (2003). "Rab GTPases are recruited to chlamydial inclusions in both a species-dependent and species-independent manner." Infect Immun **71**(10): 5855-70.
Sato, H., D. W. Frank, et al. (2003). "The mechanism of action of the Pseudomonas aeruginosa-encoded type III cytotoxin, ExoU." Embo J **22**(12): 2959-69.
Schramm, N. and P. B. Wyrick (1995). "Cytoskeletal requirements in Chlamydia trachomatis infection of host cells." Infect Immun **63**(1): 324-32.
Schuler, H. (2001). "ATPase activity and conformational changes in the regulation of actin." Biochim Biophys Acta **1549**(2): 137-47.
Shaner, N. C., J. W. Sanger, et al. (2005). "Actin and alpha-actinin dynamics in the adhesion and motility of EPEC and EHEC on host cells." Cell Motil Cytoskeleton

60(2): 104-20.
Sisko, J. L., K. Spaeth, et al. (2006). "Multifunctional analysis of Chlamydia-specific genes in a yeast expression system." Mol Microbiol **60**(1): 51-66.
Skrzypek, E., T. Myers-Morales, et al. (2003). "Application of a Saccharomyces cerevisiae model to study requirements for trafficking of Yersinia pestis YopM in eucaryotic cells." Infect Immun **71**(2): 937-47.
Smith, G. A. and D. A. Portnoy (1997). "How the Listeria monocytogenes ActA protein converts actin polymerization into a motile force." Trends Microbiol **5**(7): 272-6.
Sriram, S., W. Mitchell, et al. (1998). "Multiple sclerosis associated with Chlamydia pneumoniae infection of the CNS." Neurology **50**(2): 571-2.
Stephens, R. S. (1999). Genomic Autobiographies of Chlamydiae. Chlamydia: Intracellular Biology, Pathogenesis, and Immunity. R. S. Stephens. Washington, D.C., ASM Press**:** 9-28.
Stephens, R. S., S. Kalman, et al. (1998). "Genome sequence of an obligate intracellular pathogen of humans: *chlamydia trachomatis*." Science **282**(5389): 754-9.
Stephens, R. S., G. Myers, et al. (2009). "Divergence without difference: phylogenetics and taxonomy of Chlamydia resolved." FEMS Immunol Med Microbiol **55**(2): 115-9.
Strachan T. and Read AP. (1999). Leptospira. In: Human Molecular Genetics, Wiley-Liss. (via NCBI Bookshelf) ISBN 0-471-33061-2.
Stradal, T. E. and G. Scita (2006). "Protein complexes regulating Arp2/3-mediated actin assembly." Curr Opin Cell Biol **18**(1): 4-10.
Su, H., G. McClarty, et al. (2004). "Activation of Raf/MEK/ERK/cPLA2 signaling pathway is essential for chlamydial acquisition of host glycerophospholipids." J Biol Chem **279**(10): 9409-16.
Su, H., L. Raymond, et al. (1996). "A Recombinant Chlamydia Trachomatis Major Outer Membrane Protein Binds to Heparan Sulfate Receptors On Epithelial Cells." Proceedings of the National Academy of Sciences of the United States of America **93 (20)**: 11143-11148.
Subtil, A. and A. Dautry-Varsat (2004). "Chlamydia: five years A.G. (after genome)." Curr Opin Microbiol **7**(1): 85-92.
Subtil, A., B. Wyplosz, et al. (2004). "Analysis of Chlamydia caviae entry sites and involvement of Cdc42 and Rac activity." J Cell Sci **117**(Pt 17): 3923-33.
Suchland, R. J., D. D. Rockey, et al. (2000). "Isolates of Chlamydia trachomatis that occupy nonfusogenic inclusions lack IncA, a protein localized to the inclusion membrane." Infect Immun **68**(1): 360-7.
Suetsugu, S., H. Miki, et al. (1998). "The essential role of profilin in the assembly of actin for microspike formation." Embo J **17**(22): 6516-26.
Tapon, N. and A. Hall (1997). "Rho, Rac and Cdc42 GTPases regulate the organization of the actin cytoskeleton." Curr Opin Cell Biol **9**(1): 86-92.
Tran Van Nhieu, G., R. Bourdet-Sicard, et al. (2000). "Bacterial signals and cell responses during Shigella entry into epithelial cells." Cell Microbiol **2**(3): 187-93.
Valdivia, R. H. (2004). "Modeling the function of bacterial virulence factors in Saccharomyces cerevisiae." Eukaryot Cell **3**(4): 827-34.
Vallotton, P., S. L. Gupton, et al. (2004). "Simultaneous mapping of filamentous actin flow and turnover in migrating cells by quantitative fluorescent speckle microscopy." Proc Natl Acad Sci U S A **101**(26): 9660-5.
Van Troys, M., J. Vandekerckhove, et al. (1999). "Structural modules in actin-binding proteins: towards a new classification." Biochim Biophys Acta **1448**(3): 323-48.
Vandahl, B. B., A. S. Pedersen, et al. (2002). "The expression, processing and localization of polymorphic membrane proteins in Chlamydia pneumoniae strain CWL029." BMC Microbiol **2**(1): 36.
Ward, M. E. and A. Murray (1984). "Control mechanisms governing the infectivity of Chlamydia trachomatis for HeLa cells: mechanisms of endocytosis." J Gen Microbiol **130**(7): 1765-80.
Wegner, A. (1976). "Head to tail polymerization of actin." J Mol Biol **108**(1): 139-50.

Wolf, K., E. Fischer, et al. (2000). "Ultrastructural analysis of developmental events in Chlamydia pneumoniae-infected cells." Infect Immun **68**(4): 2379-85.

Wuppermann, F. N., J. H. Hegemann, et al. (2001). "Heparan Sulfate-like Glycosaminoglycan Is a Cellular Receptor for Chlamydia pneumoniae." J Infect Dis **184**(2): 181-7.

Wuppermann, F. N., K. Molleken, et al. (2008). "Chlamydia pneumoniae GroEL1 protein is cell surface associated and required for infection of HEp-2 cells." J Bacteriol **190**(10): 3757-67.

Wyrick, P. B., J. Choong, et al. (1989). "Entry of genital Chlamydia trachomatis into polarized human epithelial cells." Infect Immun **57**(8): 2378-89.

Yang, C., M. Huang, et al. (2000). "Profilin enhances Cdc42-induced nucleation of actin polymerization." J Cell Biol **150**(5): 1001-12.

Yang, S., M. J. Cope, et al. (1999). "Sla2p is associated with the yeast cortical actin cytoskeleton via redundant localization signals." Mol Biol Cell **10**(7): 2265-83.

Yarar, D., J. A. D'Alessio, et al. (2002). "Motility determinants in WASP family proteins." Mol Biol Cell **13**(11): 4045-59.

Yarmola, E. G., T. Somasundaram, et al. (2000). "Actin-latrunculin A structure and function. Differential modulation of actin-binding protein function by latrunculin A." J Biol Chem **275**(36): 28120-7.

Yoshida, S., E. Katayama, et al. (2002). "Shigella deliver an effector protein to trigger host microtubule destabilization, which promotes Rac1 activity and efficient bacterial internalization." Embo J **21**(12): 2923-35.

Young, M. E., J. A. Cooper, et al. (2004). "Yeast actin patches are networks of branched actin filaments." J Cell Biol **166**(5): 629-35.

Zhang, J. P. and R. S. Stephens (1992). "Mechanism of C. trachomatis attachment to eukaryotic host cells." Cell **69**(5): 861-9.

Zhong, G., P. Fan, et al. (2001). "Identification of a chlamydial protease-like activity factor responsible for the degradation of host transcription factors." J Exp Med **193**(8): 935-42.

Zhou, D. and J. Galan (2001). "Salmonella entry into host cells: the work in concert of type III secreted effector proteins." Microbes Infect **3**(14-15): 1293-8.

Zhou, D., M. S. Mooseker, et al. (1999). "Role of the S. typhimurium actin-binding protein SipA in bacterial internalization." Science **283**(5410): 2092-5.

ACKNOWLEDGMENT

My thanks and gratitude first goes to ALLAH who gave me the strength, inspiration and patience to continue this research.

First of all people, I would like to express my deepest gratitude and appreciation to Prof. Dr. Johannes H. Hegemann for giving me the opportunity to work on this highly interesting project, his invaluable advice and guidance throughout the study. I will never forget his insight as a scientist, his philosophy as a person, his guidance as a teacher and his encouragement, continues help and caring in various ways as a big brother.

I am grateful to the second referee of the thesis Prof. Dr. Olaf Bossinger for his time and willingness to review my work fast.

I am also greatly appreciating PD Dr. Ursula N. Fleig for giving me the chance to use the facilities in her laboratory, her discussion and advices for my research work.

I thank Prof. Dr. Joachim Ernst and Prof. Dr. Lutz Schmitt for giving me the opportunity to use the facilities in their institutes. Dr. Sandra Beer is also greatly thanked for her advices in transfection experiments. Many thanks also to Petra Küppers for all the help in using the machines in Prof. Dr. Lutz Schmitt laboratory.

I want also to say “Dankeschön” for all past and present member of our laboratory for providing the nice atmosphere. Our laboratory work can not be achieved without the innovated and organized administrative work by Frau Chmielewski, thank you Stefanie.

Without the help of Dr. Frederik N.Wuppermann, Dr. Gabriele Köhler, Dr. Katja Mölleken and Dr. Eleni Schmidt, my PhD work would not be what it is now.

Special thanks goes to Gido Murra , Frauke Herbst and Tim Fechtner for all the computer related help. I also liked to thank Dr. Anne Kerres and Sven Boris Heick for the various types of help.

A big thank you also to the people in the “pombe” laboratory for all kinds of help during the past few years.

I am also grateful to Irina Volfson for her help concerning everything in regard to lab issues.

I want also to thank my mother for her invaluable love.

My wife Wafa, my sons Doodi and Hamoodi are the dearest and the nearest to me. Your humour and attitude have spread me from many troubles. You are my strength, and together we are equal to anything.

The PhD work financed by Sonderforschungsbereiche (SFB590) programm is gratefully acknowledged.

EIDESSTATTLICHE ERKLÄRUNG

Hiermit versichere ich, dass die vorliegende Arbeit von mir selbst verfasst wurde und dass ich keine anderen als die von mir angegebenen Hilfsmittel verwendet habe. Alle Stellen, die aus anderen Werken im Wortlaut oder dem Sinn entsprechend übernommen wurden, habe ich mit Quellenangaben kenntlich gemacht.
Rafat Zrieq